Hawker, Matthew James (2008) Detection of glaucoma in the elderly using laser scanning tomography. DM thesis, University of Nottingham.

DETECTION OF GLAUCOMA IN THE ELDERLY USING LASER SCANNING TOMOGRAPHY

by

Matthew J. Hawker

BMedSci(Hons), MBChB, MRCOphth

Division of Ophthalmology and Visual Sciences

Thesis submitted to the University of Nottingham for the degree of Doctor of Medicine

October 2006

Table of Contents

Declaration

Except where acknowledged in the acknowledgements and text, I declare that this report is my own work and is based on research that was undertaken by me in the Division of Ophthalmology and Visual Sciences, School of Medical and Surgical Sciences, University of Nottingham, from October 2004 to October 2006.

Matthew J. Hawker

October 2006

Abstract

Primary open angle glaucoma is mostly prevalent in patients over 60 years. However, studies examining the role of laser scanning tomography in detecting glaucoma hitherto have employed non-population based data drawn from younger subjects. This study employed an elderly, Caucasian, population-based cohort (minimum age 65 years, n=721). All subjects underwent ophthalmological examination including Goldmann applanation tonometry, suprathreshold automated visual field test and Heidelberg retina tomography. Normality was defined as normal visual acuity, visual field and intraocular pressure. Perimetrically normal males were found to have significantly larger optic cups than females. Normative data were used to construct three diagnostic tests: Linear regression of rim area, RADAAR (rim area/disc area asymmetry ratio) and the optic disc hemifield test (comparison of the superior and inferior rim/disc area ratios in the temporal and nasal sectors). Specificities at the 99th limit of normality were 91.4%, 95.1% and 98.3% respectively. Sensitivity was assessed using a cohort of patients (n=58) with a new diagnosis of open angle glaucoma at the Queen's Medical Centre, Nottingham within the last two years. Sensitivities at the 99th limit of normality were 72.4%, 55.6% and 27.6% respectively. Applying the regression analysis bilaterally and RADAAR simultaneously generated a specificity of 83.0% and sensitivity of 88.9%. Inclusion of the optic disc hemifield test did not further increase sensitivity. Linear regression of rim area/disc area was found to be susceptible to non-linearity and heteroscedasticity, causing reduced specificity in bigger optic discs. Modeling the relationship separately for each disc area quartile overcame this limitation to produce a diagnostic test with constant accuracy. Whilst laser scanning ophthalmoscopy can discriminate glaucoma with reasonable accuracy, it is limited by disagreement in contour placement and poor image quality in the elderly. The combination of multiple statistical tests is not ideal – application of statistical shape analysis techniques may better employ the normative data.

Financial support

The Bridlington Eye Assessment Project was funded by an unrestricted grant from Pfizer. The grant also funded my salary for 12 months. The Project is indebted also to the following organisations for financial support: Yorkshire Wolds & Coast Primary Care Trust, The Lords Feoffees of Bridlington, Bridlington Hospital League of Friends, The Hull & East Riding Charitable Trust, The National Eye Research Centre (Yorkshire), The Rotary Club of Bridlington, The Alexander Pigott Wernher Memorial Trust, Bridlington Lions Club, The Inner Wheel Club of Bridlington, Soroptimist International of Bridlington, and The Patricia and Donald Shepherd Charitable Trust.

Acknowledgements

It is a pleasure to thank the many people who have made this work possible:

My grateful thanks go to Mr Stephen Vernon, Consultant Ophthalmologist at Queen's Medical Centre, Nottingham for giving me the opportunity to be involved with the Bridlington Eye Assessment Project. I am indebted to him not only for the quality of the data I have been privileged to analyse, but also his sturdy supervision, encouragement and friendship.

I would like to thank Professor Harminder Dua for his friendly guidance and supervision of my thesis. His insightful comments have helped sharpen my scientific writing, and I am grateful for his advice in conducting and publishing research.

I am grateful to Gerard Ainsworth who, as a Specialist Registrar at Queen's Medical Centre, started the research that led to chapters 1 and 2. He taught me how to contour optic nerve heads on HRT images, as well as export data. From this solid start I was then able to move this work onwards to publication.

I thank Dr David Crabb (Reader in Statistics and measurement in vision at City University, London) for his interest in BEAP and for periodic statistical advice. The nature of the advice was general and advisory, I conducted all statistical analyses myself.

I am grateful to Christopher L Tattersall who, as a research nurse at Queen's Medical Centre, compiled the dataset of glaucoma patients used in the work of Chapters 8-11.

I am grateful to Kamron Khan who, as a Senior House Officer in Ophthalmology at Queen's Medical Centre assisted me in the compiling of results and initial drafting of Chapters 10 and 11.

A successful period of full-time research would not have been possible without the efficient administration of Mrs Alison Adair, Research Coordinator to Mr SA Vernon. Thank you Alison for your support and friendship!

I acknowledge Drs Jonathon Hillman and Hamish MacNab (General Practitioners in Bridlington), Mrs Sheila MacNab (BEAP Manager), Linda Sanderson (Receptionist), the nursing staff, and Mr S Brown, Mrs J Button, Mr G Langton, and Mr M Kunz (Optometrists) for their hard work with BEAP. I also thank Mr J Bapty, Mr N Connell, Mr P Jay, and Mrs G Poole for their work as the charity trustees of the Project. None of my work would have been possible without the BEAP team that so enthusiastically collected the data.

Finally, I thank my wife Selina for her love and support.

Matthew J. Hawker October 2006

Abbreviations

BEAP	Bridlington Eye Assessment Project
GON	Glaucomatous optic neuropathy
HRT	Heidelberg Retina Tomograph
LDF	Linear discriminant function
MLC	Machine learning classifier
MPHSD	Mean pixel height standard deviation
MRA	Moorfields Regression Analysis
OCT	Optical Coherence Tomography
ONH	Optic nerve head
POAG	Primary open angle glaucoma
RADAAR	Rim area-to-disc area asymmetry ratio
RGC	Retinal ganglion cell
RNFL	Retinal nerve fibre layer
SAP	Standard automated perimetry
SVM	Support Vector Machine
SWAP	Short-wavelength automated perimetry

List of Tables

List of Figures

Presentations arising from this work

Platform Presentations

1. Laser scanning tomography of the optic nerve head in a normal elderly population: The Bridlington Eye Assessment Project.
Hawker MJ, Vernon SA, Ainsworth G, Hillman JG, MacNab HK, Dua HS.
The 9th Nottingham Eye Symposium and Research Meeting, Nottingham, January 2005 and Imaging Morphometry Association for Glaucoma in Europe, Milan, April 2005 and United Kingdom and Eire Glaucoma Society Annual Meeting, December 2004 (presented by G Ainsworth, won 1st prize).

2. The specificity of the Heidelberg Retina Tomograph's diagnostic algorithms in classifying optic nerve heads in a normal elderly population.
Hawker MJ, Vernon SA, Ainsworth G. Imaging Morphometry Association for Glaucoma in Europe, Milan, April 2005.

3. Observer agreement using HRT II in a population-based cross-sectional study of normal elderly patients: The Bridlington Eye Assessment Project.
Hawker MJ, Ainsworth G, Vernon SA, Dua HS. Oxford Ophthalmological Congress, 2005.

4. Linear Regression Modeling Of Rim Area To Discriminate Between Normal And Glaucomatous Optic Nerve Heads: The Bridlington Eye Assessment Project.
Hawker MJ, Vernon SA, Tattersall CL, Dua HS.
United Kingdom and Eire Glaucoma Society Annual Meeting, December 2005 (won 1st prize), The 10th Nottingham Eye Symposium and Research Meeting, Nottingham, January 2006 (won the Nottingham Research Prize), The Royal College of Ophthalmologists Annual Congress, Manchester, 2006, and the Benjamin Gooch Prize Presentation, Norfolk and Norwich University Hospital, Norwich, 2006 (won 2nd Prize).

5. Detecting Glaucoma With RADAAR (Rim Area/Disc Area Asymmetry Ratio): The Bridlington Eye Assessment Project.
Vernon SA, **Hawker MJ**, Tattersall CL, Dua HS.
The Royal College of Ophthalmologists Annual Congress, Manchester, 2006.

Poster Presentations

1. Asymmetry in optic disc morphometry as measured by Heidelberg Retina Tomography in a normal elderly population: The Bridlington Eye Assessment Project.
Hawker MJ, Vernon SA, Ainsworth G, et al. Association for Research in Vision and Ophthalmology, May 2005 and Royal College of Ophthalmologists Annual Congress, May 2005.

2. Laser scanning tomography of the optic nerve head in a normal elderly population: The Bridlington Eye Assessment Project.
Hawker MJ, Vernon SA, Ainsworth G, Hillman JG, MacNab HK, Dua HS.
Royal Society of Medicine Registrars Meeting, June 2005.

3. The Optic Disc Hemifield Test: The Bridlington Eye Assessment Project.
Khan K, **Hawker MJ**, Vernon SA, Tattersall CL, Dua HS.
The 10th Nottingham Eye Symposium and Research Meeting, Nottingham, January 2006.

Publications arising from this work

1. Vernon SA, **Hawker MJ**, Ainsworth G, *et al.* Laser scanning tomography of the optic nerve head in a normal elderly population: The Bridlington Eye Assessment Project. *Invest Ophthalmol Vis Sci.* 2005;**46**:2823-2828.

2. **Hawker MJ**, Vernon SA, Ainsworth G, *et al.* Asymmetry in optic disc morphometry as measured by Heidelberg Retina Tomography in a normal elderly population: The Bridlington Eye Assessment Project. *Invest Ophthalmol Vis Sci.* 2005;**46**:4153-4158.

3. **Hawker MJ**, Vernon SA, Ainsworth G. The specificity of the Heidelberg Retina Tomograph's diagnostic algorithms in a normal elderly population: The Bridlington Eye Assessment Project. *Ophthalmology* 2006;113(5):778-785.

4. Linear Regression Modeling Of Rim Area To Discriminate Between Normal And Glaucomatous Optic Nerve Heads: The Bridlington Eye Assessment Project.
Hawker MJ, Vernon SA, Tattersall CL. *J Glaucoma* 2007;16(4):345-51.

5. Detecting Glaucoma With RADAAR (Rim Area/Disc Area Asymmetry Ratio): The Bridlington Eye Assessment Project.
Hawker MJ, Vernon SA, Tattersall CL, Dua HS. *Br J Ophthalmol* 2006;90(6):744-748.

6. Observer Agreement Using the Heidelberg Retina Tomograph: The Bridlington Eye Assessment Project.
Hawker MJ, Ainsworth G, Vernon SA, Dua HS. *J Glaucoma 2007: In press.*

1.0 General Introduction

1.1 General Introduction

Primary open angle glaucoma (POAG) remains a major cause of blindness worldwide.[1] It has been estimated that at the end of the 20th century, over 60 million people were affected by glaucoma worldwide, and nearly 10% of those affected were blind in both eyes.[2] POAG is a chronic, slowly progressive, multifactorial optic neuropathy which usually affects both eyes. Structurally, glaucoma involves loss of retinal ganglion cells (RGCs) with associated axonal degeneration and loss of neuroretinal tissue at the optic nerve head (ONH). The functional consequence of this process is visual field loss. Early detection of structural and functional loss is an important goal if glaucoma is to be diagnosed and treated in its earliest stages.

Death of the RGC and its associated loss of neuroretinal (axonal) tissue observed at the ONH is the hallmark of glaucomatous optic neuropathy (GON). RGCs are classified into two major groups. Parasol ganglion cells are found throughout the retina and, as part of the magnocellular visual pathway, they subserve motion perception, low spatial resolution with high contrast sensitivity and stereopsis.[3] Midget ganglion cells are more concentrated in the central retina[4] and, as part of the parvocellular visual pathway, subserve central visual acuity, colour perception, low contrast sensitivity at high spatial resolution, static stereopsis and shape. Previous work, mainly reporting histological findings, has suggested that glaucoma preferentially affects parasol RGCs[5, 6] that project to the magnocellular layers of the lateral geniculate nucleus.[7-9] However, other data have demonstrated that both RGC types are affected,[10] whilst not all work has supported selective RGC death.[11] Discriminating glaucoma from normality based on structural parameters is not straightforward. There is substantial variation in the total number of RGCs between normal eyes with the number of fibres in the normal optic nerve varying from 600,000 to 1.2 million in different reports.[12-14] Additional normal variability is found in the age-dependent reduction in the number of optic nerve fibres,[15, 16] a process which may accelerate after middle-age.[14] Histological studies have estimated that 10,000 nerve fibres are

lost every year after the age of 40 years. This represents a loss of up to 40% of the approximately 1.2 million nerve fibres present in each optic nerve by an individual's 9th decade. Whilst some work supports a concurrent decrease in rim area at the ONH with age,[17] this finding is not universal.[18]

1.2 Morphological Characteristics of the Optic Nerve Head

GON, amongst all optic neuropathies, shows characteristic morphological changes at the ONH that enable glaucoma to be distinguished from normality in the majority of cases. Many continuous biological variables show overlap in parameters between the normal and disease states – and GON is no exception. As POAG is a slowly progressive condition, the early stages of the disease process may be difficult to detect at the ONH. Highly accurate and reproducible objective measures of the ONH may improve disease detection, especially when statistical limits of normality are applied. To correctly apply these technologies in the clinical setting, however, an understanding of the differences in morphology of the normal and glaucomatous ONH is required.

1.2.1 The Normal Optic Nerve Head

The ONH comprises several qualitative and quantitative parameters to be described. These are size and shape of the disc; size and shape of the neuroretinal rim (comprising RGC axons); width and depth of the optic cup in relation to the size of the disc; position of the central retinal vessel trunk on the ONH; presence of optic disc haemorrhages; presence and configuration of parapapillary chorioretinal atrophy; and the visibility of the RNFL. The normal ONH shows considerable variability between individuals. ONH size can vary from 0.8 mm2 to almost 6.0 mm2 in normal Caucasian populations.[19] Increase in size of the ONH with growth ceases after the age of around 3 to 10 years. The degree of refractive error is correlated with disc size, with discs being significantly smaller beyond +5 dioptres, and significantly larger beyond -8 dioptres, than in emmetropic eyes.[20, 21] However, within the range of -5 to +5 dioptres optic disc size shows very little correlation with refractive error.[20, 22] Optic disc size is also dependent on racial factors, being smaller in Caucasians

than Asians and African-Americans.[22, 23] In one study disc area was 2-3% larger in males than females,[22] although this finding has not been substantiated by other studies.[24] Optic disc shape may also vary significantly between individuals. The normal optic disc is vertically slightly oval, with the vertical diameter being 7-10% greater than the horizontal diameter.[20] An abnormal optic disc shape is found in a significant proportion of subjects with high myopia.[21] Such tilted optic discs are of particular significance in the context of this thesis since their aberrant configuration may affect the defining of the reference plane as used by the Heidelberg retina tomograph. In addition, tilted discs are significantly correlated with increased corneal astigmatism and amblyopia,[25] which may adversely affect image clarity.

Assessment of optic disc size is important in discriminating between normal and glaucoma since rim and cup measurements are both positively correlated with disc size.[22, 26] Anatomically, this relationship reflects the positive correlation between optic disc size and optic nerve fibre count.[27] Other reasons for the interindividual size variability of rim area include different nerve fibre counts,[13, 14, 28] different densities of axonal 'packing' with the ONH,[29] different RGC axonal diameters,[27, 29] different architecture of the lamina cribrosa,[30, 31] or different proportions of supporting glial cells within the ONH.[32] The increase in cup size in larger discs is greater than the increase in rim size,[33] although this relative difference may be modified depending upon the morphology of the cup.[24] It follows that large optic discs may have a large cup and be normal, whilst small optic discs may have a small cup and be glaucomatous. The normal neuroretinal rim also exhibits a characteristic shape, being broadest in the Inferior sector, followed by the Superior sector, the Nasal sector, and the Temporal sector (ISN'T rule).[20] This morphometry reflects the normal configuration of a vertically oval optic disc with a horizontally oval optic cup. A ONH that does not exhibit this configuration may therefore raise suspicion of GON. The cup/disc ratio is an alternative way of expressing ONH configuration that has the advantage of being robust to differences in magnification amongst imaging systems. Due to

the normal configuration described above the cup/disc ratio is smaller in the horizontal meridian than the vertical one in less than 7% of normal eyes.[20]

1.2.2 The Glaucomatous Optic Nerve Head

Loss of neuroretinal rim tissue with enlargement of the optic cup is the hallmark of GON. In contrast to glaucoma, this change in morphology is not normally seen in optic neuropathy of non-glaucomatous origin.[34] GON displays characteristic 'cupping' of the ONH resulting from a combination of loss of RGC axons along with collapse and posterior bowing of the lamina cribrosa. In GON neuroretinal rim is lost from all sectors of the optic disc, although the sequence of sector involvement may be dependent upon the stage of disease.[35, 36] One study found that early disease generally began in the inferotemporal disc region, then progressed to the superotemporal, the temporal horizontal, the inferior nasal, and finally the superonasal sectors.[37] This may reflect the differential susceptibility to glaucoma of thick and thin nerve fibres at the ONH. Thick nerve fibres originate predominantly in the retinal periphery, leading to the inferior and superior disc regions and are more susceptible to glaucoma damage.[38] Thin fibres originate from the fovea and pass to the temporal disc.[29] These fibres are less susceptible to the glaucoma process. To achieve a higher diagnostic power it is therefore better to analyse ONH rim changes by disc sector, rather than for the entirety of the ONH.[39] It should be noted that changes in rim morphology in GON seem to be entirely due to the disease process, as no change is disc size has been detected in POAG.[40] It is also of note that the local susceptibility of rim loss in a given disc sector is proportional to the distance to the exit of the central retinal vessel trunk on the surface of the lamina cribrosa.[41] The normal position of the trunk is slightly eccentrically placed in the supero-nasal disc sector[31] which may explain the early susceptibility of the infero-temporal disc sector to glaucomatous damage. Since HRT morphometry of the ONH includes the central vessel trunk in the rim area measurement,[42] an enhanced differential effect of GON on different disc sectors may be seen. An unusually eccentric exit point of the central retinal vessels, combined with a tilted disc, may induce

significant unpredictable inter-individual variation as to make comparison of rim area with normative data unreliable.

Changes in cup morphology due to GON depend upon the type of glaucoma. Generally, the optic cup enlarges in area and depth with the disease process. However, the optic cup of GON is shallower in eyes with the highly myopic and senile atrophic types of POAG compared with other descriptive subsets.[19] The presence of parapapillary atrophy may also reflect cup depth since deeper cups are associated with smaller parapapillary atrophy.[43] Cup depth is of relevance particularly in HRT scanning of the ONH where the level of the reference plane set for each individual may differentially affect cup and rim measurements where cups are of different depths.

Thus it is apparent that differences in rim and cup morphology within the ONH may be exploited to differentiate normal from glaucomatous ONHs. This short review has concentrated upon those morphological characteristics that may be detected by HRT scanning. A more extensive description has been undertaken by Jonas et al. [19, 34]

1.3 Limitations of Function Testing in the Detection of Glaucoma

POAG has a prolonged subclinical phase, with progressive loss of retinal ganglion cells demonstrable prior to the development of visual field defects on automated testing.[36, 44-48] One reason for this is the considerable overlap in receptive fields of adjacent RGCs. Consequently, unless damage is very localised standard threshold automated perimetry (SAP) may not detect visual field loss until considerable structural damage has occurred.[47, 49, 50] In addition, due to the subjective nature of visual field testing, there is considerable inter-test variability amongst individuals being screened for glaucoma.[51] Whilst short-wavelength automated perimetry (SWAP) can detect the presence and progression of glaucoma earlier in the disease process than SAP,[52, 53] SWAP unfortunately has higher inter- and intra-test variability than SAP. Larger deviations from normal values are therefore required for statistical significance.[54]

SWAP also suffers from longer test times requiring prolonged concentration, an important factor when examining elderly subjects. It is apparent, therefore, that automated perimetry has significant limitations as a tool to discriminate normal from glaucoma. Consequently, quantitative examination of the ONH and retinal nerve fibre layer (RNFL) has received much attention, particularly as more precise and repeatable objective techniques have become available.

1.4 The Heidelberg Retina Tomograph

The Heidelberg Retina Tomograph (HRT) is a semi-automated confocal scanning laser system that provides reliable and reproducible three-dimensional imaging data of the optic nerve head.[55] The first release of HRT (HRT I) was designed primarily as a research tool. The more recent release of HRT (HRT II) has redesigned ergonomics and functioning to make the machine more suitable for the clinical environment. The underlying imaging technology remains unchanged. Heidelberg GmbH's information on HRT I is given in Appendix 1, with additional information on HRT II being given in Appendix 2.

1.4.1 Principles of Operation

The HRT is a semi-automated confocal scanning laser ophthalmoscope. A monochromatic diode laser beam (wavelength 675nm) provides the light source. A confocal imaging aperture coupled with a luminance detector allows precise topographical height measurements at the ONH. Laser scanning tomography describes the sequential measurement of subsequent points within a fixed 15 degree by 15 degree frame. Adjusting the depth of the focal plane by shifting the confocal aperture allows multiple optical sections to be acquired to form a layered three-dimensional image. HRT scans between 16 and 64 individual 2-dimensional confocal planes to build a topographic map of the ONH. The first plane is focused at the posterior vitreous with the final plane lying deep in the ONH. The distance between each confocal plane is set at 62.5 microns. The image is digitized at a resolution of 384 by 384 pixels. Each pixel height is calculated at the position of peak reflectance obtained across the multiple sections. This is assumed to correspond to the position of the internal limiting

membrane. The theoretical resolution of HRT II is limited by the optics of the eye to 10 microns per pixel (transverse resolution) and 300 microns in axial resolution. HRT II automates much of the image acquisition process. A pre-scan planning mode automatically selects the optimal fine focus, scan depth and sensitivity settings to obtain the best image. To optimise the reproducibility of each pixel height measurement, three images are acquired and the mean height measurement at each pixel is calculated to create a mean topographic image.

In order to visualise the matrix of height measurements a colour-coding system is employed. Two image maps are presented. The Topographic map encodes height, with darker colours representing raised structures (such as the rim) and lighter colours representing depressed structures (such as the cup). The Reflectance image encodes intensity of light reflected to the luminance detector. Darker areas are regions of decreased reflectance, whilst brigher areas are those of greatest reflectance (such as at the base of the cup). These maps allow a subjective interpretation of the position of the ONH in order for the operator to manually mark the edge of the ONH with a contour.

1.4.2 The Reference Plane

Following the manual outlining of the ONH margin (at the inner edge of Elschnig's ring), the HRT II software automatically defines a reference plane located 50 microns posterior to the papillomacular bundle and parallel to the retinal surface (the 'standard reference plane'). The papillomacular bundle is used as a reference point because it is affected relatively late in the glaucomatous process. This reference plane approximates to the location of the deep boundary of the RNFL. Structures above the reference plane are defined as 'rim' (and RNFL at the ONH edge), those structures below the reference plane are defined as 'cup'.

The major advantage of the standard reference plane is that it better respects the individual variability of ONH morphology and orientation (e.g. oblique insertion).[56] However, great accuracy in ONH contour placement is required,

failure of which is a source of additional variability in ONH parameters.[57] This contrasts with an older definition of the reference plane which was fixed in the perpendicular plane at 320 microns (up to software version 1.10). Whilst not offering as stable a representation of ONH morphology,[58] the fixed reference plane may avoid significant parameter variability induced by variable contour placement, especially important in cross-sectional diagnostic studies.[57] Whilst other work has identified reference planes more representative of ONH morphology as judged by clinical observers,[59] and by OCT,[60] the standard reference plane remains the most commonly used.

1.4.3 Quantitative Stereometric Parameters

Following contour placement HRT II calculates the reference plane and the stereometric parameters (Table 1). Each of the morphological parameters is expressed for the global disc, and for 6 individual disc sectors (temporal 90^{o}, temporal superior 45^{o}, temporal inferior 45^{o}, nasal 90^{o}, nasal superior 45^{o}, nasal inferior 45^{o}).

Table 1. Definitions of the Stereometric Parameters.

Parameter	Definition
Disc Area (mm^2)	Area bounded by contour line.
Cup Area (mm^2)	Area enclosed by contour line which is located below the reference plane.
Rim Area (mm^2)	Area enclosed by contour line which is located above the reference plane.
Cup Volume (mm^3)	Volume enclosed by contour line which is located below the reference plane.
Rim Volume (mm^3)	Volume enclosed by contour line which is located above the reference plane.
Cup/Disc Area Ratio	Ratio of cup area/disc area.
Rim/Disc Area Ratio	Ratio of rim area/disc area.
Mean Cup Depth (mm)	Mean depth of the optic disc cup.
Maximum Cup Depth (mm)	Maximum depth of the cup.
Cup Shape Measure	Summary measure for overall 3-dimensional shape of cup. Represents the distribution frequency of the depths inside the contour line. Normal values are negative.
Height Variation Contour (mm)	Variation in height along the contour line (difference in height between the most elevated and depressed points).
Mean RNFL Thickness (mm)	Mean thickness of the RNFL (relative to the reference plane) measured along the contour line.
RNFL Cross-Sectional Area (mm^2)	Total cross-sectional area of the RNFL (relative to the reference plane) along the contour line.
Average variability (mm)	The mean standard deviation of all pixel height measurements.
FSM Discriminant Function Value	Discriminant value based on the linear discriminant function created by FS Mikelberg et al. Positive values are normal, negative values are abnormal.
RB Discriminant Function Value	Discriminant value based on the linear discriminant function created by R Burk. Positive values are normal, negative values are abnormal.

1.4.4 Reproducibility of Pixel Height Measurements

The reproducibility of each of the individual height measurements (MPHSD) obtained by HRT is in the order of 10-30 microns.[55, 61-66] In the presence of cataract, MPHSD was found to be improved by pupil dilation.[67] Similarly, image quality was found to be reduced by pupil constriction.[64] Many of these studies

found greater MPHSD in glaucomatous ONHs compared with normal ones. MPHSD was found to be greater within the ONH than the peripapillary retina, and was reduced by synchronising image acquisition with the cardiac cycle.[68] Similarly, MPHSD was found to be greater in steep areas of the topography (where there are more features) compared with flat areas.[66] One study found that three ONH scans comprising one mean topographic image allowed the optimal balance between improved reproducibility and increased image acquisition time.[65] The current HRT II therefore acquires 3 image series and computes one mean topographic image from these.

1.4.5 Reproducibility of Stereometric Parameters

The reproducibility of the computed topographic parameters has been shown to be acceptable with coefficients of variation less than 10%.[55, 64, 69-71] Test-retest variability (across five consecutively obtained images) is positively correlated with age and negatively correlated with visual acuity.[71] Using HRT I image acquisition variability is greater than contour-dependent variability,[72] although it is likely that improved image acquisition and use of a mean topographic image by HRT II has overcome this difference. Interobserver agreement in contour placement can be substantial, even with no formal discussion between investigators as to where to place the contour.[73] However, since the contour is placed at the inner edge of Elschnig's ring, where the ONH surface has a relatively steep slope, small errors in contour placement can induce large effects on parameter variability. Concordantly, placing the contour further out into the peripapillary region can reduce such variability.[74] The use of a clinical photograph of the ONH to aid contour placement appears to improve interobserver variability of HRT stereometric parameters.[75] The interobserver variability of ONH parameters appears to be better with HRT compared with both manual and computer-assisted planimetry[57, 76, 77] and a digital stereoscopic optic disc camera (Discam, Marcher Enterprises Ltd., Hereford, UK).[78]

The accurate calculation of stereometric parameters such as disc size requires use of an algorithm to correct for the effect of ametropia in individual subjects.

This is because the size of the optic disc in a fundus image is dependent on magnification due to the imaging system[79, 80] and the eye, as well as factors such as the eccentricity of the disc within the image[81] and the position of the imaging system with respect to the eye.[82] Image scaling in the HRT is based on an axial model of ametropia. The adjustment of focus settings to compensate for refractive change in eyes of stable axial length and keratometry can therefore induce a change in the stereometric parameters.[83] Change in the eye-scanner distance[84] and subject misalignment[85] can accentuate any magnification effects due to ametropia. Careful positioning of each subject is therefore a pre-requisite to good HRT image quality. Ametropia due to uncorrected astigmatism below 2.5 dioptres does not produce significant variability of stereometric parameters.[86] Whilst magnification changes may be partially compensated for in longitudinal series through image-to-image scaling and the exported contour line, the effects in cross-sectional series will be uncorrected.

1.4.6 Relationship between Structural and Functional Loss

Previous studies have examined the relationship between structural measurements of the ONH acquired using HRT and functional parameters. Visual field defects have been shown to correlate with morphometric changes at the ONH.[87-91] Unsurprisingly, this correlation is stronger when analysed for ONH sectors compared with the global ONH analysis.[92] In one study, when used to detect progression of glaucomatous damage over time (median follow up 5.5 years), HRT detected glaucoma progression more often than SAP, whilst progression on both criteria was usually detected earlier by HRT.[93] Nevertheless, there were a minority of subjects who showed progression on perimetry alone.

There is consistent evidence that ONH damage can be detected before the development of glaucomatous visual field loss on SAP.[94] This finding is in accordance with the histological evidence of marked RGC axonal loss prior to the development of visual field defects. Thus, some have previously concluded that in early glaucoma a strong correlation between structural and functional loss

will not be present. This weakness of correlation is exacerbated by the logarithmic scale of retinal sensitivity testing used in SAP, which produces a curvilinear relationship between retinal sensitivity and structural measures.[95] However, in a study examining the relationship between light sensitivity on SAP and rim area (HRT) the curvilinear (quadratic) relationship when light sensitivity was measured in decibels became linear when sensitivity was plotted on the 1/Lambert scale.[96] Thus, large changes in rim area were associated with small changes in decibel reduction of light sensitivity in early glaucoma, whilst the opposite was true in advanced glaucoma. The authors concluded that there is no ganglion cell functional reserve, but a continuous structure/function relationship. In addition, Blue-on-Yellow perimetry, which can detect defects earlier than SAP, shows a stronger correlation with HRT parameters than SAP defects.[97]

Electrophysiological functional deficits often agree with glaucomatous structural damage,[98] with a relationship also existing within ocular hypertensive patients.[99] There can, however, be notable disagreement between these measures.

1.5 HRT II Diagnostic Algorithms

1.5.1 The Moorfields Regression Analysis

The Moorfields Regression Analysis was developed to discriminate between normal and glaucomatous optic nerve heads.[17] The MRA diagnostic algorithm is incorporated into the software of HRT II as a clinical diagnostic tool. Using a database of 112 eyes of 112 normal subjects (volunteers) with a mean age of approximately 57 years, linear regression analysis was performed to determine different limits of normality for the log of the rim area corrected for disc size and age. Thus, by accounting for variation in rim area due to demographic variables, rim area changes due to GON may be more sensitively detected. Comparison of predicted limits with the log of actual measured rim area determines the ONH to be 'within normal limits' (rim area greater than the 95th lower prediction limit), 'borderline' (rim area between the 95th and 99.9th lower prediction limits) or

'outside normal limits' (rim area below the 99.9th lower prediction limit). This analysis is conducted for each of the 6 optic disc sectors in addition to a global disc analysis. The overall status for the optic disc is equal to that of the worst disc sector. This method has generated specificities of 94-96%, with lower sensitivities of 74-84%,[17, 100] and has been shown to be more sensitive than expert clinical evaluation in detecting glaucoma.[101] The MRA has also been shown to detect optic disc abnormalities in glaucoma suspects prior to the development of visual field defects.[102] ONH sectors defined as 'outside normal limits' also show reduced blood flow measured using the Heidelberg Retina Flowmeter.[103] However, diagnostic accuracy of the MRA has been found to vary with ONH area. A study opportunistically recruiting Indian normals found that specificity of the MRA decreased as disc size increased.[104] This finding was replicated in another study on Canadian subjects.[105] Conversely, however, Miglior et al found that the diagnostic ability of MRA did not change when discs less than 1.2mm^2 or more than 2.8mm^2 were excluded from the analysis.[100] The cause of variable diagnostic ability with different disc sizes is intriguing and remains elusive. Uncertain diagnostic classification due to unpredictable effects of disc size is a limitation in the clinical application of the MRA. Another limitation is the MRA's dependence on the accuracy of ONH contour placement. Variable ONH definition by different investigators causes variable measurement of rim area due to disc area and reference height variability. One study looked at the variability of classification by the MRA across 5 consecutive images obtained for each eye at one sitting. The contour was drawn on one image and the software automatically imported the contour to the other 4 images. Classification by the MRA varied in 52% of cases.[71] Another study looking at the effect of different observers placing the contour on identical images on optic nerve head measurements found significant interobserver variation in rim area measurement.[57] This variation can be reduced by the use of optic disc photographs to aid contour placement on the HRT image.[75]

1.5.2 Linear Discriminant Functions

Linear Discriminant Functions are alternative statistical techniques employed to discriminate normal from glaucomatous ONHs using HRT II. The main strength of the LDF lies in its ability to utilise many topographic parameters (as opposed to the MRA's sole use of rim area) to statistically discriminate normality from glaucoma. Using datasets of normal and glaucomatous individuals, LDFs employ individual topographic measures as weighted predictor variables to generate the function based on maximal separation of the normal and glaucomatous groups. LDF values greater than zero are interpreted as normal, with values less than zero indicating disease. Whilst they can produce reasonable diagnostic accuracy,[61, 106] they are highly dependent on the particular training sets of data used to produce the function, tending not to perform as well on subsequent testing datasets.[107] LDFs have been developed by R Burk (RB LDF; Heidelberg Retina Tomograph II Operating Instructions, Dossenheim, Germany; Table 9) and FS Mikelberg *et al.* (FSM LDF; Table 9).[106] Both LDFs are incorporated as diagnostic tools into HRT II software. The FSM LDF was developed from a database of one eye of each of 45 normal subjects (mean age 51.6 years) and 46 patients with early glaucoma (mean age 61.2 years). This LDF has generated specificities of 84-90% and sensitivities of 64-89%.[100, 106-108] However, in common with the MRA the FSM LDF also shows reduced specificity in larger optic discs.[104, 108]

1.5.3 Machine Learning Classifiers

Machine learning classifiers (MLCs) offer an alternative way to LDFs of summarising the large amoung of information generated by HRT scanning of the ONH. A disadvantage of LDFs is that they assume that data representing different groups are linearly separable. If this assumption is not well met then the LDFs diagnostic power is degraded. The major advantage of MLCs is that they can adapt to the particular distribution of the data they are trained on, rather than requiring a predefined distribution. The Support Vector Machine (SVM) is particularly suited to the task of discriminating normality from glaucoma since it is especially suitable for binary classification and for data of relatively small size

and high dimensions.[109] One study compared the diagnostic performance between LDFs and different types of MLCs in 108 glaucomatous eyes and 189 normal eyes.[107] All 17 global and 66 regional HRT parameters were employed in the functions. The areas under the ROC curve for the best performing MLC (Gaussian SVM) and the best performing LDF were 0.945 and 0.906 respectively. The application of forward selection and backward elimination optimisation techniques increased the area under ROC curve of SVM Gaussian further to approximately 0.96. The authors concluded that MLCs offer improved diagnostic power. A further study compared the diagnostic power of a Gaussian SVM trained using mean height contour at 36 points along the ONH margin compared with similar measurements further out in the parapapillary region.[109] Better diagnostic power was found at the ONH margin than in the parapapillary region (area under ROC curves 0.97 and 0.85 respectively). Other work showed that SVM classifiers trained on HRT data from glaucoma suspect eyes were somewhat more predictive of the development of visual field defects than the FSM LDF, though they were not more predictive than stereophotograph evaluation by experts or the MRA.[102]

1.5.4 Statistical Shape Analysis

A considerable limitation of the HRT operation is in the requirement for the operator to manually outline the limit of the ONH. This can be a source of considerable interobserver variability,[57] aswell as inducing variability in longitudinal image acquisitions.[110] Swindale et al. developed a method of automated analysis of ONH images acquired by HRT scanning that does not require manual outlining of the ONH. Parametric mathematical modelling of ONH shape is employed, fitting model parameters from a predefined selection to best describe the ONH topography. The parameters' values are then used as descriptors of ONH morphology to allow further analysis. Parameters of particular diagnostic power were the vertical and horizontal components of ONH convex curvature, and the steepness of the cup walls. Overall diagnostic accuracy was 89% and compared favourably with a LDF trained on the same dataset (diagnostic accuracy 84%). A further shape analysis method described

the optic cup shape using a tetrahedron model, although it's diagnostic accuracy is yet to be reported.[111] The application of statistical shape analysis techniques to HRT-acquired topography is an emerging technique that offers several advantages. Further studies are eagerly awaited.

1.6 Diagnostic Power of HRT Compared with Other Quantitative Techniques

The introduction of objective imaging of the disc promises to improve evaluation of ONH parameters by removing subjectivity. Confocal scanning laser ophthalmoscopy (HRT), scanning laser polarimetry (GDx VCC, Laser Diagnostic Technologies, Inc, San Diego, California) and optical coherence tomography (Stratus OCT, Carl Zeiss Meditec, Inc, Dublin, California) are different technologies that make use of the properties of light and retinal tissue to obtain their measurements. All have shown promising diagnostic accuracy in discriminating normal and glaucoma. Current models of each device have been shown to have similar diagnostic accuracy with moderate to substantial agreement.[112, 113] Much current research is focusing on improving diagnostic accuracy using these technologies so that sensitivity and specificity are high enough to justify population-based screening for glaucoma. Different techniques can produce different measurements of ONH parameters,[114-117] so they cannot generably be used interchangeably.

1.6.1 Clinical examination

The appearance of the normal optic nerve head can vary widely. This variability can cause expert observers of the optic disc to disagree in discriminating between normal and glaucoma.[118] With its ability to objectively compute expected rim area for a given ONH size, HRT II has been shown to be more sensitive in detecting glaucoma than expert examination of stereoscopic optic disc photographs.[101] Another study, however, found that HRT, optical coherence tomography, and scanning laser polarimetry were no better than expert examination of ONH stereophotographs in detecting glaucoma.[119] Problematic in the study of the diagnostic accuracy of clinical examination for glaucoma is the pre-emptive use of clinical examination to *define* glaucoma. The question always

remains whether glaucoma really was present. One way of overcoming this is by including glaucoma subjects only based on visual field criteria. Thus, glaucoma suspects (pre-perimetric disease) might be classified as normal. Another helpful suggestion is to define glaucoma longitudinally as those subjects with documented evidence of progression of disease.[120] This problem explains the relative lack of data comparing clinical examination and HRT in diagnosing glaucoma. One study found that clinical evaluation of the ONH cup depth showed poor agreement with HRT.[121] Further evidence of the limited accuracy of clinical evaluation of the ONH is found in its dependence on image size.[122]

1.6.2 Optical Coherence Tomography

Optical Coherence Tomography (OCT; Stratus OCT, Carl Zeiss Meditec, Inc, Dublin, California) uses optical technology (low coherence interferometry) that is analogous to B mode ultrasound imaging, except that light is utilised rather than sound to acquire high resolution images. The ONH scan consists of six radial scans in a spoke-like pattern centred on the ONH. The disc margin is automatically determined as the end of the retinal pigment epithelium/choriocapillaris layer. The reference plane is constructed 150 microns anterior to this layer, operating in the same way as that used by HRT. The OCT RNFL scan is a 360 degree circular scan around the ONH providing data on RNFL thickness. OCT imaging has been demonstrated to be similar to HRT in its ability to detect normality/glaucoma, with areas under receiver operating characteristic curves between 0.54 to 0.91.[123-126] In one study, OCT did not stand out as better than HRT in discriminating glaucoma, or as better even than subjective evaluation of ONH stereophotographs.[119] In two other studies, no significant difference was found between HRT and OCT in discriminating normality from glaucoma.[112, 113] One study found slightly higher sensitivity in detecting glaucoma using OCT compared with HRT.[126] Thus, there is no consensus to separate the diagnostic performance of the two technologies. This finding may reflect the particular selection of different statistical techniques employed in each of these studies to compare raw parameters between the

normal and glaucoma groups. It is possible that the best statistical technique for each technology was not recruited.

1.6.3 Scanning Laser Polarimetry

Scanning laser polarimetry (GDx VCC, Laser Diagnostic Technologies, Inc, San Diego, California) uses the birefringent properties of the RNFL to provide objective and quantitative measures of this structure.[127, 128] A polarization modulated laser beam (wavelength 780nm) scans the RNFL which changes the state of polarisation (retardation) of the light passing through it. The thicker the RNFL, the greater the retardation of transmitted light. However, the RNFL is not the only structure within the eye to possess birefringent qualities – the cornea and the lens also have this property. The variable corneal compensation (VCC) adaptation of the machine customises individual scans to account for corneal/lens birefringence based on measurements of the macula (which exhibits radially symmetric birefringence). An advantage of this technology is the lack of requirement for a reference plane.

Older versions of the GDx with fixed corneal compensation (FCC) have displayed areas under receiver operating characteristic curve in detecting glaucoma of 0.81 to 0.94.[119, 124, 129] Another study found sensitivity of 96% with specificity of 93%.[130] Variable corneal compensation has been found to significantly increase the diagnostic performance of the GDx.[131] In comparison with other technologies, one study found no difference between the best performing parameter of GDx VCC, OCT and HRT in detecting glaucoma. [112] Another study found that whilst areas under the receiver operating characteristic curves did not differ significantly between the technologies, sensitivities tended to be lower using the GDx.[113]

1.7 Rationale For This Study

To date there have been no studies using HRT to examine ONH morphometry specifically in the elderly. This is significant since the majority of patients with acquired glaucoma are aged over 60 years.[132] If glaucoma is to be detected,

then a more informed definition of 'normal' within this age group is required. In addition, most HRT studies' recruitment of subjects was opportunistic and not population-based. Even when clinically examined to exclude disease, volunteers recruited as 'normals' may represent a biased sample of normality. If the potential role of HRT examination in screening for glaucoma at a population level is to be quantified then the present limitations within the literature of age relevance and sampling methodology need to be addressed.

Both the FSM and RB LDFs, together with the MRA, MLCs and statistical shape analysis offer statistical means of discriminating normal from glaucoma. Since these techniques rely on the integrity of the normal range data, it is significant that previous larger-scale normal subject samples have not been population-based, with a mean age well below the age profile of glaucoma patients,[17, 133-137] the majority of whom are aged over 60 years.[132]They have yet to be tested on a population-based sample of elderly subjects, the most important age group to be targeted in screening for glaucoma. The BEAP recruited only subjects over the age of 65 years, and employs a robust population-based sampling methodology. BEAP therefore offers an opportunity to address the limitations outlined above.

2.1 Aims

1. Establish normative data for optic nerve head (ONH) morphology using HRT II scanning of a population-based sample of normal elderly subjects. Describe the effects of demographic variables and optic disc size on normal ONH morphology.
2. Establish normative asymmetry data for ONH morphology in the sample of normal elderly subjects. Describe the effects of demographic variables and optic disc size on normal asymmetry of ONH morphology.
3. Establish the specificity of current HRT II diagnostic algorithms in the sample of normal elderly subjects. Describe the effects of demographic variables and optic disc size on specificity.
4. Investigate inter- and intra-observer variability induced by different observers placing the ONH contour on HRT images. Describe the relative effects of variability upon different topographic parameters.
5. Model normal variability of rim area using multiple linear regression techniques to create a diagnostic algorithm to discriminate between normal and glaucomatous optic neuropathy (GON).
6. Employ normative asymmetry data to create a diagnostic algorithm to discriminate between normal and GON.
7. Develop a diagnostic algorithm to discriminate normal from GON by comparing the superior and inferior hemidiscs (analogous to the Glaucoma Hemifield Test).
8. Investigate whether the three diagnostic algorithms described above may be usefully combined to enhance diagnostic utility on a uniocular and binocular basis.

3.0 Methodology of the Bridlington Eye Assessment Project

3.1 Methodology of the Bridlington Eye Assessment Project

3.1.1 Inception and Organisation of the Project

The Bridlington Eye Assessment Project was conceived by Mr SA Vernon (Consultant Ophthalmologist at Queen's Medical Centre, Nottingham) and Drs JG Hillman and HK MacNab (General Practitioners, Bridlington). The primary purpose was to investigate the utility of screening for eye disease in the elderly and the Project was offered to the community of Bridlington both as a service and a research exercise. The elderly population of Bridlington is relatively stable with little migration and therefore offered an ideal opportunity for a screening project. The Project is organised by a Project Manager and administered by two receptionists. The Project is a registered charity (Charity No. 1091980) with a board of Trustees. Further staff employed by the project are one registered nurse, and four local optometrists. A local research ethics committee application was approved for all methodology of the Project which adhered to the tenets of the Declaration of Helsinki guidelines for research in human subjects.

3.1.2 Eligibility Criteria

All individuals registered with a General Practitioner in Bridlington and aged at least 65 years on the 5th November 2002 were eligible for examination by the Project. Subjects known to be registered blind or partially sighted, bed-bound or with significant dementia, and those moving into or out of the area during the study were excluded. Subjects were invited by letter on a street-by-street basis in ascending numerical order of postcode. When contacted, each subject was invited to telephone the Project to make an appointment to be examined. Apart from two subjects examined, all individuals were Caucasian. The Project saw its first subject on 5/11/2002 and had seen 1246 subjects at the start of this research in January 2004. To date the Project has examined just over 3000 subjects. Informed consent was obtained from all participants. Chapters 4-8 are based on normal subjects selected from the first 1246 subjects examined by January 2004. When the work for chapters 9-11 was undertaken further subjects had been examined by the Project and thus a total of 880 normal subjects

selected from the first 2065 individuals examined by the Project were included. A flowchart detailing subject recruitment for the entire BEAP is given in Figure 1.

3.1.3 Examination Scheme

A trained nurse obtained a relevant standardized medical history (diabetes, stroke, hypertension) together with the subject's drug history. Distance and reading spectacle requirements were noted in addition to any history of amblyopia, ocular surgery, or any other ocular disease. Specifically, any history of glaucoma, diabetic retinopathy, or macular degeneration was noted. Family history of glaucoma was determined, together with the subject's driving status and social circumstances. Uncorrected, corrected and pinhole logMAR visual acuity was then obtained (Bailey Lovie #4 Chart, National Vision Research Institute of Australia). The subject was then examined by one of four optometrists trained specifically for the project. Each of the four optometrists provided their services to the project on a daily rotational basis. Standardized slit lamp examination of the anterior segment and Goldmann applanation tonometry was performed. Following instillation of dilation drops, automated visual field analysis was then performed by the Henson Pro 5000 perimeter with software version 3.1.4 (Tinsley Instruments, Croydon, UK). A single stimulus, supra-threshold central 26 point test was employed. This was automatically extended to a 68 point test if a defect was detected. Lens opacities were classified using the Lens Opacities Classification System III (LOCS III).[138] The optic disc, macula, and peripheral retina were then specifically examined using slit lamp biomicroscopy with 90D lens. Decisions on appropriate further management of the subject were made before high-resolution digital fundus photographs (Topcon TRC NW6S, Topcon, Tokyo, Japan) and Heidelberg Retina Tomograph II images (HRT II, Software Version 2.01, Heidelberg Engineering GmbH, Dossenheim, Germany) were obtained. All history and examination findings were systematically noted on a specific proforma. If the clinical findings warranted further action, a specific proforma was used to arrange referral to the appropriate provider (optician, general practitioner, Hospital Eye Services) stating the reason for referral. Where subjects were referred to Hospital Eye

Services a proforma was provided for the reviewing clinician to complete with details of the diagnosis and further management.

Data collected were entered onto an Excel spreadsheet by a receptionist dedicated to the task. Data were entered in identical format to the proforma. Any questionable proforma entries were flagged for interpretation by MJH. After several hundred data entries one in 10 entries was checked for accuracy which was found to be 99%.

Figure 1. Flow chart of subject recruitment by BEAP

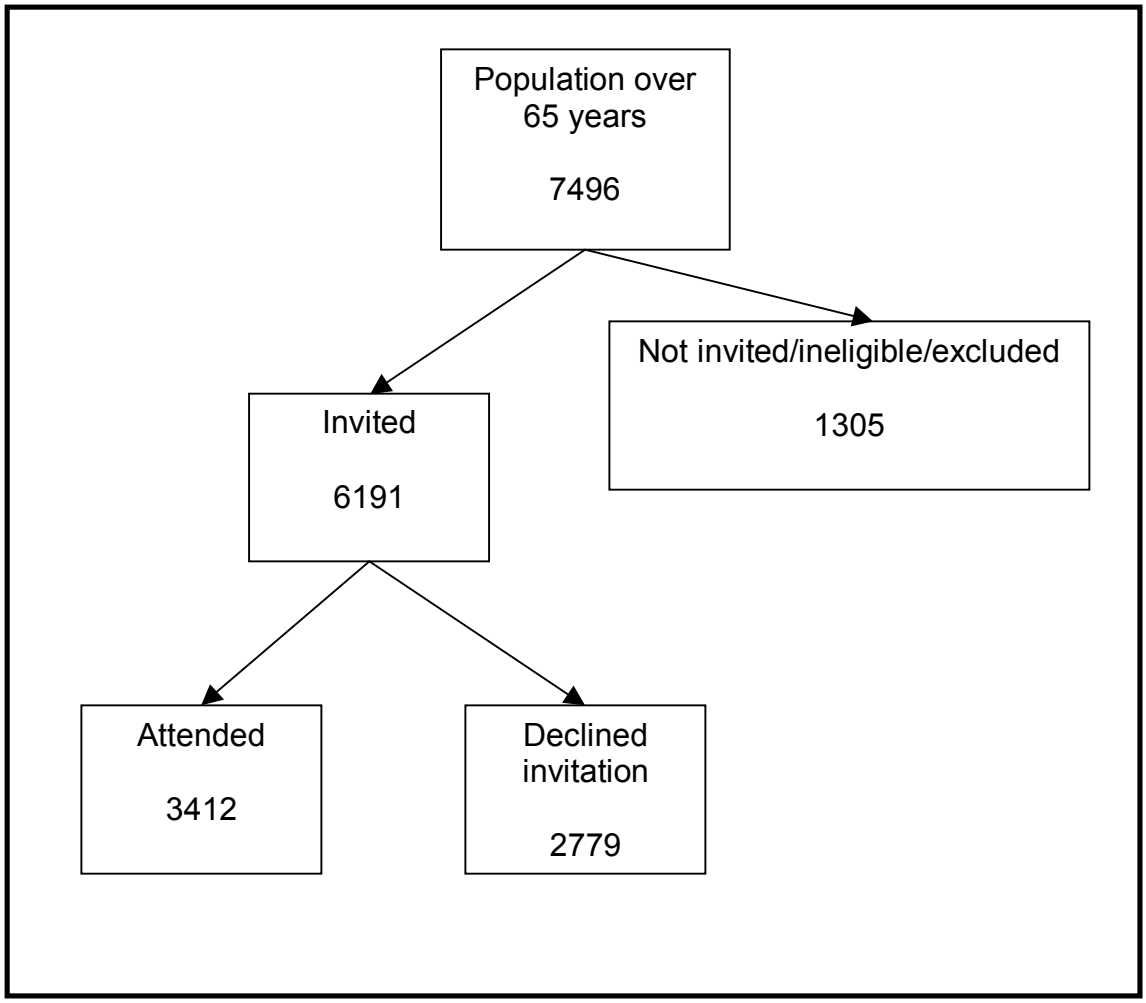

3.1.4 Acquisition of HRT II Images

Subjects were imaged with HRT II, with the scanner's focus being adjusted according to the subject's refraction, and to obtain the best image. One mean topographic image was acquired per eye. Much of the acquisition process using HRT II is automated. If the machine stated that astigmatism was significantly impairing the image then the image was obtained through the subject's spectacles. If the image acquired was visually unacceptable then the process was repeated to obtain an acceptable image, although this was not possible in a minority of subjects.

3.1.5 Further Analysis of HRT II Images

The optic disc contour line was drawn by two investigators (MJH and GA) to mark the edge of the optic disc at the inner border of Elschnig's scleral ring. Each investigator underwent training in placing the contour line by the senior investigator (Mr SA Vernon). MJH also underwent instruction by GA. Contour lines were placed on separate database copies so that each investigator could not see the contour line drawn by the other. Contour line placement is based on subjective judgement and inevitably generates intrinsic variability. Using the mean parameter value attempts to reduce this variability, improving the applicability of the results beyond the individual investigator. Following contour placement HRT II calculated disc area (mm^2) and 12 further stereometric parameters. The parameters were cup area (mm^2), rim area (mm^2), cup-to-disc area ratio, rim-to-disc area ratio, cup volume (mm^3), rim volume (mm^3), mean cup depth (mm), maximum cup depth (mm), height variation contour (mm), cup shape measure, mean retinal nerve fibre layer (RNFL) thickness (mm) and RNFL cross-sectional area (mm^2). Each of these parameters was expressed for the global disc, and for 6 individual disc sectors (temporal, temporal superior, temporal inferior, nasal, nasal superior, nasal inferior). Each parameter was expressed as a mean between the two investigators.

The average variability (MPHSD) of the three HRT images comprising the mean topographic image was 34 microns. Due to the large range of MPHSD (0 to 258

microns) discs with the largest 10% of average variability were excluded on a subject-wise (eye pair) basis (a further 91 subject exclusions). The maximum MPHSD was then 68 microns, with a mean (SD) of 26.8 (13.3) microns. This was comparable to previous investigations and gave acceptable data quality for the purposes of generating a reference range.[17]

3.1.6 Definition and Selection of Normal Subjects

In this study, data from the first 1246 subjects were examined. 576 subjects were defined as normal for the purposes of this study with an intraocular pressure less than 22 mmHg in both eyes, a normal visual field determined by suprathreshold automated examination, and corrected logMAR acuity of at least 0.3 (Snellen equivalent 6/12). Good visual acuity was a requirement to produce a reliable visual field test. Subjects with a history of glaucoma, or use of ocular pressure-lowering treatment were excluded. Of the 576 normal subjects, a further 16 were excluded because of absent or visually unacceptable HRT II images. A further 10 subjects were excluded because splinter haemorrhages were observed clinically on one or both of their optic discs. Subjects were purposely not excluded on the basis of an optic disc clinically suspicious of glaucoma.

4.0 Laser scanning tomography of the optic nerve head in a normal elderly population

4.1 Introduction

The appearance of the normal optic nerve head can vary widely. This variability can cause expert observers of the optic disc to disagree in discriminating between normal and glaucoma.[118] The introduction of objective imaging of the disc promises to improve evaluation of optic nerve parameters by removing subjectivity. HRT II is a semi-automated confocal scanning laser system that provides reliable and reproducible three-dimensional imaging data of the optic nerve head.[55] If HRT II were to offer an acceptable screening modality for glaucoma it would need to demonstrate good discrimination between normal and disease, with high sensitivity and specificity. Previous studies have sought to define the normal range of HRT II optic nerve head parameters, and thus to define disease as "non-normal". Using this approach, the Moorfields Regression Analysis has generated specificities of 94-96% with lower sensitivities of 74-84%.[17, 100] An alternative statistical technique has been employed in which individual topographic measures are used as weighted predictor variables to generate a linear discriminant function separating glaucoma and normals.[61, 106, 108] However, this has failed to sufficiently improve discrimination for the purposes of mass screening, which in a population setting requires sensitivity and specificity to be very high to avoid significant numbers of false positives and false negatives. Since these techniques rely on the integrity of the normal range data, it is significant that previous larger-scale normal subject samples have not been population-based, with a mean age well below the age profile of glaucoma patients,[17, 133-137] the majority of whom are aged over 60 years.[132] Data obtained from subjects screened by BEAP are presented. The purpose of this study was to generate reference range data for the HRT II optic nerve head parameters on a population-based sample of normal elderly subjects.

4.2 Methods

4.2.1 Subjects: The Bridlington Eye Assessment Project

The selection and examination of subjects is described in Chapter 3. This study was performed using the first 1246 subjects to be examined by BEAP, of whom 576 were defined as normal.

4.2.2 Quality of HRT II Images

The average variability (SD) of the three HRT images comprising the mean topographic image was 34 microns. Due to the large range of average variability (0 to 258 microns) discs with the largest 10% of average variability were excluded on a subject-wise (eye pair) basis (a further 91 subject exclusions). The maximum average variability was then 68 microns, with a mean (SD) of 26.8 (13.3) microns. This was comparable to previous investigations and gave acceptable data quality for the purposes of generating a reference range.[17]

4.2.3 Data Analysis

Optic nerve head parameters were analysed using SPSS for Windows version 12.0 (Statistical Package for Social Sciences, SPSS, Inc, Chicago, Illinois). Parameter indices were assessed visually for normality using histograms and objectively using the Kolmogorov-Smirnov test. As expected, all parameters produced a bell-shaped distribution apart from those related to the cup area and volume (which has a minimum value of zero and is not therefore normally distributed). Nearly all parameters with a bell-shaped distribution showed significant departure from normality with the Kolmogorov-Smirnov test. For this reason, and because parameter comparisons could not be truly classified as paired or independent, the Mann-Whitney U test was used assess significance of differences in parameters between right and left eyes, and between males and females. Two-tailed tests were used throughout. With a large dataset which was not found to be normally distributed, the 95th and 99th percentile limits of normality (reference range) are employed.

Linear regression analysis was used to determine which variables were related to disc area. In no case was R^2 greater than 0.37. Thus, with relatively small

dependent effects, and non-normally distributed data, Spearman's rank correlation was used to assess the *relative* strength of relationship between disc area and the ONH parameters. The effect of age on global disc parameters was assessed using the Kruskal-Wallis test by dividing the sample into quartiles based on age. Statistical significance for this study was set at the 5% level. However, for multiple comparisons amongst the 12 HRT parameters a Bonferroni correction was applied with resulting significance at $p<0.004$.

4.3 Results

4.3.1 Demographics

A total of 918 eyes of 459 subjects were included in the study. All subjects were white and of European extraction. The mean age of the subjects (262 female and 197 male) was 72.6 years (SD 5.1), with a range of 65.5 – 89.3 years. The mean age of males and females was not significantly different (72.9 and 72.4 years respectively; $p=0.41$). Of those subjects who were excluded 57.0% were female. The mean age of excluded subjects was significantly higher than those who were included (75.0 vs. 72.6 years; $p<0.0001$).

4.3.2 Optic nerve head parameters

The mean disc area was 1.98mm^2 (SD 0.36). The mean, standard deviation, median, and 2.5th/97.5th and 0.5th/99.5th percentiles for all global parameters are presented in Table 2. Global disc area showed a bell-shaped distribution with a degree of positive skew. As expected, global cup area, and all cup-related variables did not show bell-shaped distributions (Figure 2). Table 3 shows the global disc parameters for each eye in the 459 subjects. Global height variation contour and cup shape measure were significantly different between the two eyes, although the differences in mean values were very small. When the effects of laterality were examined for each sex separately, differences approaching significance were observed in cup shape measure in males only (mean values –0.166 and –0.182 for right and left eyes respectively; $p=0.009$), and height variation contour in females only (mean values 0.372 and 0.397 for right and left

eyes respectively; p=0.008). No other significant differences contrary to those found in the global right/left and male/female analyses were observed.

Sex-related differences in some ONH parameters were observed. Rim volume, mean RNFL thickness, and RNFL cross-sectional area were significantly greater in females than males (P<0.001;Table 4). Correspondingly, cup area and volume, and cup/disc area ratio all tended to be smaller in females than males, though the differences were not statistically significant following the application of the Bonferroni correction. Given the consistent nature of the differences between males and females, the 5% and 1% reference ranges are quoted separately for these groups. There were clinically relevant differences in these normal range references between the sexes in the cup- and rim–related parameters.

Cup area was found to have the strongest association with global disc area (Table 5). All other parameters had small to moderate degrees of association apart from height variation contour. When subjects were divided into quartiles based on age, no significant effects of age were found for any ONH parameter, although global rim/disc area ratio and mean RNFL thickness tended to fall with increasing age, with a concurrent increase in cup area (Figure 3).

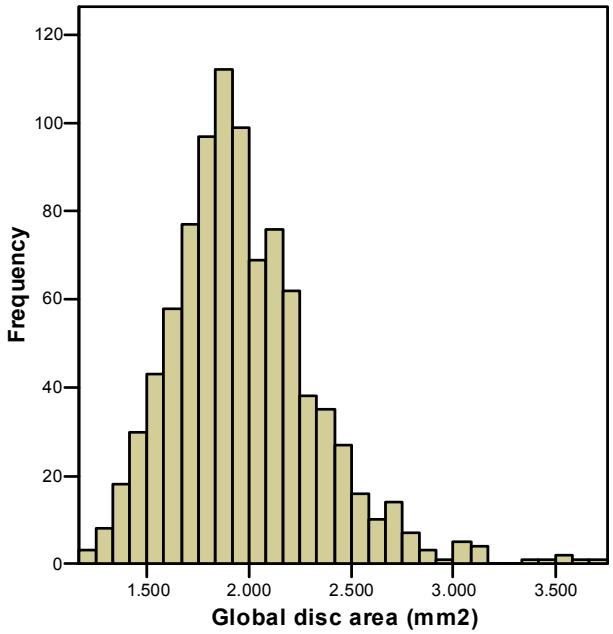

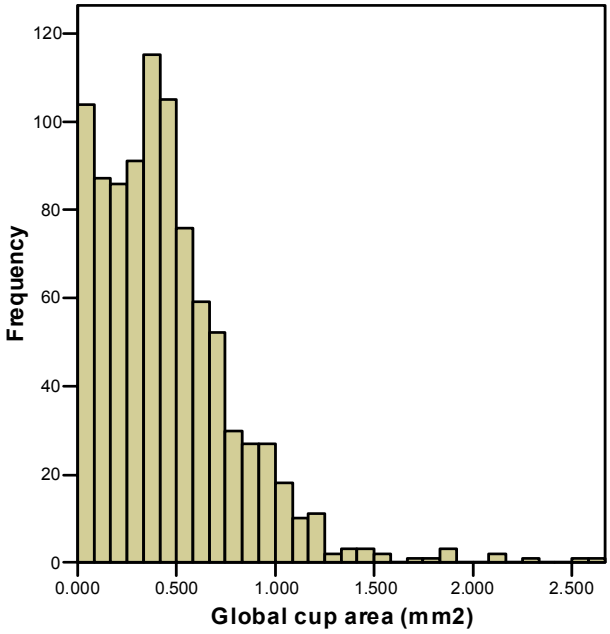

Table 2. HRT II measurements of the optic nerve head of 459 normal elderly subjects (n=918 eyes).

Global Parameter	Mean (SD)	Median	Range	2.5/97.5 percentiles	0.5^{th}/99.5^{th} percentiles
Disc area (mm^2)	1.98 (0.36)	1.93	1.20-3.73	1.40/2.81	1.28/3.49
Cup area (mm^2)	0.45 (0.35)	0.40	0.00-2.61	1.06*	1.79†
Rim area (mm^2)	1.52 (0.31)	1.49	0.32-3.34	1.03/2.24	0.58/2.65
Cup-to-disc area ratio	0.22 (0.14)	0.21	0.00-0.89	0.45*	0.62†
Cup volume (mm^3)	0.09 (0.11)	0.06	0.00-0.82	0.30*	0.52†
Rim volume (mm^3)	0.40 (0.15)	0.38	0.02-1.17	0.17/0.77	0.07/1.05
Mean cup depth (mm)	0.19 (0.08)	0.18	0.01-0.50	0.04/0.38	0.02/0.45
Maximum cup depth (mm)	0.52 (0.21)	0.51	0.02-1.36	0.12/0.97	0.06/1.19
Height variation contour (mm)	0.37 (0.10)	0.37	0.14-0.92	0.21/0.59	0.15/0.72
Cup shape measure	-0.18 (0.06)	-0.18	-0.38-0.05	-0.30/-0.06	-0.36/-0.02
Mean RNFL thickness (mm)	0.23 (0.07)	0.23	-0.08-0.48	0.09/0.35	0.04/0.41
RNFL cross-sectional area (mm^2)	1.11 (0.33)	1.12	-0.43-2.54	0.43/1.76	-0.17/2.03

* 95^{th} percentile (lowest value=0)
† 99^{th} percentile (lowest value=0)

Table 3. HRT II global optic disc parameters in 459 healthy elderly subjects' right and left eyes.

Parameter	Right eyes Mean (SD)	Right eyes 2.5/97.5 percentile	Left eyes Mean	Left eyes 2.5/97.5 percentile	*P*
Disc area (mm^2)	1.98 (0.35)	1.42/2.82	1.97 (0.36)	1.38/2.78	0.60
Cup area (mm^2)	0.46 (0.34)	1.06*	0.44 (0.36)	1.05*	0.12
Rim area (mm^2)	1.52 (0.31)	1.01/2.26	1.53 (0.31)	1.06/2.22	0.61
Cup-to-disc area ratio	0.22 (0.14)	0.46*	0.21 (0.14)	0.45*	0.12
Cup volume (mm^3)	0.09 (0.10)	0.29*	0.09 (0.11)	0.32*	0.28
Rim volume (mm^3)	0.39 (0.15)	0.15/0.77	0.41 (0.15)	0.19/0.81	0.04
Mean cup depth (mm)	0.19 (0.08)	0.04/0.36	0.19 (0.09)	0.04/0.38	0.46
Maximum cup depth (mm)	0.51 (0.21)	0.11/0.93	0.53 (0.22)	0.13/0.99	0.37
Height variation contour (mm)	0.36 (0.09)	0.20/0.55	0.39 (0.10)	0.21/0.62	0.001
Cup shape measure	-0.17 (0.06)	-0.30/ -0.06	-0.18 (0.06)	-0.31/-0.06	0.004
Mean RNFL thickness (mm)	0.22 (0.07)	0.08/0.35	0.23 (0.07)	0.10/0.36	0.23
RNFL cross-sectional area (mm^2)	1.10 (0.33)	0.41/1.76	1.13 (0.34)	0.47/1.77	0.44

*95^{th} percentile (lowest value=0)

Table 4. Sex-related differences in optic nerve head topography of a normal elderly population.

Parameter	**Males** (n=197) Mean (SD)	$2.5^{th}/97.5^{th}$ percentiles	$0.5^{th}/99.5^{th}$ percentiles	**Females** (n=262) Mean (SD)	$2.5^{th}/97.5^{th}$ percentiles	$0.5^{th}/99.5^{th}$ percentiles	*P*
Disc area (mm^2)	2.00 (0.37)	1.40/2.82	1.30/3.56	1.96 (0.34)	1.40/2.77	1.26/3.49	0.10
Cup area (mm^2)	0.49 (0.38)	1.16*	1.93†	0.42 (0.32)	0.98*	1.52†	0.02
Rim area (mm^2)	1.51 (0.32)	0.99/2.23	0.39/2.57	1.53 (0.30)	1.03/2.24	0.89/2.90	0.12
Cup-to-disc area ratio	0.23 (0.15)	0.47*	0.78†	0.21 (0.13)	0.43*	0.61†	0.02
Cup volume (mm^3)	0.10 (0.12)	0.32*	0.59†	0.08 (0.10)	0.27*	0.47†	0.02
Rim volume (mm^3)	0.38 (0.14)	0.15/0.72	0.02/0.92	0.41 (0.16)	0.17/0.84	0.11/1.05	<0.001
Mean cup depth (mm)	0.19 (0.09)	0.05/0.40	0.01/0.47	0.18 (0.08)	0.04/0.36	0.02/0.45	0.16
Maximum cup depth (mm)	0.53 (0.21)	0.14/0.98	0.04/1.28	0.51 (0.22)	0.11/0.96	0.07/1.16	0.20
Height variation contour (mm)	0.36 (0.09)	0.20/0.55	0.14/0.67	0.38 (0.10)	0.21/0.61	0.16/0.78	0.002
Cup shape measure	-0.17 (0.06)	-0.30/-0.06	-0.37/-0.02	-0.18 (0.06)	-0.30/-0.06	-0.34/-0.01	0.13
Mean RNFL thickness (mm)	0.21 (0.06)	0.08/0.33	-0.05/0.40	0.23 (0.07)	0.09/0.37	0.03/0.44	<0.001
RNFL cross-sectional area (mm^2)	1.06 (0.32)	0.42/1.60	-0.29/2.01	1.15 (0.34)	0.43/1.83	0.13/2.11	<0.001

* 95^{th} percentile (lowest value=0)
† 99^{th} percentile (lowest value=0)

Table 5. Spearman's rank correlation between optic nerve head topographic parameters and global disc area (n=918 eyes).

Parameter	r_s	P
Cup area (mm^2)	0.54	<0.0001
Rim area (mm^2)	0.47	<0.0001
Cup volume (mm^3)	0.45	<0.0001
Cup-to-disc area ratio	0.38	<0.0001
Mean cup depth (mm)	0.34	<0.0001
Cup shape measure	0.29	<0.0001
Maximum cup depth (mm)	0.25	<0.0001
Mean RNFL thickness (mm)	-0.15	<0.0001
RNFL cross-sectional area (mm^2)	0.14	<0.0001
Rim volume (mm^3)	0.12	<0.0001
Height variation contour (mm)	-0.03	0.31

Figure 3. Changes in global rim/disc area ratio between the four age quartile groups of 918 eyes of 459 normal elderly subjects.

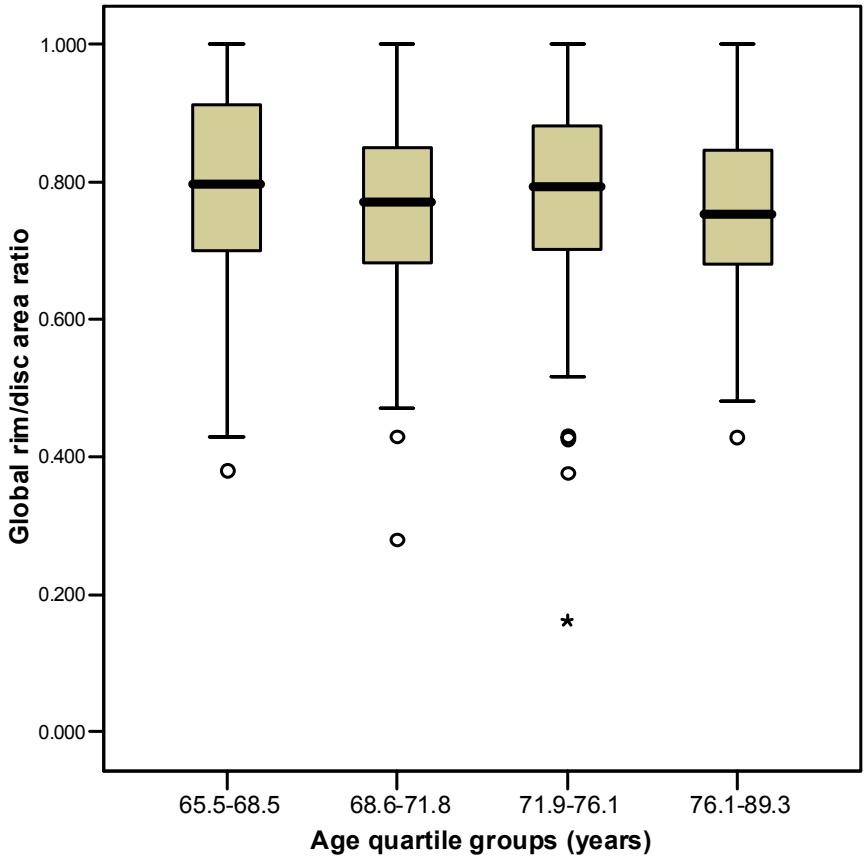

Table 6. HRT II measurements of the optic nerve head of 397 normal elderly subjects (n=794 eyes) where both eyes produced images with MPSHD not greater than 50 microns.

Global Parameter	Mean (SD)	Median	Range
Disc area (mm^2)	1.97 (0.35)	1.93	1.20-3.63
Cup area (mm^2)	0.45 (0.34)	0.40	0.00-2.61
Rim area (mm^2)	1.52 (0.29)	1.49	0.40-2.78
Cup-to-disc area ratio	0.22 (0.14)	0.21	0.00-0.85
Cup volume (mm^3)	0.09 (0.11)	0.06	0.00-0.82
Rim volume (mm^3)	0.40 (0.14)	0.38	0.02-1.17
Mean cup depth (mm)	0.19 (0.08)	0.18	0.01-0.50
Maximum cup depth (mm)	0.52 (0.21)	0.51	0.02-1.36
Height variation contour (mm)	0.37 (0.09)	0.37	0.14-0.82
Cup shape measure	-0.18 (0.06)	-0.18	-0.38-0.05
Mean RNFL thickness (mm)	0.23 (0.06)	0.23	-0.08-0.48
RNFL cross-sectional area (mm^2)	1.13 (0.32)	1.12	-0.43-2.54

4.4 Discussion

Due largely to the overlap in ONH parameter ranges between normal and glaucoma, some previous studies have shown that HRT II has poor sensitivity as a screening modality for glaucoma and therefore these authors concluded that HRT II cannot currently be recommended for screening.[105, 139] On the other hand, other researchers have shown that HRT classifications techniques and stereophotograph assessment can detect optic disc topography abnormalities in glaucoma-suspect eyes before the development of standard achromatic perimetry abnormalities. These data support strongly the importance of optic disc examination for early glaucoma diagnosis.[102] Normal range data for optic

nerve head parameters measured by HRT II based on a large, population-based sample of elderly subjects is presented. With a mean age of 72.6 years, this sample is more representative of the glaucoma population than previous studies (mean age range 36-56 years[133, 134, 136, 137, 140]), and more pertinent to discriminant analyses attempting to separate normals and glaucoma. With this pragmatic purpose in mind, this study defined 'normal' based on visual field, intraocular pressure, and visual acuity, and not optic disc appearance.

This study has demonstrated consistent differences in optic nerve head parameters between the sexes. Females had significantly greater rim volume, and mean RNFL thickness and cross-sectional area, and tended to have a smaller cup area and volume, and cup/disc area ratio. There was no significant difference in mean age between males and females to account for the observed differences. The sex-related differences in cup-related parameters did not reach statistical significance, although non-parametric tests with a Bonferroni correction return a conservative result (increasing the risk of Type II errors).[141] It is noted that analyses performed using the unpaired Student's *t*-test (equality of variances not assumed) returned significant differences between the sexes for all cup and rim-related variables at the 0.5% level. Hermann *et al* found that rim volume was significantly greater in the right eye in females compared with males, though they found no other significant differences between the sexes.[133] This study did not reproduce their finding. Other studies have found no significant difference in parameters based on sex.[104, 142, 143] In contrast to this study, using digitized photographic optic disc images, Rudnicka *et al* found females to have smaller rim areas and larger cup areas (differences of marginal statistical significance).[144] Using stereoscopic optic disc images, Ramrattan *et al* found males to have significantly larger disc area and rim area.[145] These variations are not due to racial factors as nearly all subjects in these studies were Caucasian. The mean age of subjects in many of these previous studies was considerably lower than in this study. Given that elderly males have twice the prevalence of open angle glaucoma compared to females,[132] the findings of

smaller rim volumes and tendency to larger cup-related measurements in males than females may reflect the progression of a greater proportion of males towards glaucoma. Having found significant sex-related differences, for the purposes of using this data to distinguish normal and glaucoma, sex-specific normal ranges should be stated for HRT II optic nerve head parameters.

This study found significant differences between right and left eyes in height variation contour and cup shape measure. When the effects of laterality were examined for each sex, cup shape measure differed significantly only in males, and height variation contour differed significantly only in females. These differences, however, were small and of little clinical significance. A recent study found no systematic differences based on laterality [134], previous studies having found conflicting differences in mean RNFL thickness and cross-sectional area which were clinically small.[133, 136] To date, no consistent differences in optic nerve head parameters based on laterality have been demonstrated.

Although rim and nerve fibre-related measurements tended to decrease with age, a significant effect of age on ONH parameters was not found in this study. However, with a minimum age of 65 years, it is likely that the sample lacks power in detecting a significant effect without younger subjects for comparison. Using image analysis of stereoscopic disc photographs, another population-based study with a minimum age of 55 also detected no age effect on ONH parameters.[145] Studies with a larger age range have detected significant enlargement of cup measurements, with reduction in rim/nerve fibre layer measurements with increasing age.[133-135, 146, 147]

In common with previous research, this study has shown many ONH parameters to be dependent on disc size.[17, 134, 135] Height variation contour was found to be the only parameter independent of disc area. Cup shape measure, which Durukan *et al.* found to be independent of disc area[134], did have a significant association with disc area in this study. Whilst cup shape measure has shown

promise in glaucoma detection and progression[148, 149] any variability due to disc area will widen the confidence limits of normality.

Heidelberg Engineering recommend that images of low quality (MPHSD greater than 50 microns) should not be used in a follow-up (change) analysis. Even by excluding 10% of subjects with the greatest MPHSD, the maximum MPHSD in this sample was 68 microns. Although this should be considered as a limitation, it is not unexpected in this sample with a minimum age of 65 years. Previous studies have found that image variability increases with age,[71] and with the presence of cataract,[67] though the effect of cataract was much reduced by acquiring images through a dilated pupil. Exclusion of subjects with MPHSD over 50 microns would preferentially exclude more elderly subjects, and limit one of the main novelties of this study as an analysis of HRT II imaging in the elderly. Subjects were included on an eye-pair basis. Thus, a significant number of individuals would be lost (120 eyes in 60 subjects further excluded) if they were excluded because even one eye had a MPHSD over 50 microns. Subjects with the greatest 10% of MPHSD were therefore excluded to remove outlying subjects with MPHSDs not representative of the group as a whole. When the sample was re-analysed with subjects with a MPHSD over 50 microns excluded, all global parameter means and SDs remained essentially unchanged, with no significant differences caused by the new exclusion criteria (Table 6). It is anticipated that in a cross-sectional study the effect of MPHSD is less critical than in longitudinal studies due to the principal of regression to the mean. In this study only one mean topographic image was acquired per eye. The focusing dial of the machine was adjusted according to the subject's refraction, and to obtain the clearest image. Much of the acquisition process using HRT II is automated. If the machine stated that astigmatism was significantly impairing the image then the image was obtained through the subject's spectacles. If the image acquired was visually unacceptable then the process was repeated to obtain an acceptable image, although this was not possible in a minority of subjects. The causes of poor image quality are important, especially in this age group for the

reasons outlined above. It is possible that the use of previous drops and applanation tonometry reduced image quality. However, tonometry was performed before dilation, and HRT II image acquisition was not performed until at least 20 minutes after instillation of drops. The effects are therefore likely to have been minimal. Ultimately, significant numbers of subjects ineligible due to poor image quality will limit the usefulness of HRT II in screening for glaucoma in this age group with the highest prevalence of the disease. An analysis of the effect of image quality on observer agreement is given in Chapter 7.

Of 1246 subjects examined by BEAP, the definitions of normality have excluded the majority. This limitation of the study arises mainly from the lack of best corrected visual acuity using a contemporary refraction, and a large number of false positive suprathreshold visual field tests. In this elderly age group false positive fields are common, and represent a major hindrance to the use of visual field tests in screening for glaucoma. In this study, individual reading glasses were used when available. Otherwise, based on focimetry of the subject's spectacles, the optometrist recommended a spherical reading 'add' (wide lens spectacles) to be worn whilst performing the test. All subjects had received mydriatics prior to performing the visual field test. Whilst the effect of mydriasis is not expected to be uniform, in this elderly age group dilation reduces the effect of senile miosis on the visual field tests. This is especially relevant in the presence of cataract. With the minimum age of 65 years in the sample conferring significant presbyopia, significant variability due to reduced accommodation because of mydriasis is not anticipated. Overall, the visual field test conditions are likely to have produced some false positive abnormal results resulting in exclusion from the study. However, even with many exclusions of potentially "normal" subjects, this data provide a reference range of normality for HRT II parameters drawn from a population-based sample with an age range relevant to glaucoma. Further work will assess whether this new reference range utilising both eyes of normals can improve discrimination between normal and glaucoma.

5.0 Asymmetry In Optic nerve head morphology In A Normal Elderly Population

5.1 INTRODUCTION

The evaluation of neuroretinal rim morphology is key in the diagnosis of glaucoma. For glaucoma screening to be successful, an objective, reproducible evaluation of the neuroretinal rim would be required to achieve sufficiently high sensitivity and specificity. The Heidelberg retina tomograph (HRT) is a semi-automated confocal scanning laser system that provides reliable and reproducible three-dimensional imaging data of the optic nerve head (ONH).[55] However, previous studies that developed diagnostic criteria for glaucoma based on HRT parameters have failed to generate sufficient sensitivity and specificity for the purposes of mass screening,[17, 61, 100, 106, 108] which in a population setting requires sensitivity and specificity to be very high to avoid significant numbers of false positives and false negatives. Whilst specificities of over 95% can be achieved, sensitivities are universally lower, due largely to the wide overlap in HRT parameters between normal and glaucomatous optic discs.[105] Additionally, variability in optic nerve head parameters due to factors other than disease creates background "noise", reducing diagnostic facility. Variation in age,[133-135] sex,[150] disc area,[17, 134] refraction,[135] image acquistion,[72] and contour placement on the optic disc[57] have all been shown to influence ONH parameters.

Asymmetry of neuroretinal rim configuration is a well-recognised component in the diagnosis of glaucoma.[132] It is also a risk factor for progression of ocular hypertensive patients to glaucoma.[151] Asymmetry has the potential to reduce parameter variability by providing a measure which accounts for inter-individual variation due to factors such as age, sex, and disc size. Thus inter-individual comparisons in cross-sectional (diagnostic) studies may become more valid. In spite of this potential, we found only one study examining the usefulness of asymmetry measures in glaucoma diagnosis using HRT.[152] The authors constructed the RADAAR measure (rim area to disc area asymmetry ratio) and found it was significantly correlated with intraocular pressure and degree of glaucomatous optic nerve damage in glaucoma patients. However, they were

unable to test the ability of RADAAR to discriminate between normal and glaucoma in the absence of a suitable reference range developed on normal subjects.

The purpose of this study was to generate reference range data for asymmetry of HRT II optic nerve head parameters on a population-based sample of elderly subjects.

5.2 METHODS

5.2.1 Subjects: The Bridlington Eye Assessment Project

The selection and examination of subjects is described in Chapter 3. The dataset of normal subjects used in this study is the same as that described in Section 4.2.1. Images were selected according to image quality as described in Section 4.2.2.

5.2.2 Data Analysis

HRT II parameters for this study were derived as a mean value of parameters generated by the two individual investigators (MJH and GA). Parameter asymmetries were generated for all global parameters by subtracting the value of the smaller disc from that of the larger. Rim/disc area ratio asymmetries were also calculated, using the same method, for the global and six sectoral measures.

Optic nerve head parameters were analysed using SPSS for Windows version 12.0.2 (Statistical Package for Social Sciences, SPSS, Inc, Chicago, Illinois). The Mann-Whitney U test was used to assess significance of differences in parameters between males and females. To examine the effects of age on asymmetry, the sample was divided into age quartiles. The groups were divided at 68.5, 71.8, and 76.1 years. To examine the relationship between magnitude of difference in disc area and the asymmetry parameters, the sample was divided into quartiles based on disc area difference. The groups were divided at 0.07, 0.14, and 0.25 mm^2 difference. The Kruskal-Wallis test was used to assess

the significance of differences in parameters between the four age and disc area difference quartile groups. Spearman's rank correlation coefficient was calculated to investigate the relationship between mean intraocular pressure and central corneal thickness with each asymmetry parameter. Two-tailed tests were used throughout. Statistical significance was set at $p<0.05$.

5.3 RESULTS

5.3.1 Demographics

A total of 918 eyes of 459 subjects were included in the study. The mean age of the subjects (262 female and 197 male) was 72.6 years (SD 5.1), with a range of 65.5 – 89.3 years. The mean age of males and females was not significantly different (72.9 and 72.4 +/- 5.4 years respectively; p=0.41).

5.3.2 Asymmetry parameters

Mean (SD) and 5% percentile limits of normality for the right and left eyes of 459 normal elderly subjects are shown in Table 3. Rim volume, cup shape measure and height variation contour reached statistically significant levels of difference between eyes. The differences, however, were very small and clinically insignificant.

Figure 4 illustrates the distribution of values for the global rim/disc area ratio asymmetry parameter. The normal curve (with the same mean and standard deviation) is shown for reference. The values display a bell shaped distribution with significant positive kurtosis and departure from the normal distribution. The 5% and 1% limits of normality for the global and sectoral rim/disc area ratio asymmetry measures are given in Table 7. Figure 5 depicts global rim/disc area ratio asymmetry in males and females. The distribution of differences was similar in both sexes. There was no significant difference in any global or sectoral rim/disc area ratio asymmetry measure between the sexes or the four age quartiles (p>0.05). Figure 6 shows data distributions (box and whisker plots) for other selected global HRT II parameter asymmetries. The differences in data dispersion largely reflect differences in the data range of HRT II global

parameters. No significant difference in disc area asymmetry, or any of these other global HRT II parameter asymmetries was found between the sexes or the four age quartiles.

The median difference in disc area was 0.14 mm^2 (minimum and maximum differences were 0.00 and 0.64 mm^2 respectively). Increases in the difference in disc area (bigger disc – smaller disc) were significantly related to increases in the difference in global rim area (p<0.001;Figure 7). However, increasing disc area difference was related to only a small change in the magnitude of global rim/disc area ratio asymmetry of marginal significance (p=0.055). Table 8 compares the magnitudes of association between the difference in disc area and various asymmetry parameters by means of Spearman's rank correlation. The magnitude of asymmetry of rim area and cup area was positively associated with increasing disc area asymmetry. This relationship was a negative one for all rim/disc area ratio asymmetries. The magnitude of association with disc area asymmetry was much greater for the raw rim area and cup area asymmetries compared with the rim/disc area ratio asymmetry.

Mean (SD) intraocular pressure and central corneal thickness in the sample was 16.1 (2.5) mmHg and 543.5 (35.9) microns respectively. No statistically significant correlation existed between any of the asymmetry measures presented and mean IOP/CCT (p>0.05).

Figure 8 shows the distribution of vertical cup/disc ratio asymmetry graded clinically during the screening examination. There is a positive skew in the data indicating proportionately larger cup/disc ratios in larger discs. The median asymmetry value was 0 with 2.5^{th} and 97.5^{th} percentile limits of normality of –0.2 and +0.25 respectively. There was no significant difference in the amount of clinical cup/disc ratio asymmetry based on sex or between the difference in disc area quartile groups. Additionally, no significant difference in clinical cup/disc ratio was found between the sexes or the age quartiles.

Table 7. Difference in rim/disc area ratio (bigger disc – smaller disc) for global and sectoral measures of 918 eyes of 459 normal elderly subjects.

Rim/disc area asymmetry ratio	Mean (SD)	Median	2.5^{th}/97.5^{th} percentiles	0.5^{th}/99.5th percentiles
Global	-0.021 (0.097)	-0.016	-0.212/0.154	-0.431/0.379
Temporal	0.019 (0.155)	-0.011	-0.351/0.324	-0.614/0.420
Temporal/superior	-0.028 (0.151)	-0.020	-0.341/0.252	-0.672/0.507
Temporal/inferior	-0.023 (0.151)	-0.010	-0.331/0.261	-0.568/0.473
Nasal	-0.021 (0.104)	-0.001	-0.260/0.144	-0.484/0.439
Nasal/superior	-0.026 (0.126)	-0.008	-0.277/0.213	-0.643/0.418
Nasal/inferior	-0.012 (0.115)	0.000	-0.251/0.216	-0.407/0.299

Figure 4. Differe[illegible]) for 918 eyes of 459

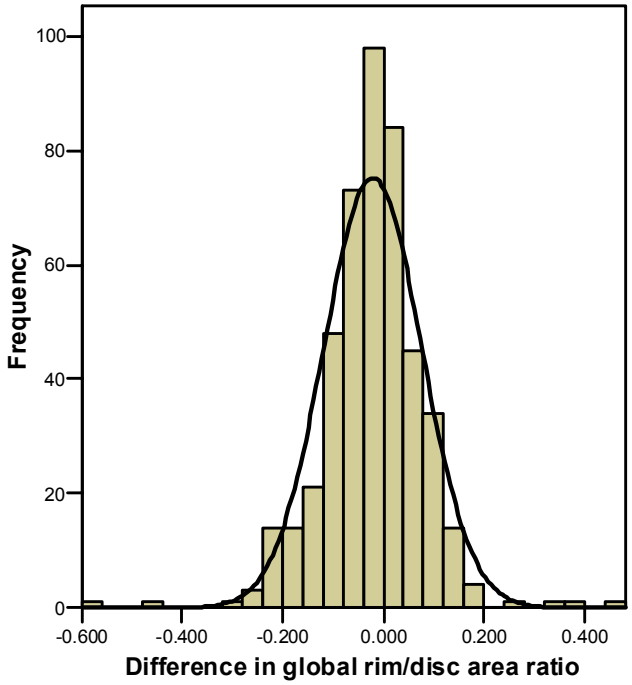

Figure 5. Difference in global rim/disc area ratio (bigger disc – smaller disc) in 197 males and 262 females in the normal elderly population.

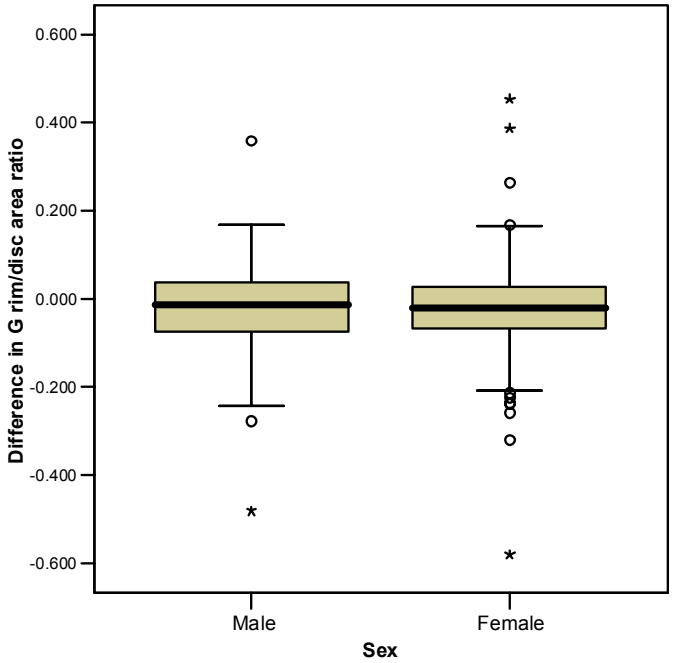

Figure 6. Box and whisker plots showing data distributions of various global HRTII parameter asymmetries (bigger disc – smaller disc) in 459 normal elderly subjects.

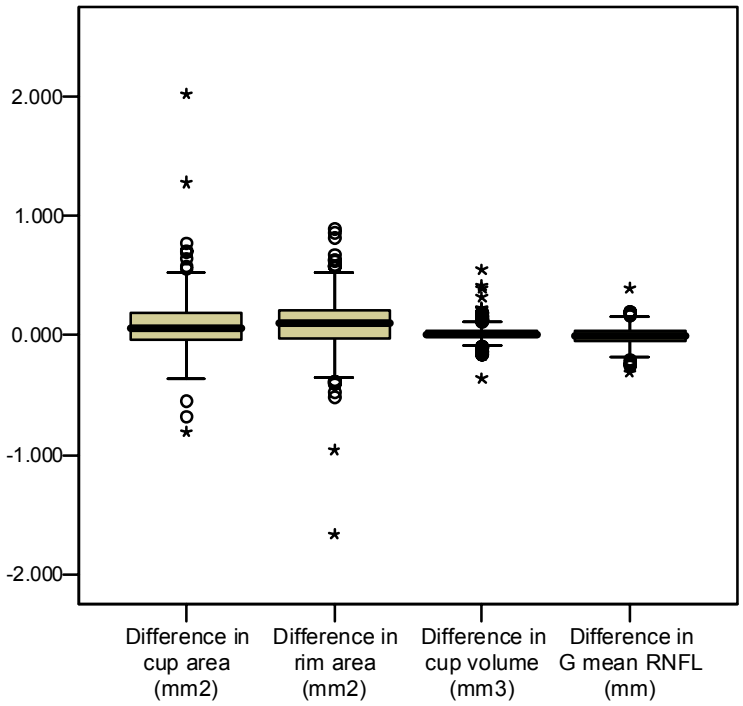

Figure 7. Box and whisker plots showing the differences in global rim area and global rim/disc area ratio (bigger disc – smaller disc) in relation to the difference in disc area (quartiles). Data drawn from 459 normal elderly subjects.

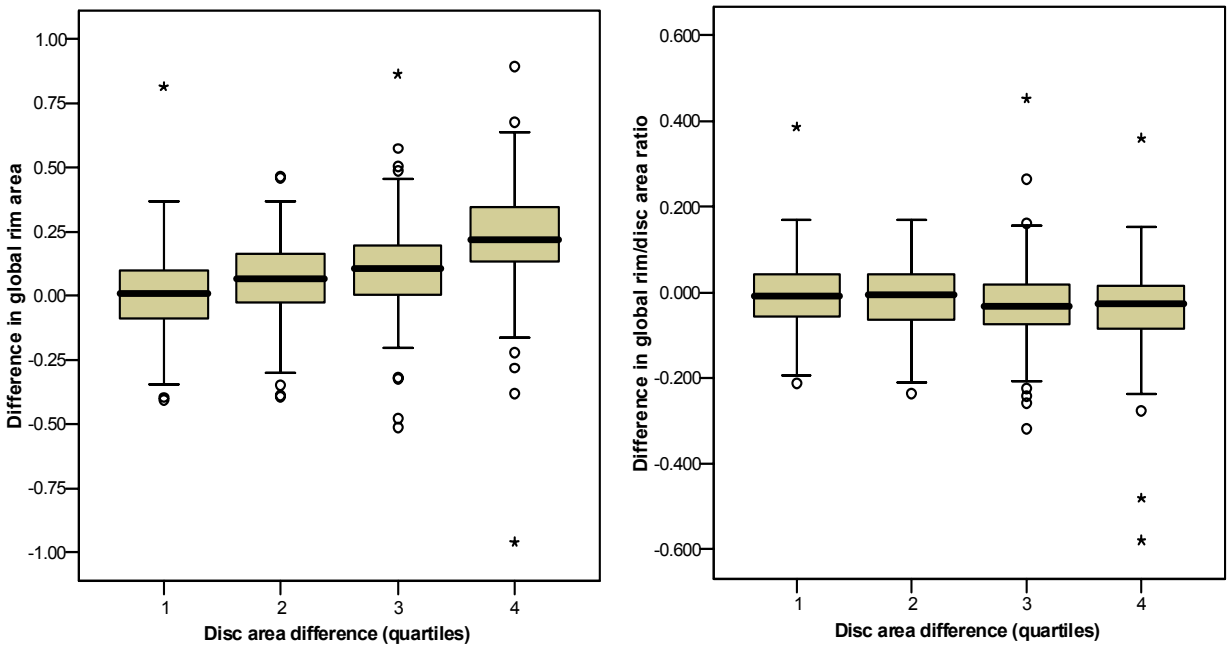

Table 8. Spearman's rank correlation between various asymmetry parameters (bigger disc – smaller disc) and difference in disc area in 459 normal elderly subjects.

Asymmetry parameter	r_s	P
Global rim area	0.41	<0.001
Global cup area	0.29	<0.001
Global cup volume	0.24	<0.001
Temporal-superior rim/disc area ratio	-0.15	0.002
Global rim/disc area ratio	-0.13	0.004
Temporal-inferior rim/disc area ratio	-0.10	0.03

(bigger disc – displayed for

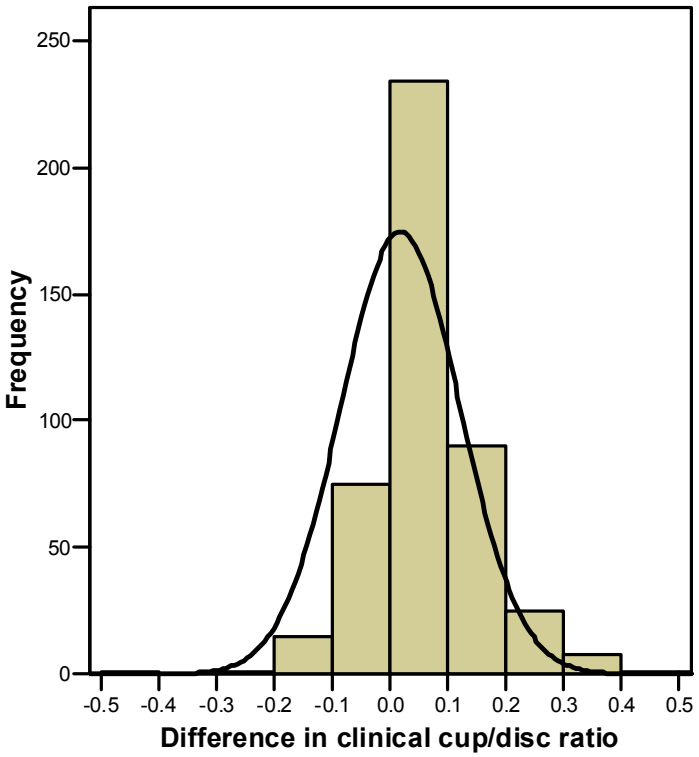

5.4 DISCUSSION

It has been previously demonstrated that HRT classification techniques and stereophotograph assessment can detect optic disc topography abnormalities in glaucoma-suspect eyes prior to the development of standard achromatic perimetry abnormalities. Thus, optic disc examination is very important in detecting early glaucoma.[102] However, variation due to factors such as disc size, sex, and age can have a significant effect on the quoted normal range of ONH parameters.[150] Thus, the specificity of various diagnostic functions based on HRT scanning has been found to decrease significantly with increasing disc size.[61, 104, 105] However, these factors seem to have much less of an effect on the normal limits of asymmetry than on the direct measurements for individual eyes. This study found no significant effect of variation in age or sex on asymmetry of cup or rim area or volume. Similarly, asymmetry of rim/disc area ratio was not affected by variation in age or sex. The major advantage of rim/disc area ratio asymmetry was in its relative immunity to the effects of variation in disc area asymmetry, compared with the absolute rim and cup measurements. This study found increasing disc area asymmetry to be much more strongly associated with changes in rim and cup asymmetry compared with rim/disc area ratio asymmetries. On this basis, rim/disc area ratio asymmetry is likely to be the most useful parameter in defining normality, and perhaps discriminating normal and glaucoma.

The choice of method in calculating asymmetry measures is important. Most of the previous studies calculating asymmetry parameters did so on a left/right basis,[133, 142, 153] though the recent study by Harasymowycz *et al.* used a bigger disc/smaller disc comparison.[152] It has been previously demonstrated that cup area increases to a larger degree than rim area with increases in disc size.[33] In this study's sample, comparison of the largest and smallest quartiles of disc size showed a relative increase in rim area of 1.30 with a corresponding relative increase in cup area of 2.91.[150] This difference needs to be handled consistently to generate well defined limits of normality for asymmetry. No systematic

difference in ONH measurements between right and left eyes was found. Asymmetry measures should therefore be calculated by comparing eyes on the basis of disc size, rather than laterality. The standard deviations of asymmetry measures in this sample calculated by subtracting the left eye value from the right eye value were up to 8% higher compared with the bigger disc minus smaller disc method (data not shown). In contrast with the RADAAR measure,[152] this study compared eyes not on a relative scale, but an absolute one. Comparing the results between eyes by division rather than subtraction results in a loss of potentially useful information.

Using a 90D Volk lens, the 95% limits of clinical vertical cup/disc ratio asymmetry were –0.2 to +0.25. These tolerances are similar to previous studies.[132, 153] The slight asymmetry in the limits may indicate that CDR estimation is biased by disc size, or simply reflect the finding that disc cups are proportionately larger in larger discs (as found with HRT).

The quality of the HRT image was a limitation in this study. Even by excluding subjects with the greatest MPHSD, the maximum MPHSD in this study was 68 microns. This issue was discussed in Section 4.4.

Generating a reference range for normality necessarily requires strict entry criteria, and it is likely that this study has falsely rejected a significant number of normals in order to maintain as pure a dataset as possible. It is very difficult to predict the effect of these exclusion criteria on the tolerances of normality for asymmetry parameters. This is the first study to generate a reference range for normal asymmetry based on HRT parameters in a large sample of normal, elderly subjects. It has been shown that the rim/disc area ratio asymmetry measure is likely to be the most useful parameter in describing normality with consistency. Further work will investigate whether it achieves sufficient precision in discriminating normal from glaucoma for the purposes of screening.

6.0 Specificity Of HRT II Diagnostic Algorithms In A Normal Elderly Population

6.1 Introduction

Primary open angle glaucoma remains a major cause of blindness in the world. The disease has a prolonged subclinical phase, with progressive loss of retinal ganglion cells that may go unnoticed before advanced visual field loss occurs. Detection of glaucoma in its early stages through analysis of the optic nerve head may therefore help to prevent significant morbidity. However, subjective evaluation of the optic disc, even by expert observers, has failed to generate sufficient agreement to be reliable in the diagnosis of glaucoma.[118, 154] The introduction of objective imaging of the optic disc promises to improve the evaluation of optic nerve parameters by removing subjectivity. One such system is the Heidelberg Retina Tomograph (HRT II) – a semi-automated confocal scanning laser system that provides reliable and reproducible three-dimensional imaging data of the optic nerve head.[55] Using this instrument the Moorfields Regression Analysis was developed to discriminate between normal and glaucomatous optic nerve heads.[17] Using a database of 112 eyes of 112 normal subjects with a mean age of approximately 57 years, linear regression analysis was performed to determine the 99% limit of normality for the log of the rim area corrected for disc size and age (Table 9). This method has generated specificities of 94-96%, with lower sensitivities of 74-84%,[17, 100] and has been shown to be more sensitive than expert clinical evaluation in detecting glaucoma.[101] Alternative statistical techniques called Linear Discriminant Functions (LDFs) have been developed by R Burk (RB LDF; Heidelberg Retina Tomograph II Operating Instructions, Dossenheim, Germany), and FS Mikelberg *et al.* (FSM LDF; Table 9).[106] Using datasets of normal and glaucomatous individuals, LDFs employ individual topographic measures as weighted predictor variables to generate the function. LDF values greater than zero are interpreted as normal, with values less than zero indicating disease. The FSM LDF was developed from a database of one eye of each of 45 normal subjects (mean age 51.6) and 46 patients with early glaucoma (mean age 61.2). This LDF has generated specificities of 84-90% and sensitivities of 64-89%.[100, 106-108] These diagnostic tools, which were developed on individuals with a mean age less than

60 years, have yet to be tested on a population-based sample of elderly subjects, with an age profile which better reflects the rising prevalence of glaucoma in age groups over 60 years.[132] Even with the greater prevalence of glaucoma in the elderly, glaucoma is still considerably less prevalent than non-glaucoma. A successful screening test for the disease should therefore have a high specificity to avoid generating a significant number of false positives.

This study aimed to investigate the diagnostic performance of the MRA and RB and FSM LDFs in the sample of normal subjects from BEAP. It also aimed to describe the level of diagnostic agreement between two investigators (MJH and GA) separately placing the contour on the same image obtained from each subject.

Table 9. The Moorfields Regression Analysis and Linear Discriminant Functions formulae.

Diagnostic tool	Formula
MRA*	Rim area = 1.021 + 0.443 x disc area - 0.006 x age
RB LDF†	F = 4.197 x (contour line height difference temporal - temporal superior) + (5.642 x contour line height difference temporal - temporal inferior) - (3.885 x temporal superior cup shape measure) - 0.974
FSM LDF‡	F = (rim volume x 1.95) + (height variation contour x 30.12) – (corrected cup shape x 28.52) – 10.08, where corrected cup shape = cup shape + [0.0019 x (50 – age)]

* Moorfields Regression Analysis[106]
† R Burk Linear Discriminant Function (Heidelberg Retina Tomograph II Operating Instructions, Dossenheim, Germany)
‡ FS Mikelberg Linear Discriminant Function

6.2 METHODS

6.2.1 Subjects: The Bridlington Eye Assessment Project

The selection and examination of subjects is described in Chapter 3. The dataset of normal subjects used in this study is the same as that described in Section 4.2.1. Images were selected according to image quality as described in Section 4.2.2.

6.2.2 Moorfields Regression Analysis and Linear Discriminant Functions

Using a built-in diagnostic function HRT II categorised the optic disc by comparing the percentage share of rim area and cup area (globally, and for each segment) with the percentage share of rim area predicted by the Moorfields Regression Analysis. Diagnostic categories used were: 'Within normal limits' if the percentage share of rim area was greater than or equal to the 95% limit, 'Borderline' if it was between the 95% and 99.9% limit, and 'Outside normal limits' if it was below the 99.9% limit. These categories were returned for each disc sector, globally, and as a summary category. The summary category was an overall classification equal to the category of the

worst global or sector category. It is notable that some of the optic discs in the BEAP sample were larger than the largest disc in the normal database. This will reduce the reliability of the MRA's diagnostic accuracy.

The HRT software also calculated the Linear Discriminant Functions according to Burk and Mikelberg (Table 9). Positive values indicated a normal disc, and negative values indicated a diseased disc. 2 discs in the sample returned a value of zero for investigator 1 and were therefore unable to be classified.

6.2.3 Data Analysis

One eye was chosen randomly from each of the 459 subjects included in the study. All data were analysed using SPSS for Windows version 12.0.2 (Statistical Package for Social Sciences, SPSS, Inc, Chicago, Illinois). HRT II optic disc parameters for this study were derived as a mean value of parameters generated by the two individual investigators. The Mann-Whitney U test was used to assess significance of differences in parameters between males and females and between right and left eyes. To examine the effects of disc size and age on the results of the diagnostic functions, the sample was divided into quartiles on the basis of disc area and age respectively. The strength of linear association between these quartiles and the diagnostic categories returned was assessed using the Chi squared test for trend. Although the value of X^2 for trend will always be less than X^2 for the overall comparison, this is a powerful method of analysis because the test statistic occupies a distribution with one degree of freedom rather than the *k*-1 degrees of freedom for the standard X^2 test. If most of the variation is due to a trend across the groups, then the test for trend will yield a much smaller P value. The strength of directional association was assessed using Somers' d. This is a measure of association between two ordinal variables that ranges from –1 to 1. Values close to an absolute value of 1 indicate a strong relationship between two variables, and values close to 0 indicate little or no relationship between the variables. The strength of agreement between the diagnostic categories generated by each investigator was assessed using Cohen's kappa, a measure used to evaluate how much

better than chance is the agreement between categorical assessments. Statistical significance was set at $p<0.05$ throughout.

6.3 RESULTS

6.3.1 Demographics

459 eyes of 459 subjects were included in the study. The mean age of the subjects (262 female and 197 male) was 72.6 years (SD 5.1), with a range of 65.5 – 89.3 years. The mean age of males and females was not significantly different (72.9 and 72.4 years respectively; $p=0.41$).

6.3.2 Heidelberg Retina Tomograph measurements

The results of optic nerve head imaging using HRT II in the 459 normal elderly subjects are given separately for each sex in Table 10. Females had larger rim-related measurements than males, males having larger cup-related measurements. No significant differences in rim- or cup-related measures were detected between right and left eyes. No significant difference in disc size based on sex or laterality was detected.

6.3.3 Moorfields Regression Analysis

The summary classifications by the Moorfields Regression Analysis (MRA) of the 459 optic discs of 459 elderly subjects are given for each investigator in Table 11. 83.2% and 83.0% of discs were classified as normal for investigators 1 (MJH) and 2 (GA) respectively. The classifications of individual disc sectors, and for the global disc, are given in Table 12. The classifications of optic discs by MRA are compared across the four disc area quartile groups for each investigator in Figure 9. The MRA was increasingly likely to return a 'borderline' or 'outside normal limits' result with larger disc area quartiles. The percentage of optic discs classified 'outside normal limits' in the smallest and largest disc area quartiles was 0.9% and 7.0%, and 0.9% and 14.9% for Investigators 1 and 2 respectively. The association between MRA classification and disc area quartile groups was found to be significant for Investigators 1 and 2 (X^2_{trend} =13.2 and 23.5 respectively, $p<0.001$). The strength of directional association was assessed using Somers' d and found to be similar for the two investigators (0.23

and 0.29 for investigator 1 and 2 respectively; $p<0.001$). The classification of optic discs by MRA (Investigator 2) are compared across the four disc area quartiles for each sex in Figure 10. In males, a marked increase in classification as 'borderline' and 'outside normal limits' was seen in larger disc area quartile groups (X^2_{trend} =21.6, $p<0.001$). In females this trend was not significant (X^2_{trend} =2.9, p=0.09; Somers' d=0.40, *p<0.001* and 0.13, p=0.21 in males and females respectively). Similar results were obtained by Investigator 1. No statistically significant linear association between MRA classification and age quartile groups was detected (X^2_{trend} =0.11, p=0.74). Table 13 is a crosstabulation examining the agreement between the two investigators in MRA classification. There were a minority of cases of outright disagreement over normality, and overall inter-rater agreement was only moderate (Cohen's kappa(SE)=0.54(0.05), $p<0.001$). Agreement was most substantial in the temporal/superior sector (κ=0.78(0.08), $p<0.001$), and tended to be greater in this sector than the temporal and temporal/inferior sectors (κ=0.61(0.12), and 0.48(0.08), $p<0.001$ respectively). Agreement in the nasal, nasal/superior and nasal/inferior sectors was similar (κ=0.59(0.08), 0.53(0.08) and 0.58(0.06), all $p<0.001$ respectively). When 'borderline' cases were treated as test negative, agreement was slightly worse (κ=0.48(0.10); $p<0.001$); when 'borderline' cases were treated as test positive, agreement improved (κ=0.64(0.05); $p<0.001$).

Table 10. Optic nerve head measurements using HRT II in a normal elderly population (197 males and 262 females).

Parameter	**Males** (n=197) Mean (SD)	2.5th/97.5th percentiles	0.5th/99.5th percentiles	**Females** (n=262) Mean (SD)	2.5th/97.5th percentiles	0.5th/99.5th percentiles	*P*
Disc area (mm^2)	1.99 (0.38)	1.38/3.00	1.22/3.56	1.95 (0.33)	1.39/2.79	1.23/3.40	0.20
Cup area (mm^2)	0.50 (0.39)	1.16*	2.51†	0.41 (0.30)	0.96*	1.51†	0.05
Rim area (mm^2)	1.50 (0.32)	1.00/2.23	0.32/2.53	1.53 (0.29)	1.06/2.16	0.93/2.95	0.15
Cup-to-disc area ratio	0.24 (0.15)	0.47*	0.84†	0.20 (0.13)	0.43*	0.59†	0.04
Cup volume (mm^3)	0.10 (0.12)	0.32*	0.65†	0.08 (0.10)	0.27*	0.39†	0.06
Rim volume (mm^3)	0.37 (0.12)	0.15/0.66	0.02/0.72	0.42 (0.15)	0.18/0.82	0.13/1.06	0.002
Cup shape measure	-0.17 (0.07)	-0.35/-0.05	-0.38/-0.03	-0.18 (0.06)	-0.30/-0.06	-0.33/0.02	0.13
Mean RNFL thickness (mm)	0.21 (0.06)	0.10/0.33	-0.03/0.39	0.24 (0.07)	0.10/0.37	0.08/0.47	<0.001
RNFL cross-sectional area (mm^2)	1.05 (0.29)	0.49/1.61	-0.18/1.83	1.17 (0.32)	0.53/1.78	0.37/2.39	<0.001

* 95th percentile (lowest value=0)
† 99th percentile (lowest value=0)

Table 11. Summary classification by the Moorfields regression analysis (MRA) of 459 optic nerve heads of 459 normal elderly subjects when contoured by two different investigators.

MRA Result (%)	Investigator 1	Investigator 2
Within normal limits	83.2	83.0
Borderline	12.9	11.3
Outside normal limits	3.9	5.7

Table 12. Summary classification of the different disc sectors by the Moorfields Regression Analysis (MRA) of 459 optic nerve heads of 459 normal elderly subjects. Results are shown for the global disc analysis and individual disc sectors for the two investigators (investigator 2 in parentheses).

MRA Result (%)	Global	Temporal	Temp/Sup	Temp/Inf	Nasal	Nasal/Sup	Nasal/Inf
Within normal limits	97.4 (95.6)	97.2 (98.3)	97.8 (97.2)	95.6 (92.2)	95.6 (94.3)	93.7 (93.7)	91.1 (90.0)
Borderline	2.0 (2.8)	2.4 (1.3)	0.9 (1.3)	3.3 (5.7)	3.1 (4.4)	5.7 (5.2)	7.0 (6.1)
Outside normal limits	0.7 (1.5)	0.4 (0.4)	1.3 (1.5)	1.1 (2.2)	1.3 (1.3)	0.7 (1.1)	2.0 (3.9)

Figure 9. Summary classification of 459 optic discs of 459 normal elderly subjects by the Moorfields Regression Analysis (MRA) according to disc area quartile groups. Results are shown for both investigators.

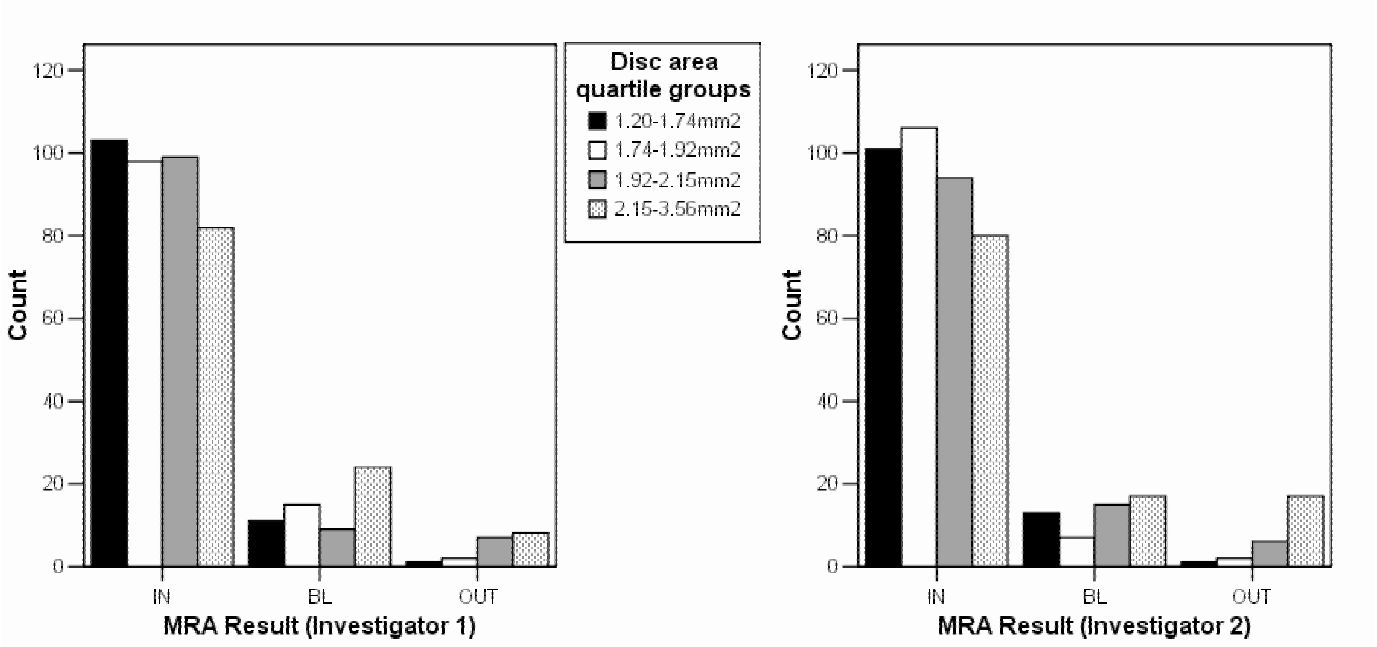

Figure 10. Summary classification of 459 optic discs of 459 normal elderly subjects by the Moorfields Regression Analysis (MRA) according to disc area quartile and sex (197 males, 262 females). Results are shown for Investigator 2.

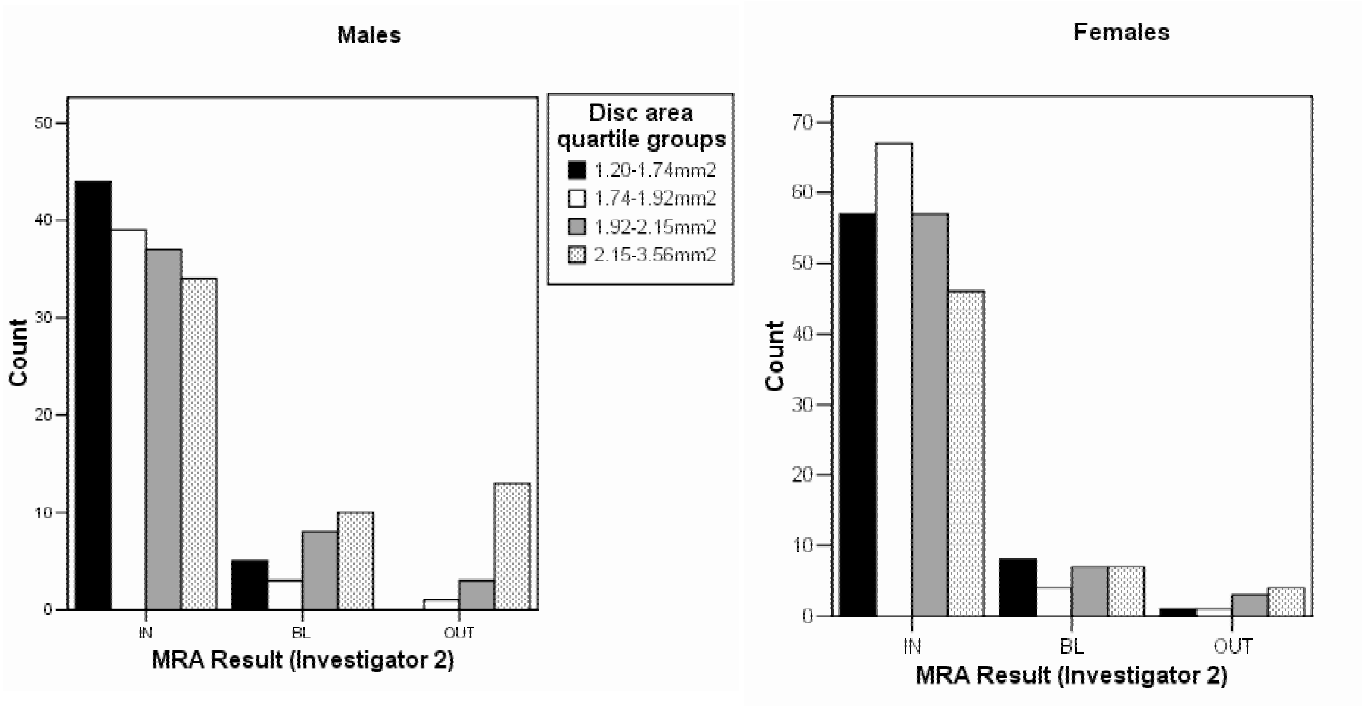

Table 13. Crosstabulation examining agreement between two investigators in summary classification of 459 optic discs of 459 normal elderly subjects using the Moorfields Regression Analysis (MRA).

		MRA Result (Investigator 2)			
		IN	BL	OUT	**Total**
MRA Result (Investigator1)	IN	358	20	4	382
	BL	20	28	11	59
	OUT	3	4	11	18
	Total	381	52	26	**459**

IN Within normal limits
BL Borderline
OUT Outside normal limits

6.3.4 Linear Discriminant Functions

Using the RB and FSM LDFs, investigator 1 classified 7.4% and 10.0% of discs as "disease" respectively. For investigator 2 the respective figures were 6.8% and 11.8%. Table 14 shows the crosstabulation examining agreement between the two LDFs for each investigator. The kappa statistics for investigator 1 and 2 respectively were 0.48(0.07; p<0.001) and 0.42(0.07; p<0.001). Figure 11 displays the classification of discs by both LDFs according to disc area quartiles in the two sexes for Investigator 2. For Investigator 2, the RB LDF classified 0.0% and 15.8% of male discs as diseased in the smallest and largest quartiles respectively (X^2_{trend} =9.8, *p*=0.02; Somers' d=0.46, *p*<0.001). Respective figures for female discs were 3.0% and 3.5%, the relationship between disc area quartile and diagnosis not being significant in this sex (X^2_{trend} =0.1, *p*=0.73). For the same investigator, the FSM LDF classified 10.2% and 19.3% of male discs as diseased in the smallest and largest quartiles respectively, although this trend was not significant (X^2_{trend} =1.98, *p*=0.16; Somers' d=0.16, *p*=0.16). Respective figures for female discs were 6.1% and 8.8%, representing a non-significant trend (X^2_{trend} =0.8, *p*=0.39; Somers' d=0.11, *p*=0.32). Similar results were obtained for Investigator 1. No statistically significant association was found between the results of any of the LDFs for either investigator and the age quartiles in this sample of subjects.

Table 14. Crosstabulation examining agreement between two investigators in classification of 459 optic discs of 459 normal elderly subjects by the R Burk (RB) and FS Mikelberg (FSM) Linear Discriminant Functions (LDFs).

Investigator 1 (458 discs)	*RB LDF*		**Investigator 2** (459 discs)	*RB LDF*	
FSM LDF	Normal	Disease	*FSM LDF*	Normal	Disease
Normal	399	13	Normal	394	34
Disease	25	21	Disease	11	20

Figure 11. Classification of 459 optic discs of 459 normal elderly subjects by the R Burk (RB) and FS Mikelberg (FSM) Linear Discriminant Functions (LDFs) according to disc area quartile and sex (197 males, 262 females). Results are shown for Investigator 2.

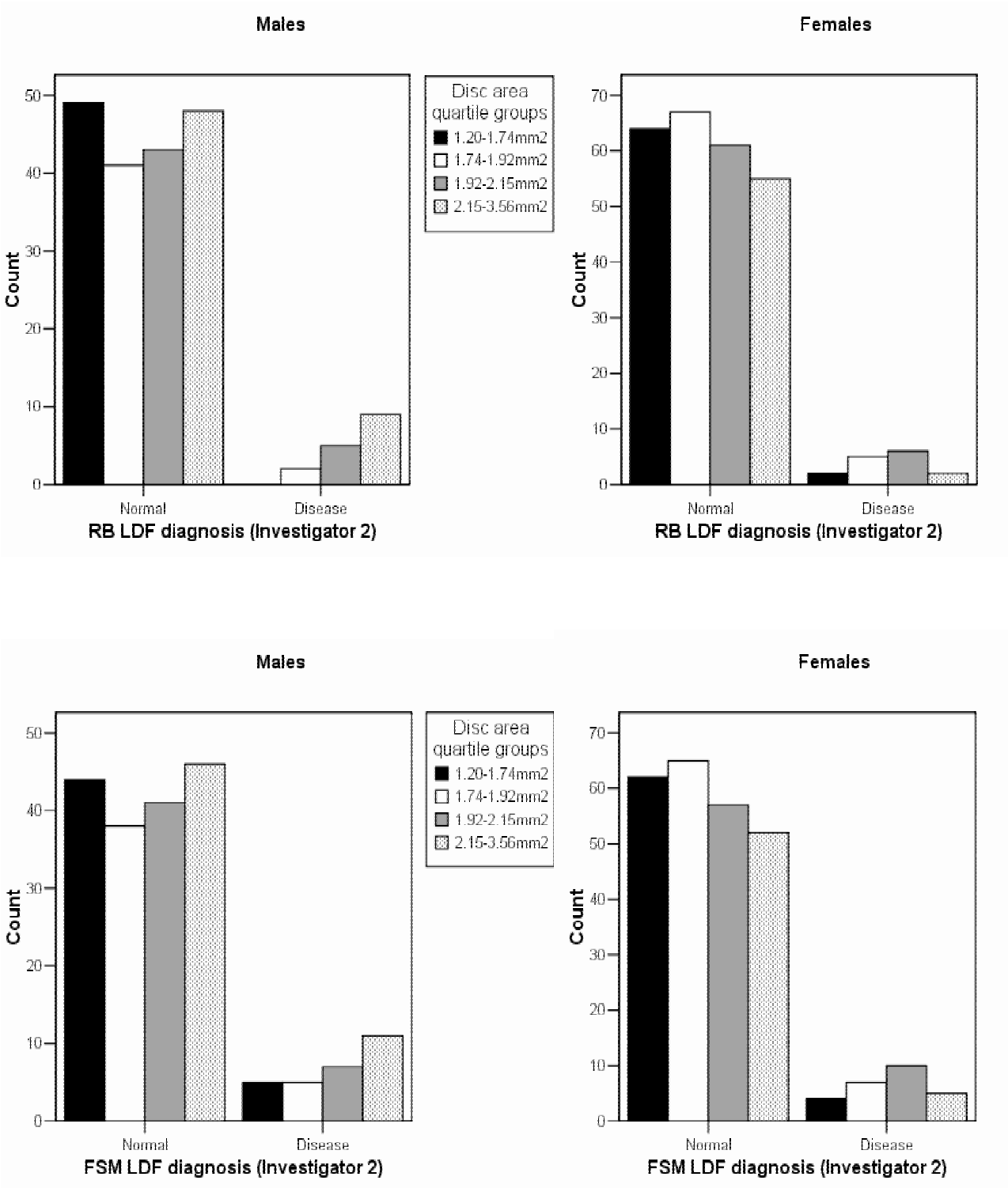

6.4 DISCUSSION

The Moorfields Regression Analysis has been shown to be more sensitive at discriminating normal from glaucoma than expert clinical observers of the optic disc.[101] The MRA is also able to detect optic disc abnormalities in glaucoma suspects prior to the development of visual field defects.[102] However, in this sample of normal elderly subjects, which was defined on visual field and not optic disc appearance, the Moorfields Regression Analysis (MRA) classified a significant number of discs as abnormal. When "borderline" cases were considered normal, the specificity of the classification was 96.1% and 94.3% for each investigator. When "borderline" cases were considered disease specificity fell to 83.2% and 83.0% for each investigator. Counting "borderline" cases as normal, previous researchers have found MRA specificities between 85% and 98.2%.[100, 104, 105] Overall in this sample, the specificity of the RB and FSM LDFs was 96.2% and 90.0% respectively for Investigator 1. Specificities were similar for investigator 2. The specificity of the FSM LDF was similar overall to that found by Iester *et al.*,[108] although other studies have found specificity to be as low as 65%.[155] Miglior *et al*. found that the specificity of the FSM LDF when analysing normals plus suspects vs POAG was 64%. However, specificity was found to be much lower when glaucoma suspects were included in the normals group.[156] BEAP's definition of normality was based on visual field, intraocular pressure and visual acuity, and not optic disc appearance. There may be individuals in this dataset with preperimetric glaucomatous optic neuropathy, which these diagnostic algorithms may be detecting, contributing to the reduced specificity. However, these linear discriminant functions were developed using patients with perimetric glaucoma, classifying discs on the basis of visual field changes and not on optic disc appearance. This study's definition of normality is therefore expected to provide a valid test of specificity. Additionally, subject age was not associated with a diagnosis of disease by MRA or the two LDFs. This suggests that this study's subjects came from a population representative of normals, since glaucoma is increasingly common with advancing years.

This study confirms in a population-based sample what other studies have also observed in selected subjects, namely reduced specificity of the MRA and the RB LDF with increasing disc size.[61, 105, 108] Interestingly, this effect was only significant in males. The FSM LDF tended to a lower specificity with larger discs in males more than females, although the relationships were not statistically significant. These findings are likely to be related to the larger cup measurements in this sample's males compared with females. This divergence in the population was not predicted by the MRA which was developed on a younger sample of normal subjects with a mean age of approximately 57 years.[17] No previous studies reporting sex differences in the relationship between diagnostic specificity and disc size were found. One study recruiting "opportunistic" Indian normals found, using HRT, that specificity of the MRA and FSM LDF decreased as disc size increased, though no gender differences were observed.[104] Interestingly, Miglior et al found that the diagnostic ability of MRA did not change when discs less than 1.2mm^2 or more than 2.8mm^2 were excluded from the analysis.[100]

The kappa statistic for agreement was only moderate when discs were contoured separately by two investigators and classified by MRA. However, agreement seemed better viewed in percentage terms, 86.5% of discs were classified identically, 12.0% disagreed by one level, and 1.5% disagreed by two levels. No previous studies were found reporting the effect on MRA classification of different operators placing contours on the same image acquired for each eye. One study looked at the variability of classification by the MRA across 5 consecutive images obtained for each eye at one sitting. The contour was drawn on one image and the software automatically imported the contour to the other 4 images. Classification by the MRA varied in 52% of cases.[71] Another study looking at the effect of different observers placing the contour on identical images on optic nerve head measurements found significant interobserver variation.[57] This variation can be reduced by the use of optic disc photographs to aid contour placement on the HRT image.[75] Any disagreement in classification

methods will limit the clinical usefulness of HRT classification tools in the normal elderly population, and further research is required to develop more reproducible techniques.

Reduced image quality associated with high MPHSD was a significant limitation in this study. This issue was discussed in Section 4.4. To check for an effect of SD in this sample, subjects who had a MPHSD over 50 microns were excluded and the analysis repeated. No change was observed in the significance levels of any of this study's findings, the data remaining largely unchanged.

Non-glaucoma is considerably more common than glaucoma. Any screening exercise for this disease in the population will therefore encounter a lot of normals. High test specificity is therefore required to avoid significant numbers of false positives. With specificities of 96.1%, 92.6% and 90.0% for the MRA, RB and FSM LDFs respectively, these diagnostic tools would generate significant numbers of false positives if used in a screening context in the general elderly population. In addition, decreasing specificity of these diagnostic tools was found with increasing disc size. The tools were developed on younger samples than this elderly sample, and did not predict the differences in normal tolerances for males and females. Further research will develop diagnostic algorithms for the HRT appropriate to the elderly population using data from BEAP.

7.0 Observer Agreement Using The Heidelberg Retina Tomograph

7.1 INTRODUCTION

HRT II generates ONH parameters using a mean topographic image which is computed from a series of three acquired images, giving improved reproducibility of the topographic height measurements.[65] However, HRT II requires the investigator to subjectively mark the edge of the ONH with a contour before the software can calculate the ONH parameters. This process adds a source of additional variability to the imaging data,[57, 75, 77] beyond that of image acquisition[55, 71, 72, 85] and individual patient variation. Such additional variability will limit the advantages of objective ONH assessment over expert clinical judgement. HRT II uses the standard reference plane, which is defined for each individual parallel to the peripapillary retinal surface and is located 50 microns posteriorly to the retinal surface at the papillo-macular bundle. The area below the reference plane defines cup, with the area above defining rim. Since the position at which the ONH contour crosses the papillo-macular bundle may vary between investigators, consequent variation in the height of the reference plane may introduce parameter variability which is significant in cross-sectional (diagnostic) studies.[57] As discussed in Chapter 3 there are several issues related to data variability in the normal elderly age group. Image acquisition variability (quantified by HRT II as mean pixel height standard deviation across the three images) is known to increase with age[71] and the presence of cataract.[67] Additionally, variability in optic disc contour placement is greater for normal discs than glaucomatous discs, probably due to the thicker nerve fibre layer of normal discs obscuring Elschnig's ring.[57] Whilst longitudinal (change) analyses are more affected by variability induced by sequential image acquisition, cross-sectional (diagnostic) analyses such as those used in this study are more limited by variation due to disc contour placement.

The aims of this study were to quantify the variability of contour placement in normal elderly subjects between two investigators, and to investigate variation of each ONH parameter in relation to variation in reference plane height and disc area, lens opacity and image quality. It also aimed to determine whether the use

of high-resolution digital fundus photographs to aid contour placement might improve inter- and intraobserver agreement.

7.2 SUBJECTS AND METHODS

7.2.1 Subjects: The Bridlington Eye Assessment Project

The selection and examination of subjects is described in Chapter 3. The dataset of normal subjects used in this study is the same as that described in Section 4.2.1. To enable the effect of image quality on parameter agreement to be studied no further selection was applied based upon MPHSD.

7.2.2 Interobserver variability

Interobserver variability in optic nerve head (ONH) parameters for all 550 eyes was assessed with the use of Bland Altman plots to examine bias and 95% limits of agreement. Interobserver difference (investigator 1 (MJH) minus investigator 2 (GA)) was plotted against the mean of the two investigators. Coefficient of variation (standard deviation of the differences divided by the mean multiplied by 100) was calculated for each parameter to allow comparison of the degree of variability of different parameters. Significance testing for bias between the investigators was achieved with use of a one sample Student's t test of the mean differences against a hypothesized value of zero. Linear regression was used to assess the magnitude of relationship between the difference in ONH parameters (as dependent variables) and differences in reference height and disc area (as the independent variables) induced when each disc was contoured by separate investigators. Non-linearity of relationship was assessed through analysis of the residuals. No evidence of non-linearity was found for any of the relationships. Spearman's rank correlation was used to look for relationships between parameter differences and LOCS score and MPHSD. For this analysis the differences were expressed without any minus sign to indicate a unidirectional magnitude of difference.

50 eyes were randomly selected from the group and both observers traced the disc contour with the aid of a high-resolution digital photograph. A period of at

least 3 months had passed since the initial contouring of discs. Interobserver variability was assessed using the methods described above.

7.2.3 Intraobserver variability

10 eyes were chosen for intraobserver variation analysis. 5 eyes were selected randomly from the 58 discs that fell outside of the 95% limits of agreement for disc area. A further 5 eyes were selected randomly from the 66 discs that fell within the 5% limit of agreement for disc area. Each disc was then contoured ten times by each investigator in one session. Measures of variability were employed as above.

7.3 RESULTS

7.3.1Demographics

Table 15 displays summary data for age, sex ratio, and MPHSD parameter, together with LOCS III score for the whole group of 550 eyes, and the subset of 50 optic discs contoured with the aid of a fundus photograph. Subjects selected for contouring with the aid of a photograph were slightly younger than the whole sample (mean age 73.2 and 71.2 years, p=0.05). Both groups had similar image quality (mean MPHSD 34.6 and 35.8 microns in the whole group and subset respectively, p=0.78).

7.3.2 Interobserver variability

Table 16 displays agreement statistics for disc area (globally and for each sector) when contoured by each investigator. Mean difference in disc area between the two investigators was negative in all sectors, indicating that Investigator 2 consistently traced larger contours than Investigator 1. Resulting bias was statistically significant in all but one sector (temporal-inferior sector p=0.06). The coefficient of variation (CV) for global disc area was 13.1%. The Bland Altman plot (mean plotted against difference in the two measurements) for agreement in global disc area is given in Figure 12. The 95% limits of agreement for global disc area were +/- 0.50mm^2. Table 17 shows agreement statistics for the 12 optic nerve head parameters, in addition to MPHSD and reference height. Bias between the 2 investigators was not apparent for all parameters. Cup area

and rim area were both significantly larger for Investigator 2. CV varied markedly for different parameters being greatest for rim volume (25.1%). Rim/disc area ratio showed much smaller CV compared with cup/disc area ratio (5.9% and 19.9% respectively). Scatterplots displaying the relationships between difference in rim and cup area versus difference in reference height and disc area are given in Figure 13. Differences in rim area showed an obvious relationship with differences in disc area though not with differences in reference height. The opposite relationships were found with cup area. The results of linear regression analysis exploring the relationship between the differences in each global parameter and the difference in reference height and disc area are given in Table 18. Rim measurement differences were mostly related to disagreement in disc area, whereas cup and RNFL measurement differences were mostly related to disagreement in reference height. No significant correlation was found between the LOCS score for nuclear, cortical, or posterior subcapsular cataract and magnitude of any of the differences in optic disc sector area or reference height. No significant correlation between average MPHSD and magnitude of difference in disc area was found in any disc sector. Magnitude of difference in reference height was weakly correlated with average MPHSD (r_s=0.12, p=0.004).

7.3.3 Interobserver variability using digital photographs

Table 19 examines the effect on optic disc parameters of using a photograph to aid contour placement compared with no photograph for each investigator. No significant systematic effect due to the use of photographs was demonstrated. Both investigators traced larger contours when using photographs though the bias was not significant.

7.3.4 Intraobserver variability

The 10 optic discs included in the intraobserver variability analysis were drawn from 6 right eyes and 4 left eyes of 2 males and 8 females. Figure 14 displays intraobserver variation data for Investigator 1. Cup-related measures had greater variability than rim-related ones. Rim/disc area ratio had the lowest variability (1.6%). Similar results were obtained for investigator 2. Figure 15

shows intraobserver variability for Investigator 1 when contouring optic discs in the best 5% and worst 5% of interobserver agreement. Intraobserver variability was notably worse where poor interobserver agreement existed. The cup-related measurements were worst affected, with rim/disc area ratio maintaining a very high repeatability. Results were similar for Investigator 2.

Table 15. Summary data for the whole group and the subset of discs contoured with the aid of a fundus photograph.

Parameter	Whole group	Subset contoured with photo	P Value (Mann-Whitney test)
Number (eyes)	550	50	-
Mean (SD) age (years)	73.2 (5.4)	71.2 (4.8)	0.05
Male:female ratio	230:320	22:28	0.78[†]
Mean (SD) MPHSD (microns)	34.6 (27.7)	35.8 (31.9)	0.78
LOCS score (median)			
Nuclear colour	2.5	2.0	0.05
Cortical	1.0	1.0	0.06
Posterior subcapsular	1.0	1.0	0.34

[†] Chi square test

Table 16. Bias and agreement between two investigators in defining disc area. Data shown for the mean, mean (SD) of the differences and coefficient of variation. Results shown for 550 eyes of 550 normal elderly subjects.

Disc area (mm^2)	Mean	Mean (SD) difference	Bias significance *P*	Coefficient of variation (%)
Global	1.96	-0.052 (0.256)	<0.001	13.1
Temporal	0.48	-0.018 (0.065)	<0.001	13.5
Temp/Sup	0.25	-0.004 (0.036)	=0.01	14.6
Temp/Inf	0.26	-0.003 (0.038)	=0.06	14.4
Nasal	0.49	-0.017 (0.065)	<0.001	13.4
Nasal/Sup	0.25	-0.003 (0.037)	=0.04	15.1
Nasal/Inf	0.24	-0.008 (0.038)	<0.001	16.1

Figure 12. Bland-Altman plot showing agreement in disc area when contoured by two investigators. Data shown for 550 eyes of 550 normal elderly subjects. Reference lines correspond to the mean difference and 95% limits of the differences.

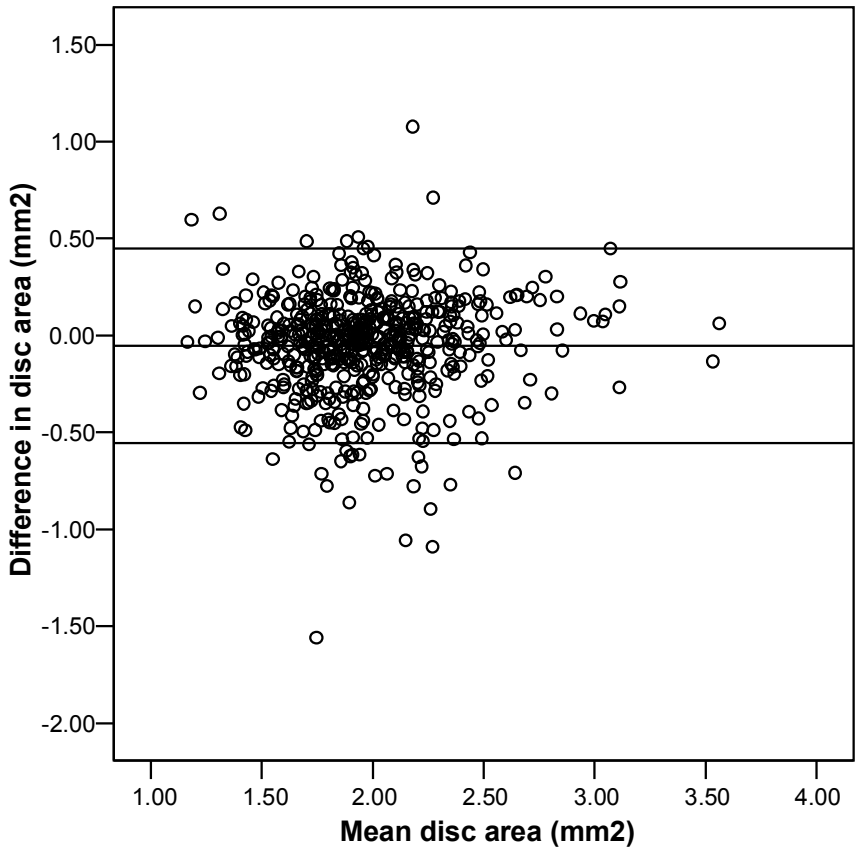

Table 17. Bias and agreement between two investigators in global disc parameters. Data shown for the mean, mean (SD) of the differences and coefficient of variation. Results shown for 550 eyes of 550 normal elderly subjects.

Parameter	Mean	Mean (SD) difference	Bias significance *P*	Coefficient of variation (%)
Cup area (mm^2)	0.46	-0.007 (0.090)	0.06	19.1
Rim area (mm^2)	1.49	-0.045 (0.254)	<0.001	17.0
Cup/disc area ratio	0.23	-0.003 (0.045)	0.18	19.9
Rim/disc area ratio	0.77	0.003 (0.045)	0.18	5.9
Cup volume (mm^3)	0.09	-0.001 (0.022)	0.53	23.7
Rim volume (mm^3)	0.39	-0.007 (0.098)	0.11	25.1
Mean cup depth (mm)	0.19	0.002 (0.011)	<0.001	5.6
Max. cup depth (mm)	0.52	0.001 (0.032)	0.43	6.0
Height variation contour	0.38	0.005 (0.054)	0.03	14.3
Cup shape measure *	-0.17	0.006 (0.026)	<0.001	-14.9
Mean RNFL thickness (mm)	0.22	0.004 (0.037)	0.01	16.8
RNFL cross-sectional area (mm^2)	1.08	0.005 (0.188)	0.51	17.3
MPHSD (microns)	34.6	-0.06 (6.69)	0.82	19.4
Reference height (mm)	0.27	0.004 (0.041)	0.02	14.9

MPHSD Mean pixel height standard deviation

Figure 13. Scatterplots showing difference in rim area and difference in cup area against difference in disc area and difference in reference height when contoured by two investigators. Data shown are for 550 eyes of 550 normal elderly subjects.

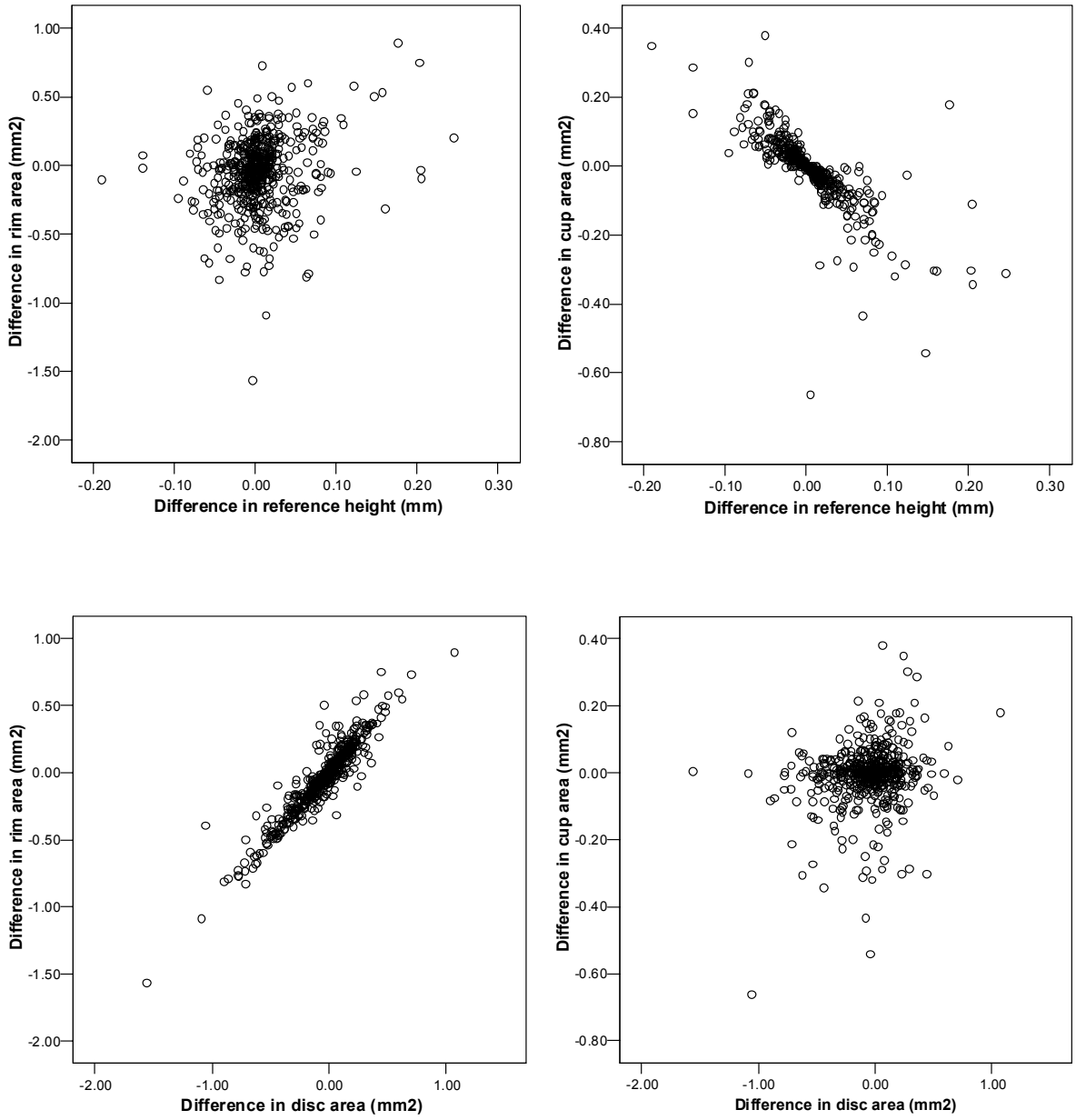

Table 18. Linear regression analysis of the relationship between the differences in optic nerve head measurements and the difference in reference height and disc area when disc contour placed by two different observers. Data shown for 550 eyes of 550 normal elderly subjects.

	Difference in reference height			**Difference in disc area**		
Parameter difference	**R^2**	**B (SE)**	***p***	**R^2**	**B (SE)**	***p***
Cup area (mm^2)	0.62	-1.71 (0.06)	<0.001	0.02	0.05 (0.01)	<0.001
Rim area (mm^2)	0.07	1.71 (0.06)	<0.001	0.88	0.95 (0.01)	<0.001
Cup/disc area ratio	0.56	-0.87 (0.03)	<0.001	0.12	-0.06 (0.00)	<0.001
Cup volume (mm^3)	0.48	-0.38 (0.02)	<0.001	0.02	0.01 (0.00)	<0.001
Rim volume (mm^3)	0.41	1.54 (0.03)	<0.001	0.50	0.29 (0.01)	<0.001
Mean cup depth (mm)	0.10	-0.03 (0.01)	<0.001	0.09	-0.01 (0.00)	<0.001
Height variation contour	0.35	0.78 (0.05)	<0.001	-	-	0.14
Cup shape measure	0.23	-0.05 (0.00)	<0.001	-	-	0.07
Mean RNFL thickness (mm)	0.84	0.83 (0.02)	<0.001	0.01	-0.01 (0.00)	<0.001
RNFL cross-sectional area (mm^2)	0.71	4.00 (0.09)	<0.001	0.09	0.22 (0.01)	<0.001

Table 19. Bias in optic disc parameters as defined by two different investigators when using a photograph to aid contour placement compared with no photograph. Results based on 50 discs randomly selected from 550 normal elderly subjects.

	Investigator 1		**Investigator 2**	
Parameter	Mean (SD) difference	Bias significance P	Mean (SD) difference	Bias significance P
Disc area (mm^2)	-0.010 (0.190)	0.71	-0.041 (0.331)	0.38
Cup area (mm^2)	0.004 (0.094)	0.75	-0.035 (0.135)	0.07
Rim area (mm^2)	-0.014 (0.186)	0.60	-0.006 (0.290)	0.89
Cup/disc area ratio	-0.001 (0.046)	0.92	-0.012 (0.051)	0.12
Rim/disc area ratio	0.001 (0.046)	0.92	0.012 (0.051)	0.12
Cup volume (mm^3)	-0.001 (0.027)	0.74	-0.008 (0.034)	0.10
Rim volume (mm^3)	-0.016 (0.084)	0.19	0.000 (0.120)	0.99
Mean cup depth (mm)	-0.001 (0.008)	0.38	-0.002 (0.011)	0.26
Max. cup depth (mm)	0.002 (0.013)	0.23	0.002 (0.017)	0.34
Height variation contour	-0.004 (0.053)	0.56	0.018 (0.069)	0.08
Cup shape measure	-0.002 (0.020)	0.47	-0.014 (0.030)	0.002
Mean RNFL thickness (mm)	-0.002 (0.043)	0.74	0.008 (0.059)	0.35
RNFL cross-sectional area (mm^2)	-0.014 (0.202)	0.64	0.034 (0.287)	0.41
Reference height (mm)	-0.005 (0.050)	0.51	0.009 (0.069)	0.35

RNFL Retinal nerve fibre layer

Figure 14. Boxplot displaying the intraobserver variability (coefficient of variation) for Investigator 1. Plot based on 10 optic discs each contoured 10 times.

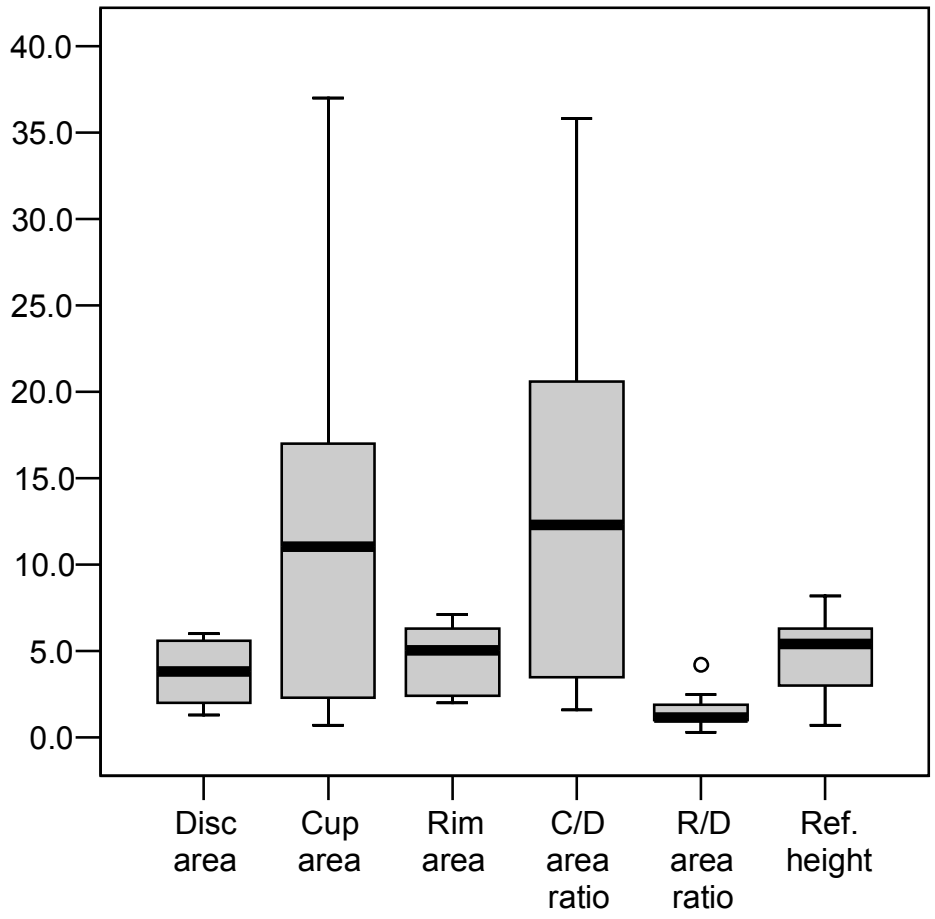

Figure 15. Boxplot displaying intraobserver variability (coefficient of variation) for 10 optic discs contoured 10 times each. Data are shown for five discs sampled from the best 5% of interobserver agreement, and for five discs sampled from the worst 5%. Results are shown for Investigator 1.

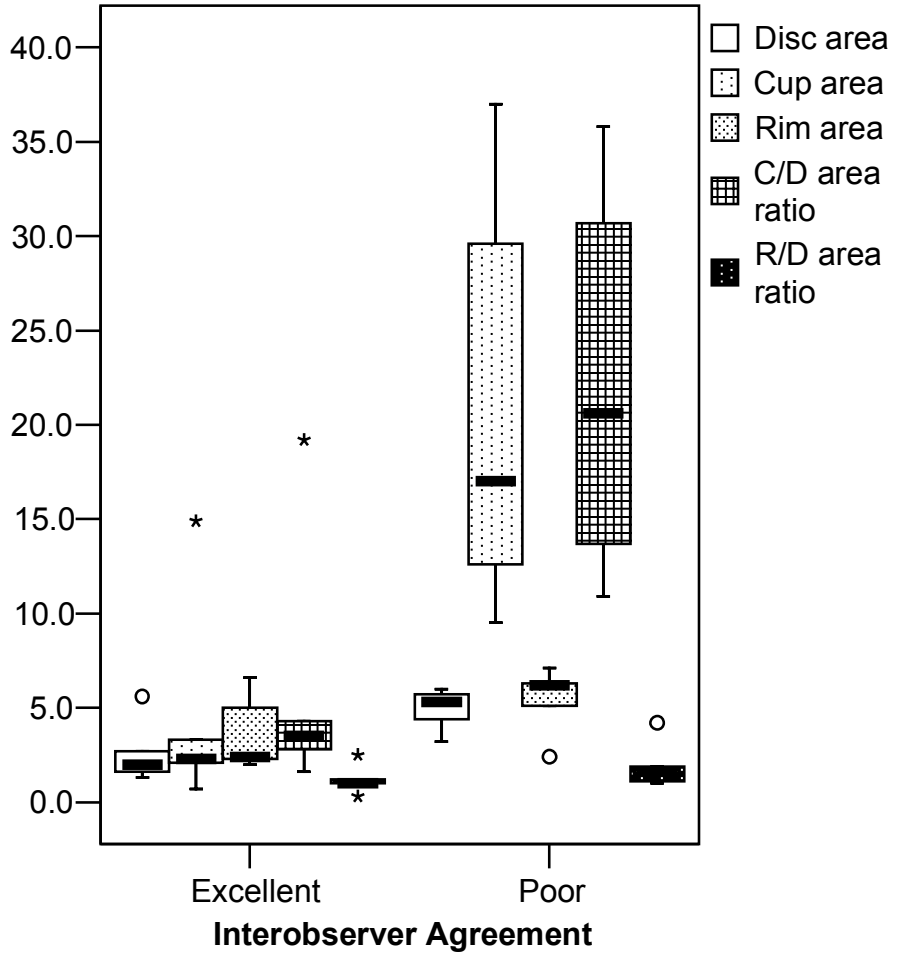

7.4 DISCUSSION

Heidelberg retina tomography (HRT) is an objective means of characterising the optic nerve head (ONH) with superior inter-observer repeatability over planimetry.[77] Further, inter-observer agreement is dependent upon operator experience with planimetry, though may not be with HRT.[57] The reproducibility of the computed topographic parameters has been shown to be acceptable with coefficients of variation less than 10%.[55, 64, 69] With only two separate

investigators, this study is not designed to demonstrate the reproducibility of HRT II parameters in general. Rather, it is designed to compare the relative variability of the different parameters when variability in disc contouring exists. In this study, one investigator consistently traced larger ONH contours than the other resulting in significant bias. In addition, agreement in disc area also showed large variation (within +/- 0.50 mm^2 95% of the time). However, interobserver agreement was differentially manifest for different parameters. Rim volume (mean 0.39mm^3) had a larger coefficient of variation than rim area (1.49mm^2; CV 25.1% and 17.0% respectively). This may be due to the smaller value of the former measure compared with the resolution of the machine (HRT II exports parameters to three decimal places). In addition, changes in reference height impact rim volume measurements in three dimensions, but rim area in only two dimensions. Rim/disc area ratio had the lowest CV of the rim measures (5.9%), showing also the greatest level of intraobserver repeatability. This was much lower than cup/disc area ratio (19.9%) which is simply the inverse of rim/disc area ratio. This may again be explained by the smaller value of the measure giving rise to very large CV values, though may also reflect the relationship that cup area variability showed with differences in reference height (discussed below).

Rim area, which is used by the Moorfields Regression Analysis (MRA) in a cross-sectional diagnostic manner, had a similar coefficient of variation (CV) to cup area, although the variation in each of these measures was explained by different factors. Linear regression demonstrated a minimal effect of disagreement in disc area (as traced by the contour) on variation in cup area, but a large effect on variation of rim area. The converse was true for disagreement in reference height. Thus, use of the standard reference plane in cross-sectional studies, which has been questioned by other observers, may not be a source of significant variability when using the MRA. Indeed, the major advantage of the standard reference plane is that it better respects the individual variability of ONH morphology and orientation (e.g. oblique insertion).[56] Rather,

variation in disc contour size can introduce significant disagreement in rim area and therefore the diagnostic category determined by the MRA. Interestingly, a longitudinal study of rim area repeatability found that variability in reference height accounted for a significant amount of rim area variability.[70] In this study the contour was drawn by one observer on the first acquired image and imported onto subsequent images. By maintaining a constant contour area, therefore, the differential effects of contour area and reference height were not explored. In the current study, the rim/disc area ratio was a highly reproducible measure in inter- and intra-observer analyses. By dividing rim area by disc area, this measure accounts for differences in contour area between observers, thus minimising variability. Further research is required to assess whether other reference planes judged to be more representative of ONH morphology by clinical observers,[59] and by OCT,[60] offer lower variability amongst observers of a population.

This study found no clinically significant relationship between LOCS III score of lens opacification or mean pixel height standard deviation and magnitude of difference in disc area or reference height. Thus, these indicators of image quality did not seem to affect agreement. However, images that caused poor interobserver agreement also led to poor intraobserver repeatability, suggesting that image quality can reduce repeatability. Additionally, use of a photograph to aid contour placement did not lead to any systematic difference in the contouring process for either investigator. This suggests that disagreement created during contour placement is specifically related to the investigator's interpretation of the optic disc edge on the HRT image. In contrast, a previous study using HRT I found that for 2 out of 4 observers the use of a clinical photograph of the ONH to aid contour placement improved interobserver variability of stereometric parameters.[75] It may be that the current study failed to detect a significant effect using photographs by studying only 2 investigators. Whilst the utility of photographs to improve HRT interobserver variability may still be open to question, HRT imaging has been shown in several studies to be superior in

reproducibility over photographic-based techniques, whether manual or computer-assisted,[57, 76, 77], or digital stereoscopic (Discam, Marcher Enterprises Ltd., Hereford, UK).[78]

This study highlights the limitations of describing ONHs using derived ONH parameters dependent on subjective operator input. In particular, rim area as used by the Moorfields Regression Analysis to create diagnostic categories, is prone to variability amongst investigators due to variability in the size of optic disc contour. Rim/disc area ratio was robust to such variability and may therefore be a more suitable parameter for use in diagnostic classification at a population level. The latest version of the technology, HRT III, employs an additional diagnostic tool utilising statistical shape analysis techniques. This does not require operator-dependent contouring of the ONH, [157] and therefore is only open to degradation of repeatability due to image acquisition variability. Studies assessing the repeatability of this technique are awaited.

8.0 Linear Regression Modeling Of Rim Area To Discriminate Between Normal And Glaucomatous Optic Nerve Heads

8.1 INTRODUCTION

Chronic open angle glaucoma has a prolonged subclinical phase, with progressive loss of retinal ganglion cells that may go unnoticed before advanced visual field loss occurs. Detection of glaucoma in its early stages through analysis of the optic nerve head may therefore help to prevent significant morbidity. However, the current gold standard of clinical evaluation of the optic disc, even by expert observers, generates sufficient disagreement to be unreliable in the diagnosis of glaucomatous optic neuropathy (GON).[118, 154] The introduction of objective imaging of the optic disc promises to improve the evaluation of optic nerve parameters by removing subjectivity. One such system is the Heidelberg Retina Tomograph (HRT) – a semi-automated confocal scanning laser system that provides reliable and reproducible three-dimensional imaging data of the optic nerve head.[55] Using this instrument the Moorfields Regression Analysis was developed to discriminate between normal and glaucomatous optic nerve heads.[17] Using a database of 112 eyes of 112 normal volunteers with a mean age of approximately 57 years, linear regression analysis was performed to determine the lower prediction limits for the log of the rim area corrected for disc size and age. Thus, by accounting for variation in rim area due to demographic variables, rim area changes due to GON may be more sensitively detected. Comparison of predicted limits with the log of actual measured rim area determines the ONH to be 'within normal limits' (rim area greater than the 95th lower prediction limit), 'borderline' (rim area between the 95th and 99.9th lower prediction limits) or 'outside normal limits' (rim area below the 99.9th lower prediction limit). This method has generated specificities of 94-96%, with lower sensitivities of 74-84%,[17, 100] and has been shown to be more sensitive than expert clinical evaluation in detecting glaucoma.[101] However, the diagnostic precision of MRA is not uniform across all disc sizes, with larger discs returning lower specificity and higher sensitivity compared with smaller discs.[104, 105] In addition, the sample of 'normals' used to generate MRA was not population-based, with a mean age below the age profile of patients with acquired GON, most of whom are aged more than 60 years.[132] In chapter 4 the

finding that normal elderly males have larger cup-related variables than normal elderly females is described.[158] Thus, to accurately describe normal neuroretinal rim variability in the elderly, subject sex should be considered as an independent variable in the regression model in addition to age and disc size.

Using a similar approach to Wollstein et al.,[17] the aim of this study was to generate a multiple linear regression model of rim area adequately corrected for demographic-based variation using the prospective population-based sample of normal elderly subjects. Then the aim was to assess the specificity of the algorithm in these normal subjects, and its sensitivity when applied to patients with a new diagnosis of GON recruited retrospectively from the practice of a consultant ophthalmologist specialising in glaucoma (SAV).

8.2 PATIENTS AND METHODS

8.2.1 Normal Subjects: The Bridlington Eye Assessment Project

BEAP saw it's first subject on 5/11/2002 and had seen 2065 subjects at the start of this study in October 2004. Of these, 880 were defined as normal based on the criteria stated in Chapter 3. The methodology of subject recruitment, examination and selection is described in full in Chapter 3.

8.2.2 Glaucoma Patients

The most preferable source of glaucoma patients for this study would have been from BEAP. However, there were two major reasons why these patients were not suitable. First, diagnosis of glaucoma could not be standardised, and was based on many different criteria e.g. history, examination by optometrist, diagnosis by local ophthalmologist. Second, BEAP used a supra-threshold visual field test, and thus standard research perimetric criteria for glaucoma could not be applied. Glaucoma patients were therefore recruited retrospectively over 2 years from the practice of a glaucoma consultant (SAV) at Queen's Medical Centre, Nottingham. Patients were included if they met all of the following criteria: (1) New diagnosis of open angle glaucoma, including pseudexfoliative and pigmentary glaucoma, made by the Consultant or Senior

Fellow. (2) Visual field loss consistent with glaucoma and (3) Corrected logMAR acuity of at least 0.3. Minimal criteria for glaucomatous visual field defect were as follows: Glaucoma hemifield test outside normal limits, pattern standard deviation with a P value of<5%, or a cluster of 3 points in the pattern deviation plot in a single hemifield (superior or inferior) with P value of <5%, one of which must have a P value of <1%. A visual field test was excluded if any of the reliability indices was 20% or greater. A total of 95 patients fitting the above criteria for glaucoma were recruited. Where both eyes fulfilled the criteria for glaucoma, one eye was selected randomly for inclusion in the study by tossing a coin.

8.2.3 Confocal Scanning Laser Ophthalmoscope assessment

The scanning acquisition process employed for normal subjects is detailed in Section 3.1.4. In the glaucoma group, all images were acquired within 6 months of the index visual field test. One mean topographic image was acquired per eye. All images were acquired by one operator (CLT). The optic disc contour line was drawn on all images by one investigator (MJH) to mark the edge of the optic disc. HRT II then calculated disc area (mm^2), reference height (mm) and 12 further stereometric parameters. The parameters were cup area (mm^2), rim area (mm^2), cup/disc area ratio, rim/disc area ratio, cup volume (mm^3), rim volume (mm^3), mean cup depth (mm), maximum cup depth (mm), height variation contour (mm), cup shape measure, mean retinal nerve fibre layer (RNFL) thickness (mm) and RNFL cross-sectional area (mm^2). Each of these parameters was expressed for the global disc, and for 6 individual disc sectors (temporal, temporal superior, temporal inferior, nasal, nasal superior, nasal inferior). Images with a mean pixel height standard deviation greater than 50 microns were excluded from further analysis. Optic nerve head parameters were analysed using SPSS for Windows version 12.0.2 (Statistical Package for Social Sciences, SPSS, Inc, Chicago, Illinois). Two-tailed tests were used in all statistical analyses. Statistical significance was set at $p<0.05$.

8.2.4 Linear Regression Analysis

Wollstein et al. developed prediction intervals for log rim area corrected for disc area and age by fitting a linear regression model.[17] This study aimed to use similar methodology.

Figure 16. Scatterplot of log rim area versus disc area for the global disc in 712 normal elderly subjects. The dotted lines represent the linear regression (mean and 95th prediction intervals) and the solid line represents the Loess regression (locally weighted regression).

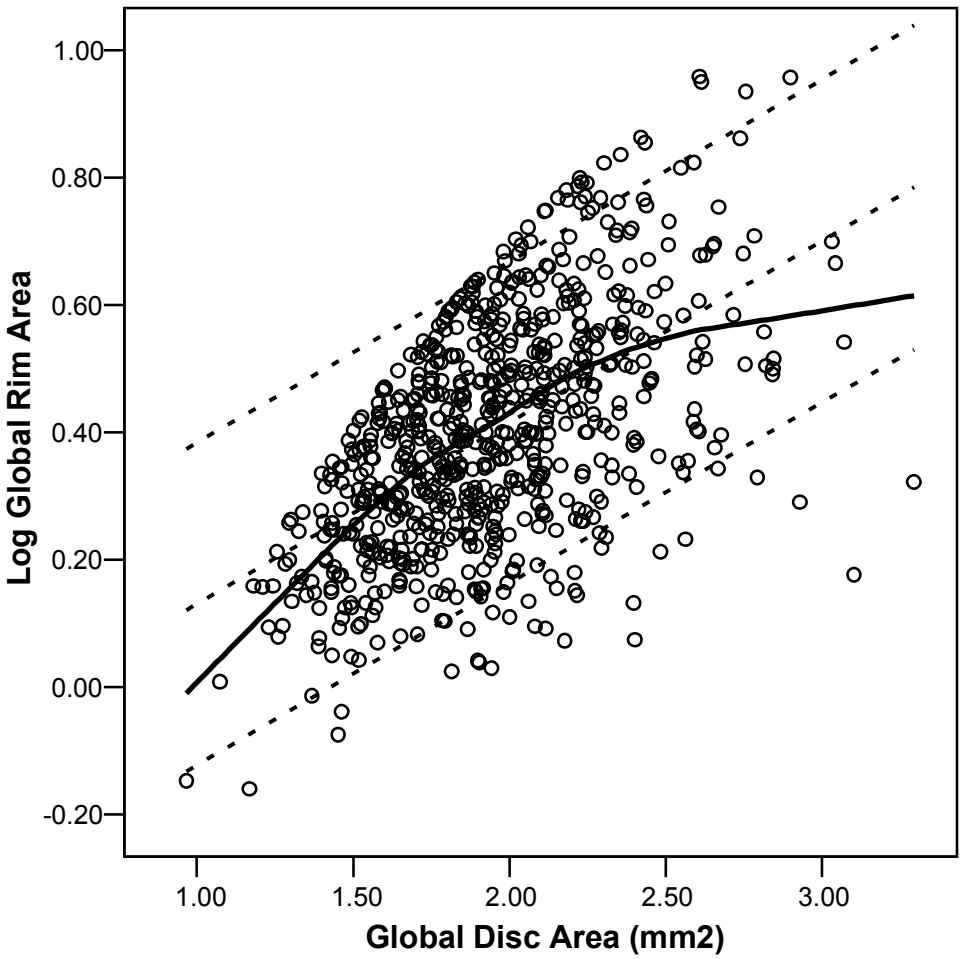

Figure 16 shows a scatterplot of log global rim area against global disc area, displaying fit lines developed by linear regression and Loess (abbreviation for 'local regression') regression methods. Linear regression fits a straight line to the data based on the sum of least squares of the residuals. Critical assumptions of this method are that variability of the dependent variable is

constant for all values of the independent variable (homoscedascity), and that the relationship between the variables is linear. Loess regression combines the simplicity of linear least squares regression with the flexibility of nonlinear regression to produce a function that describes the deterministic part of the variation in the data point by point.[159] As observed by Wollstein et al., the variability of rim area increased with increasing disc area. This phenomenon, called heteroscedasticity, is in part due to the maximum possible rim area of a disc being defined by the disc area. Log transformation of rim area did not remove heteroscedasticity in the BEAP data (Levene statistic for homogeneity of variance 8.53, $p<0.001$), although it did reduce it compared with the untransformed rim area (slope of spread of rim area versus level (disc area quartile) plot 0.53 and 2.37 respectively). However, log transformation of rim area markedly increased the curve of the Loess regression, and thus the departure of the relationship from linearity. This non-linearity and heteroscedasticity may explain the known reduction in specificity and rise in sensitivity with increased disc size of the MRA.[104, 105] Since the Loess regression described a lognormal relationship (which was expected, since increases in disc area are not matched by equal increases in rim area[33]) log transformation of disc area was a more appropriate transformation to achieve linearity across the whole range of data. Heteroscedasticity remained, however, so to overcome both issues linear regression analysis was conducted on four separate groups according to disc area quartile. I am grateful to Mr A Rotchford, Specialist Registrar in Ophthalmology at Queen's Medical Centre for his suggestion to use this method. The quartile cut-offs were 1.70mm2, 1.92mm2 and 2.17mm2 (minimum disc area 0.97mm2, maximum 3.30mm2). Visual analysis of scatterplots revealed 9 extreme outliers which were removed from further analysis. Multiple linear regression was then performed with log rim area as the dependent variable and disc area, reference height, age and sex as independent (predictor) variables. Predictor variables were selected for each model using a backward elimination method (sequential removal of variables not contributing significantly to the model using a probability limit of 0.10) for each of

the 4 regression analyses in each disc sector. The global and temporal sectors in the 4th disc area quartile did not produce a significant linear regression model. For these sectors the lower limits of log rim area were determined by the relevant nonparametric percentiles. The 95th and 99th lower limits of the prediction interval for log rim area generated by the multiple linear regression were compared with actual log rim area in the normal and glaucomatous eyes. Actual values greater than the 95th prediction limit were deemed 'Within normal limits', those between the 95th and 99th limits were 'Borderline' and those less than the 99th limit were 'Outside normal limits'. This classification was conducted for each disc sector, with the overall disc classification being equal to the status of the worst disc sector. The 99th prediction interval was chosen as the cut-off for 'outside normal limits' (in contrast with the MRA as employed by HRT software which used the 99.9th prediction interval) as a compromise between better specificity and reduced sensitivity. Variables included in the multiple linear regression model for the global sector are shown in Table 20. Frequency tables were used to analyse the relationship between disc area quartile and diagnostic classification. The X^2 statistic was used, with Yates' correction applied if a 2x2 table was analysed. Because of the small sample size of glaucoma patients causing small expected frequencies in some cells, the relationship between diagnostic classification and disc size was analysed in a 2x2 table between diagnostic classification (Normal/Abnormal separated at the 95th prediction interval) and 2 disc area groups separated at the 50th centile.

8.3 RESULTS

After exclusion of subjects with unacceptable image quality, the final study sample consisted of 712 normal subjects, and 58 patients with glaucoma. Characteristics of the datasets are given in Table 21. Mean age was significantly lower in the glaucoma group compared with the normal individuals (62.6 vs 72.8 years respectively; $p<0.001$). In the glaucoma dataset mean (SD) MD of the visual field test closest to the date of HRT imaging was –5.7 (5.1) dB (range –0.2 to –23.0 dB). Corresponding mean (SD) PSD was 6.6 (3.3) dB (range 1.8 to 13.8 dB).

Table 22 displays the mean values of HRT II parameters in the normal and glaucoma individuals. All HRT II parameters were significantly different when the two groups were compared. Figure 17 displays receiver operating characteristic (ROC) curves examining separation between normal and glaucoma using neuroretinal tissue-related measurements. Best separation was achieved with the rim/disc area ratio parameter (area (SE) under ROC curve 0.88(0.03)). Corresponding figures for mean retinal nerve fibre layer (RNFL) thickness were 0.72(0.04). Table 23 displays the area under ROC curves for all HRT II parameters. The worst performing parameter was height variation contour (area (SE) under ROC curve 0.59(0.05)).

Table 20. Independent predictor variables entered into a multiple linear regression model of log rim area for the global disc of 712 normal elderly subjects. Independent variables were selected automatically using a backward elimination method (criteria for removal p>0.10). Results are shown for disc area quartile groups 1 and 3.

Parameters Selected	**Coefficient B (SE)**	**t**	***P* Value**
Disc Area (1)	0.517(0.060)	8.60	<0.001
Disc Area (3)	-	-	NS
Reference Height (1)	-0.129(0.060)	-2.14	0.03
Reference Height (3)	-0.269(0.105)	-2.57	0.01
Sex (1)	0.027(0.016)	1.67	0.10
Sex (3)	0.055(0.023)	2.41	0.02
Age (1)	-	-	NS
Age (3)	-	-	NS
Constant (1)	-0.538(0.096)	-5.63	<0.001
Constant (3)	0.429(0.044)	9.71	<0.001

NS not significant

Table 21. Characteristics of the study populations (Mean (SD))

	Normal subjects (n=712)	**Glaucoma patients (n=58)**	***P* Value***
Age	72.8(4.9)	62.6(13.7)	<0.001
Male:Female (%)	42:58	57:43	
Right:Left eyes (%)	49:51	64:36	
MPHSD (microns)	24.0(10.1)	28.9(10.0)	0.002

MPHSD Mean Pixel Height Standard Deviation
* Mann-Whitney U Test

Table 22. Mean (SD) of HRT II parameters in 712 normal elderly subjects and 58 patients with glaucoma.

Parameter	**Normal**	**Glaucoma**	***P* Value***
Disc area (mm^2)	1.94 (0.35)	2.06 (0.46)	0.04
Cup area (mm^2)	0.43 (0.31)	0.98 (0.47)	<0.001
Rim area (mm^2)	1.52 (0.28)	1.09 (0.31)	<0.001
Cup/disc area ratio	0.21 (0.13)	0.46 (0.17)	<0.001
Rim/disc area ratio	0.79 (0.13)	0.54 (0.17)	<0.001
Cup volume (mm^3)	0.08 (0.09)	0.25 (0.20)	<0.001
Rim volume (mm^3)	0.39 (0.14)	0.24 (0.14)	<0.001
Mean cup depth (mm)	0.18 (0.08)	0.28 (0.10)	<0.001
Maximum cup depth (mm)	0.51 (0.21)	0.64 (0.19)	<0.001
Height variation contour (mm)	0.37 (0.09)	0.35 (0.13)	0.03
Cup shape measure	-0.18 (0.06)	-0.09 (0.07)	<0.001
Mean RNFL thickness (mm)	0.23 (0.06)	0.17 (0.10)	<0.001
RNFL cross-sectional area (mm^2)	1.11 (0.30)	0.85 (0.48)	<0.001

* Mann-Whitney U test

Figure 17. Receiver operating characteristic (ROC) curves for neuroretinal tissue-related measurements in the discrimination between 712 normal eyes and 58 eyes with glaucoma.

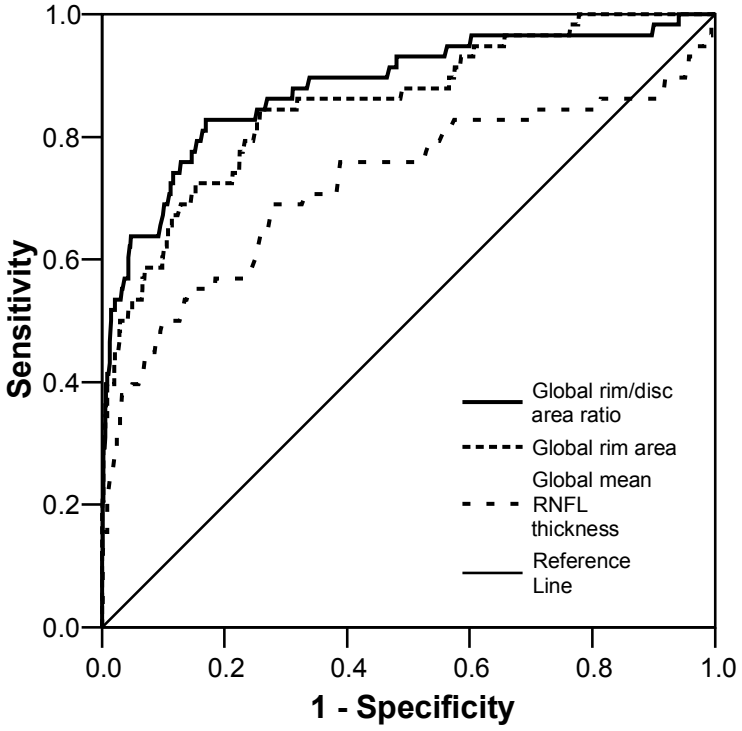

Table 23. Area under ROC curves and sensitivities (Sn) at fixed specificities (Sp) for discrimination between normal subjects (n=712) and glaucoma patients (n=58).

Parameter	ROC Curve Area (SE)	Sn/Sp (Sp>95%)	Sn/Sp (Sp>80%)
Cup area (mm^2)	0.85 (0.03)	48/95	78/80
Rim area (mm^2)	0.86 (0.03)	53/95	72/80
Cup/disc area ratio	0.88 (0.03)	64/95	83/80
Rim/disc area ratio	0.88 (0.03)	64/95	83/80
Cup volume (mm^3)	0.81 (0.03)	33/95	66/80
Rim volume (mm^3)	0.80 (0.04)	50/95	69/80
Mean cup depth (mm)	0.77 (0.03)	24/95	52/80
Maximum cup depth (mm)	0.69 (0.02)	12/95	38/80
Height variation contour (mm)	0.59 (0.05)	16/95	40/80
Cup shape measure	0.83 (0.03)	41/95	74/80
Mean RNFL thickness (mm)	0.72 (0.04)	40/95	57/80
RNFL cross-sectional area (mm^2)	0.70 (0.05)	38/95	55/80

8.3.1 Linear Regression Analysis

Multiple linear regression for log global rim area with global disc area, reference height and sex as independent variables produced a model with R^2=0.32 (residual standard deviation 0.104) for the first disc area quartile. The results of diagnostic classification of normal and glaucomatous optic nerve heads by the new linear regression analysis (NRA) are shown in Table 24. All disc sectors showed significantly different proportions of the three diagnostic categories between normal and glaucomatous eyes (Chi square tests p<0.001). Overall, at the 95th prediction limit of normality, the analysis returned a specificity of 83.3% with a sensitivity of 81%. At this same limit of normality the MRA returned a specificity of 84.4% with a sensitivity of 82.7%. Using the 99% prediction limit the NRA returned a specificity of 91.4% with a sensitivity of 72.4%. Diagnostic classification of optic nerve heads in the normal and glaucoma groups by the NRA and MRA for each of the four disc area quartile groups are shown in Figure 18. In normal individuals increasing disc area quartile had no significant effect on specificity using the new regression analysis (81.6% and 86.3% in the first

and fourth quartiles respectively; X^2=2.0 with 3 degrees of freedom, *p*=0.56) but was associated with a significant drop in specificity using the MRA (91.1% and 73.1% in the first and fourth quartiles respectively; X^2=24.2 with 3 degrees of freedom, *p*<0.001). In glaucoma patients analysed with the NRA, increasing disc area quartile was associated with a rise in the total number of 'outside normal limits' results, although not in the overall proportion of such results (75.0% and 75.0% in the first and fourth quartiles respectively; $X^2_{\text{Yates correction}}$ =0.05 with 1 degree of freedom, *p*=0.82; 2x2 table between diagnostic classification and disc area halves). In these patients analysed with the MRA, decreasing disc size was associated with significantly reduced sensitivity (58.3% and 85.0% in the first and fourth disc area quartiles respectively; $X^2_{\text{Yates correction}}$ =3.76 with 1 degree of freedom, *p*=0.05). When analysed with the NRA using a cut-off at the 95% limit there was no effect of sex on specificity (81.1% and 84.8% in males and females respectively; X^2 =1.68 with 1 degree of freedom, *p*=0.20) or sensitivity (84.8% and 76.0%; X^2 =0.73 with 1 degree of freedom, *p*=0.40). With the MRA using a cut-off at the 95% limit, specificity was significantly lower in males compared with females (80.5% and 87.2% respectively; X^2 =6.01 with 1 degree of freedom, *p*=0.01). Sensitivity did not differ using MRA between males and females (X^2 =1.41 with 1 degree of freedom, *p*=0.24). Agreement between the NRA and MRA for the normal and glaucomatous discs is shown in Table 25. Agreement was moderate between the two regression analyses for normal subjects (kappa=0.59(0.04), *p*<0.001) and substantial for glaucoma patients (kappa=0.71(0.12), *p*<0.001).

Table 24. Diagnostic classification of optic nerve heads of 712 normal elderly subjects and 58 glaucoma patients (results in parentheses) by a new linear regression analysis. Results are shown for all disc sectors and for the overall analysis.

Result (%)	**Global**	**Temp**	**TS**	**TI**	**Nasal**	**NS**	**NI**	**Overall**
WNL	97.2	96.3	96.3	96.8	94.8	95.6	95.2	83.3
	(51.7)	(75.9)	(55.2)	(58.6)	(48.3)	(43.1)	(56.9)	(19.0)
BL	2.2	2.7	2.2	1.4	2.2	2.7	2.0	8.1
	(8.6)	(8.6)	(8.6)	(1.7)	(8.6)	(10.3)	(3.4)	(8.6)
ONL	0.6	1.0	1.4	1.8	2.9	1.7	2.8	8.6
	(39.7)	(15.5)	(36.2)	(39.7)	(43.1)	(46.6)	(39.7)	(72.4)

WNL Within normal limits
BL Borderline
ONL Outside normal limits
TS Temporal/superior
TI Temporal/inferior
NS Nasal/superior
NI Nasal/inferior

Table 25. Crosstabulation examining agreement between a new regression analysis and the Moorfields Regression Analysis (MRA) when classifying optic nerve heads of 712 normal elderly subjects and 58 patients with glaucoma (results in parentheses). IN and OUT categories mark separation at the 95th prediction interval.

		MRA Result		
		IN	OUT	**Total**
New Regression Result	IN	557	36	593
		(8)	(3)	(11)
	OUT	44	75	119
		(2)	(45)	(47)
	Total	601	111	712
		(10)	(48)	(58)

Figure 18. Overall diagnostic classification of optic nerve heads of 712 normal elderly subjects and 58 glaucoma patients by a new linear regression analysis and the Moorfields Regression Analysis (MRA). Results are shown for each of the four disc area quartiles. IN and OUT categories mark the separation at the 95th prediction interval.

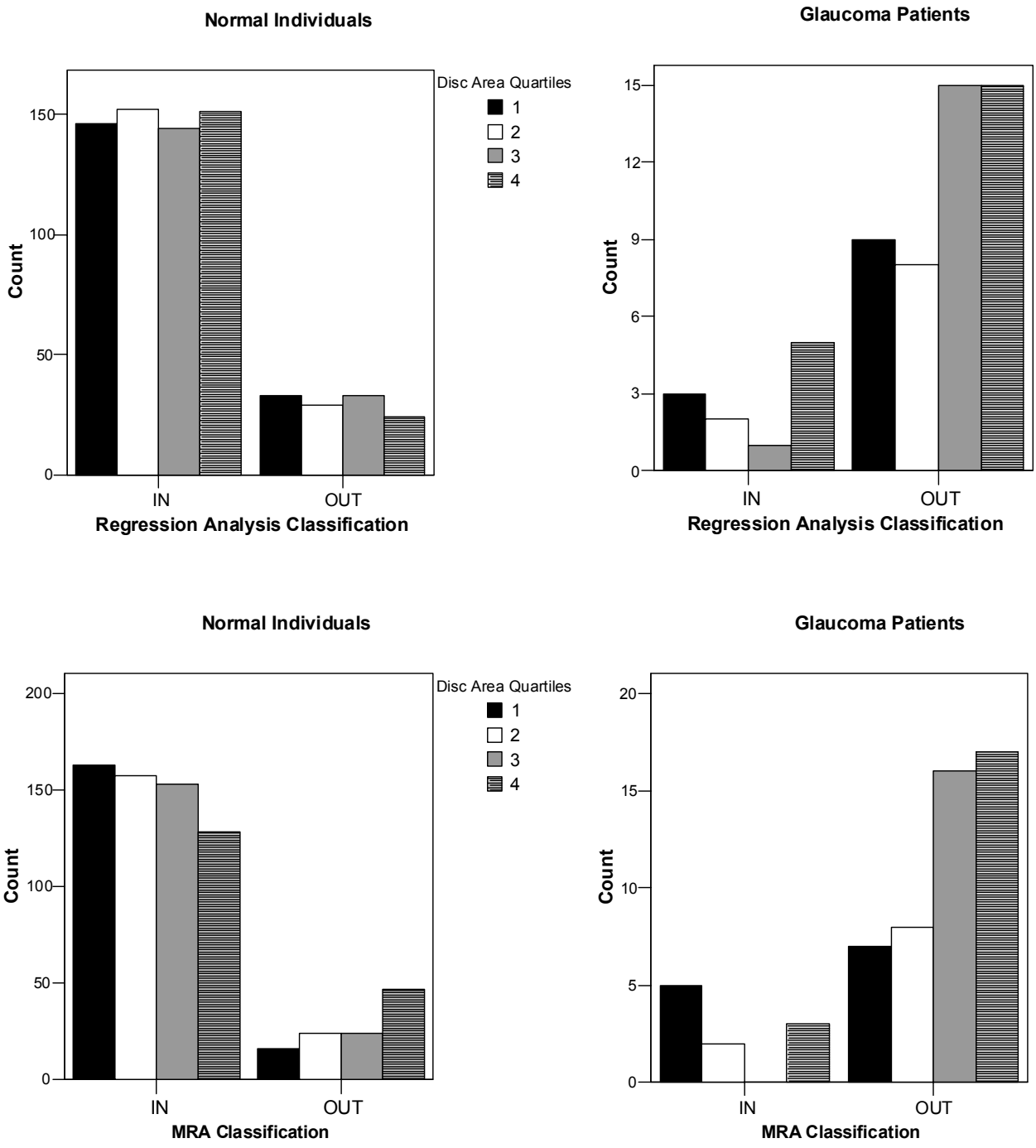

8.4 DISCUSSION

Measurements of the topography of the ONH using HRT II can identify normal and glaucomatous optic discs as separate entities using all HRT parameters. However, there remains considerable overlap between the two groups that reduces the sensitivity of diagnostic algorithms in detecting glaucoma. Using multiple linear regression to correct variability in rim area due to normal variation in disc size, age, sex and reference plane height is able to reduce the overlap between normality and glaucoma to improve sensitivity. Using this approach a diagnostic algorithm with 91.4% specificity and 72.4% sensitivity using the 99% lower prediction limit of normality has been developed. The relationship between rim area and disc area is a complex one, displaying significant heteroscedasticity and non-linearity. Modeling this relationship with linear regression across the entire range of disc size is therefore not appropriate and has resulted in inconsistent sensitivity and specificity of the MRA.[104, 105] With the advantage of a large sample of normal elderly individuals this study was able to construct linear regressions for log rim area and disc area for the four disc area quartile groups. This has significantly reduced the effects of heteroscedasticity on the regression's prediction limits and removed inconsistencies in diagnostic accuracy owing to variation in disc size in the samples of normal subjects and glaucoma patients. Additionally, by including patient sex as a predictor variable in the regression specificity between elderly males and females has been equalised, although interestingly sensitivity was unaffected. This may be due to the effects of age differences on rim area (mean age glaucoma patients 62.6 years, 72.8 years for normals). Sensitivity, however, remains the major limiting factor of the analysis, illustrating the important effect of overlap in rim area measurements between normal and glaucomatous ONHs. This is unsurprising given that the regression only explained 32% of variation in log global rim area in the first disc area quartile group. Additionally, reduction of the wealth of ONH topographic information harvested by HRT to simply 'rim area' may be a significant limiting step in describing differences between normality and GON. More comprehensive descriptors of ONH topography may improve diagnostic

accuracy, previous work using statistical shape analysis techniques having shown promising results in glaucoma detection.[111, 157] Linear discriminant functions offer an alternative way of maximising use of the available topographic information. They employ statistical techniques to select the combination of different HRT parameters that produces maximum separation between normal and glaucomatous ONHs. Whilst they can produce reasonable diagnostic accuracy,[61, 106] they are highly dependent on the particular training sets of data used to produce the function. They therefore do not tend to perform as well on subsequent testing datasets.[107] They are also susceptible to changes in the relationship between topographic parameters and disc area across the range of disc sizes.[61, 104, 108] Having corrected for this problem, the NRA could further be improved by researching the best combination of disc sectors to optimise diagnostic accuracy. The temporal sector offered the lowest sensitivity and its inclusion may unnecessarily reduce specificity. Interestingly, the nasal sectors offered the best sensitivity – a previous study using morphometric evaluation of stereo optic disc photographs found that the nasal rim area offered the lowest diagnostic precision.[160] Wollstein et al. found that the nasal sector offered comparatively poor sensitivity with the MRA.[17] It is uncertain why the NRA should have high sensitivity in the nasal sector, though it may be due to the novel inclusion of reference plane height in the regression model. The reference plane is defined individually from the height of the papillomacular bundle at the disc edge, and is therefore susceptible to variability in ONH contour placement by the investigator. Such random variability may limit the usefulness of rim area in cross-sectional (diagnostic) studies such as this.[57] Reference height inclusion in the multiple regression model may reduce this limitation. Finally, it is possible that a model constructed using the rim/disc area ratio parameter may offer better precision, given that this parameter had the greatest area under ROC curve. Further research is required in this regard.

Image quality was a significant limiting factor in this study, with poor quality images resulting in the exclusion of 19% of normal subjects and 39% of

glaucoma patients. Reasons for poor image quality in the elderly[158] such as cataract[67] and advanced age[71] have been discussed in Section 4.4. The image quality in the glaucoma group was surprisingly poor given that all images were acquired by an experienced, trained operator. Previous work has shown the mean pixel height standard deviation to be worse when imaging glaucomatous optic discs.[55, 63] Any diagnostic algorithm will be of limited usefulness if significant numbers of patients produce unusable images. Another limitation of this study repeats the problem of the difference in ages between the normal and glaucoma groups. Rim area has been previously shown to decline with age, [17, 134, 135, 143] although not all studies have confirmed this.[18, 22, 104] Although age was included for consideration in the regression model it accounted for very small effects in only a few sectors. Thus, this model may predict less rim area for normality in younger glaucoma patients than is the case, therefore accounting for a lower sensitivity in this particular set of glaucoma patients. Using image analysis of stereoscopic disc photographs, another population-based study with a minimum age of 55 years also detected no age effect on ONH parameters.[145] The likely age effect is therefore probably small, but optimum sensitivity using the NRA regression analysis may only be achieved in patients over the age of 65 years.

9.0 Detecting Glaucoma With RADAAR (Rim Area/Disc Area Asymmetry Ratio)

9.1 INTRODUCTION

Asymmetry of neuroretinal rim configuration is a well-recognised component in the diagnosis of glaucoma.[132] It is also a risk factor for progression of ocular hypertensive patients to glaucoma.[151] With the development of digital imaging technologies (such as the Heidelberg Retina Tomograph, HRT) comes the possibility of measuring asymmetry of optic nerve head parameters accurately enough to use asymmetry to discriminate normal and glaucoma. In spite of this potential, only one previous study has examined the usefulness of asymmetry measures in glaucoma diagnosis using HRT.[152] The authors constructed the RADAAR measure (rim area to disc area asymmetry ratio) and found it was significantly correlated with intraocular pressure and degree of glaucomatous optic nerve damage in glaucoma patients. However, they were unable to test the ability of RADAAR to discriminate between normal and glaucoma in the absence of a suitable reference range developed on normal subjects. Chapter 5 details normative RADAAR values based on a population-based sample of normal elderly subjects participating in the Bridlington Eye Assessment Project. By comparing the two eyes of each subject, asymmetry has the potential to reduce parameter variability by providing a measure which accounts for inter-individual variation due to factors such as age,[133-135] sex,[158] disc area,[17, 134] refraction,[135] image acquistion,[72] and contour placement on the optic disc.[57] Thus inter-individual comparisons in cross-sectional (diagnostic) studies may become more valid.

The aim of this study was to develop a diagnostic algorithm using RADAAR and to test its specificity in these normal subjects, and its sensitivity when applied to patients with a new diagnosis of glaucomatous optic neuropathy.

9.2 PATIENTS AND METHODS

9.2.1 Normal Subjects: The Bridlington Eye Assessment Project

BEAP saw it's first subject on 5/11/2002 and had seen 2065 subjects at the start of this study in October 2004. Of these, 880 were defined as normal based on

the criteria stated in Chapter 3. The methodology of subject recruitment, examination and selection is described in full in Chapter 3.

9.2.2 Glaucoma Subjects

95 patients with open angle glaucoma were recruited retrospectively over 2 years from the practice of a glaucoma consultant (SAV) at Queen's Medical Centre, Nottingham (see Section 8.2.2).

9.2.3 Confocal Scanning Laser Ophthalmoscope assessment

Individuals were imaged with HRT II, with the scanner's focus being adjusted according to the individual's refraction, and to obtain the best image. In the normal group, all data were acquired the same day. In the glaucoma group, all images were acquired within 6 months of the index visual field test. One mean topographic image was acquired per eye. The optic disc contour line was drawn on all images by one investigator (MJH) to mark the edge of the optic disc. HRT II then calculated disc area (mm^2), reference height (mm) and further stereometric parameters including rim area (mm^2) and rim/disc area ratio. Each of these parameters was expressed for the global disc, and for 6 individual disc sectors (temporal, temporal superior, temporal inferior, nasal, nasal superior, nasal inferior). Subjects with an image mean pixel height standard deviation greater than 50 microns in either eye were excluded from further analysis. Rim area/disc area asymmetry ratio (RADAAR) was calculated in a similar way to Harasymowycz et al. by dividing the the rim/disc area ratio of the eye with the larger disc by that of the smaller disc.[152] In contrast with Harasymowycz et al., for most analyses this study did not then remove the left hand tail of the histogram by taking the inverse of values less than 1 (smaller rim/disc area ratio in the smaller disc). This preserved any relevant information contained asymmetrically in the right and left sides of the curve. However, in order to plot receiver operating characteristic (ROC) curves, this transformation was performed as a unidirectional measure was required. Disc area ratio was calculated by dividing the area of the larger disc by that of the smaller disc.

9.2.4 RADAAR Diagnostic Algorithm

95% and 99% limits of normality for RADAAR were defined non-parametrically (by percentiles) globally and for each sector based on the ranked values in the sample of normal subjects. Although there was a relationship between RADAAR and disc area asymmetry, this was only significant in two sectors, even then only accounting for approximately 1% of the variance. No attempt was therefore made to account for this relationship using linear regression in the normal tolerances. For any individual, RADAAR for each sector between the 2.5th and 97.5th percentiles of normality was defined 'Within normal limits', between the 0.5th and 2.5th and 97.5th and 99.5th was defined 'Borderline', and outside of the 0.5th or 99.5th percentiles was defined 'Outside normal limits'. Overall status for each individual was equal to the worst status of any of the global or sectoral RADAAR measure. Statistical analyses were undertaken using SPSS for Windows version 12.0.2 (Statistical Package for Social Sciences, SPSS, Inc, Chicago, Illinois). Statistical significance was set at $p<0.05$.

9.3 RESULTS

9.3.1 Study group characteristics

After exclusion of subjects with unacceptable image quality, the final study sample consisted of 622 normal subjects, and 45 patients with glaucoma. These numbers are smaller than those derived from the same datasets in Chapter 8 because the image quality selection criterion (MPHSD less than or equal to 50 microns) was applied bilaterally to each subject. After subjective examination of RADAAR values, 11 normal subjects were further excluded as extreme outliers, leaving 611 normal individuals for further analysis. The exclusion was based on boxplots where extreme outliers were defined as values falling outside of the 3 x interquartile range limit. Characteristics of the two datasets are given in Table 26. Mean age was significantly lower in the glaucoma group compared with the normal subjects (62.1 vs 72.5 years respectively; $p<0.001$, Mann-Whitney U test). Average visual field mean deviation in the worse eye of each of the glaucoma patients was –6.9dB.

9.3.2 RADAAR in normal subjects and glaucoma patients

Table 27 displays RADAAR values for the 611 normal individuals and 45 patients with glaucoma. There was no significant difference in central tendency (mean) of RADAAR between the normal and glaucoma groups. The variance of RADAAR values was consistently significantly greater in the glaucoma group compared with the normal group (Levene statistic for homogeneity of variance $p<0.001$ for all sectors; shown graphically for the nasal-superior sector in Figure 19). There was no significant difference in central tendency (mean) or variance of any RADAAR measure between normal males and females. No significant correlation was found between any RADAAR measure in the normal group and age. Small but significant negative correlations were found between RADAAR in normals and disc area ratio only in the global and nasal sectors (Pearson's $r=-0.12$, $p=0.004$ and -0.09, $p=0.03$ respectively). No significant correlation between age and any RADAAR measure was found in the glaucoma group. Males and females with glaucoma showed no difference in central tendency of any RADAAR, however variance was greater in males than females for all RADAAR measures, reaching significance in the temporal-inferior and nasal-inferior sectors (Levene statistic for homogeneity of variance 14.3, $p<0.001$ and 5.1, $p=0.03$ respectively).

Table 28 displays the area under ROC curves for the global and sectoral RADAAR measures when used to discriminate between the normal and glaucoma subjects (ROC curves for selected RADAAR measures plotted in Figure 20). The global RADAAR measure had the greatest area under ROC curve, with the temporal measure having the smallest area.

Table 26. Characteristics of the study samples (mean+/-SD).

	Normal (n=611)	**Glaucoma** (n=45)	***P* Value***
Age (years)	72.5(4.8)	62.1 (14.1)	<0.001
Male:Female (%)	44:56	60:40	

* Mann-Whitney U test

Table 27. Global and sectoral RADAAR measures in 611 normal subjects and 45 patients with glaucoma (mean +/-SD).

Parameter	**Normals**	**Glaucoma**	**P value***
G RADAAR	0.97(0.11)	1.06(0.43)	0.23
T RADAAR	0.98(0.28)	1.12(0.76)	0.91
TS RADAAR	0.98(0.19)	1.10(0.67)	0.47
TI RADAAR	0.98(0.22)	1.56(1.79)	0.52
N RADAAR	0.99(0.10)	1.07(0.50)	0.55
NS RADAAR	0.98(0.13)	1.15(0.75)	0.48
NI RADAAR	1.00(0.13)	1.08(0.43)	0.99

* Student's t test

Table 28. Area Under ROC Curves and Sensitivities (Sn) at Fixed Specificities (Sp) for Discrimination Between Normal subjects (n=611) and Patients With Glaucoma (n=45).

Parameter	**ROC Curve Area (SE)**	**Sn/Sp (Sp>95%)**	**Sn/Sp (Sp>80%)**
G RADAAR	0.81(0.04)	42/95	71/80
T RADAAR	0.65(0.05)	22/95	42/80
TS RADAAR	0.73(0.04)	42/95	49/80
TI RADAAR	0.79(0.04)	36/95	58/80
N RADAAR	0.79(0.04)	40/95	64/80
NS RADAAR	0.74(0.05)	44/95	56/80
NI RADAAR	0.77(0.04)	33/95	56/80

Figure 19. Boxplot comparing nasal-superior RADAAR measure in 611 normal subjects and 45 patients with glaucoma. Bold horizontal line indicates median value, box extent indicates interquartile range, circles represent outliers and asterisks represent extreme cases.

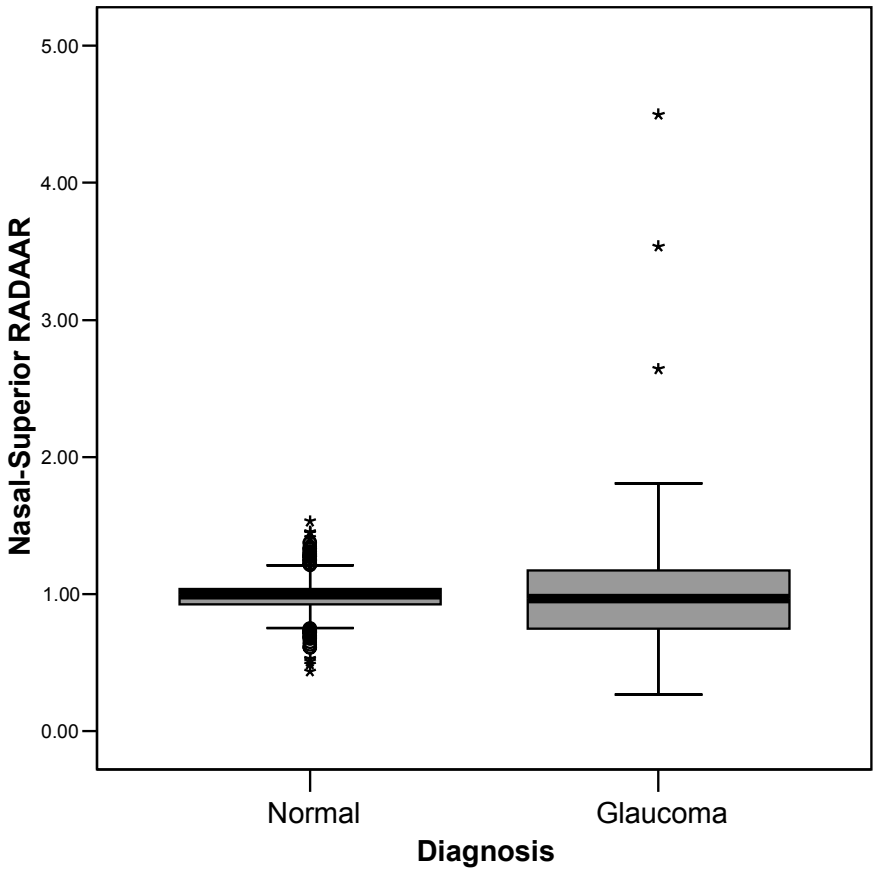

Figure 20. Receiver operating characteristic (ROC) curves for Global, Temporal and Temporal-Inferior RADAAR in discriminating 622 normal subjects and 45 patients with glaucoma.

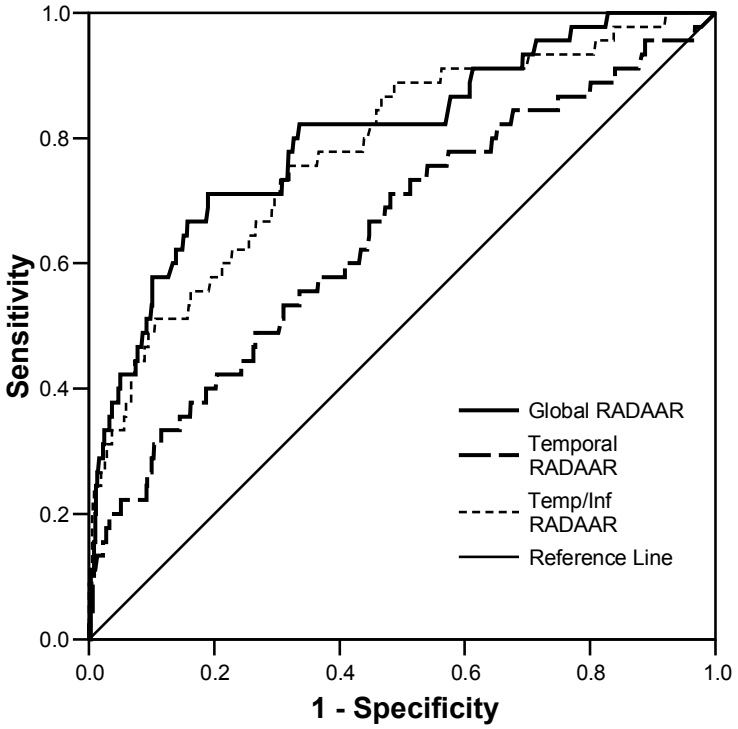

9.3.3 RADAAR Diagnostic Algorithm

Table 29 displays summary classification based on this scheme for 611 normal subjects and 45 patients with glaucoma. The best discriminating sector was the global classification with a specificity of 95.1% and sensitivity of 42.2% at the 95% limit of normality. The overall classification returned a specificity of 78.5% and a sensitivity of 80.0% at the 95% limit of normality. Chi-square tests revealed highly significant associations between diagnostic classification and actual diagnosis in all sectors and for both sexes (p<0.001). Figure 21 compares the results of the overall classification for each sex in the normal and glaucoma groups. In normal individuals the overall classification defined 77.2% of males and 79.6% of females as 'Within normal limits'. In glaucoma patients the overall

classification defined 63.0% of males and 44.4% of females as 'Outside normal limits'. This trend to increased specificity and decreased sensitivity in females compared with males was not statistically significant (Chi square 0.69 with 2 degrees of freedom, *p*=0.71 in normals, 1.71 with 2 degrees of freedom, *p*=0.43 in glaucoma patients). No statistically significant relationship was found between disc area asymmetry (when ranked in 2 groups by the median value) and overall classification based on RADAAR (at the 99% limits of normality; Chi square 1.18, *p*=0.28 and Chi square with continuity correction 0.59, *p*=0.44 in the normal and glaucoma groups respectively). The effect of asymmetry in visual field index mean deviation on sensitivity was assessed by grouping difference in mean deviation in glaucoma patients into 2 ranks by the median value (median difference MD 2.3dB, minimum 0.0, maximum 19.0dB). Of 22 glaucoma patients with difference in MD of 2.3dB or less, 9 were 'outside normal limits. Of 21 patients with a difference in MD of greater than 2.3dB, 15 were 'outside normal limits' (X^2_{trend} 3.96, *p*=0.05).

Table 29. Summary Classification of Disc Sectors by RADAAR limits of normality. Results (%) are shown for 611 normal elderly subjects and 45 patients with glaucoma (in parentheses). Results are shown for all disc sectors and for the overall analysis. RADAAR values within the central 95% of normative values were classed 'Within normal limits', between the 95% and 99% limits, 'Borderline' and outside the 99% limits, 'Outside normal limits'.

RADAAR Result (%)	Global	Temp	TS	TI	Nasal	NS	NI	Overall
Within normal limits	95.1 (57.8)	95.1 (75.6)	95.1 (60.0)	95.1 (60.0)	95.1 (57.8)	94.9 (64.4)	95.1 (64.4)	78.5 (20.0)
Borderline	3.9 (11.1)	3.9 (6.7)	3.9 (13.3)	3.9 (13.3)	3.9 (24.4)	4.3 (17.8)	3.9 (8.9)	16.6 (24.4)
Outside normal limits	1.0 (31.1)	1.0 (17.8)	1.0 (26.7)	1.0 (26.7)	1.0 (17.8)	0.8 (17.8)	1.0 (26.7)	4.9 (55.6)

TS Temporal/superior
TI Temporal/inferior
NS Nasal/superior
NI Nasal/inferior

Figure 21. Overall classification by sex according to RADAAR limits of normality. Results are shown for 611 normal elderly subjects and 45 patients with glaucoma.

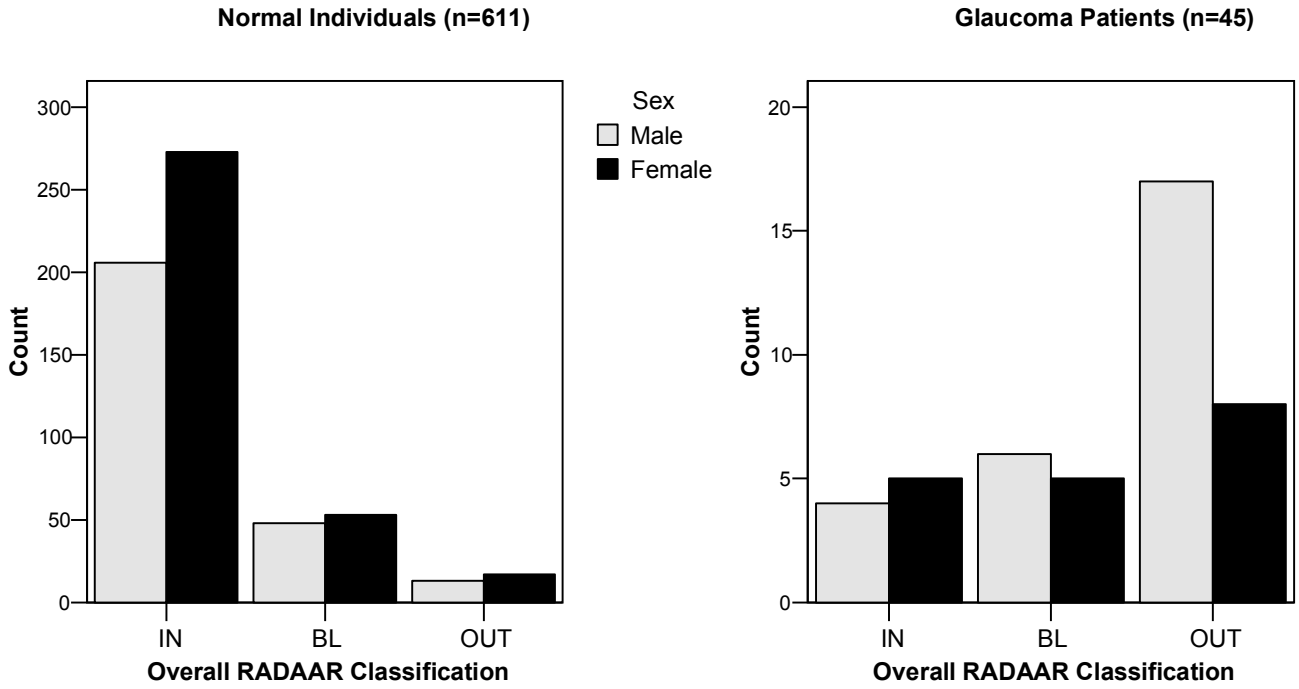

9.4 DISCUSSION

This study indicates that asymmetry in rim/disc area ratio can detect glaucoma with a sensitivity of 80% and specificity of 78.5% at the 95% limit of normality. At the 99% limit specificity rose to 95.1% with a sensitivity of 55.6%. The relatively low sensitivity reflects the overlap in RADAAR between normal and glaucoma (illustrated in Figure 19) indicating that symmetry is common in early to moderate glaucoma. In this study, RADAAR in normal subjects showed no correlation with age or sex, and only a very small correlation with disc size asymmetry. It might be therefore expected that this diagnostic tool will perform similarly if tested in other Caucasian populations because of the consistency of the measure. Further studies are needed to confirm this. As RADAAR variance was greater in glaucoma than normal for all disc sectors they were all included in the diagnostic model. However, ROC curves revealed that not all sectors were equally accurate in discriminating normal and glaucoma. Further research

is required to determine the best combination of sectors to optimise specificity and sensitivity. In glaucoma patients, males exhibited significantly greater RADAAR variance than females in the temporal-inferior and nasal-inferior sectors, although the differences in sensitivity and specificity of the overall diagnostic method were not significant using a Chi square test. No other studies demonstrating a sex difference in optic nerve head asymmetry in glaucoma patients were found. Further studies are required to confirm this finding in other populations. Previous research has also demonstrated utility in structural asymmetry measures in glaucoma. RADAAR correlates with the severity of open angle glaucoma,[152] and cup asymmetry is a risk factor for conversion from ocular hypertension to glaucoma.[151, 161] Functional asymmetry in visual evoked potential perimetry can also detect early glaucoma.[162] However, the Blue Mountains Eye Study found that vertical cup/disc ratio (CDR) asymmetry was not useful in identifying patients with glaucoma.[153] The study measured optic disc parameters from stereo photographs, and derived asymmetry measures by subtracting the value of the right eye from that of the left eye. Possible reasons for the insensitivity of the method include the consideration of only vertical CDR asymmetry that may miss glaucoma manifesting in other disc sectors. Additionally, as argued in Chapter 5, asymmetry should be calculated on a bigger disc/smaller disc comparison, rather than on a right/left basis.[163] This ensures that the greater increase in cup size compared with rim size in bigger discs does not introduce additional 'noise' into the asymmetry measure.

Image quality was a significant limiting factor in this study, with poor quality images resulting in the exclusion of 29% of normals and 53% of glaucoma patients. This issue is discussed in Section 8.4. Another limitation of this study was the lack of data on refractive status. The Blue Mountains Eye Study found significant anisometropia (defined as greater than or equal to 1.0D spherical equivalent difference between eyes) in 14.7% of older individuals, with higher rates found in more elderly individuals and those with cataract.[164] Anisometropia may cause differential effects on image size, thus introducing inconsistency into

the RADAAR measure. However, by dividing rim area by disc area, it is anticipated that the ratio of rim/disc area asymmetry should remain relatively unaffected.

10.0 The Optic Disc Hemifield Test

10.1 INTRODUCTION

Characterisation of optic nerve head (ONH) topography is integral to the diagnosis of glaucoma. However, clinical evaluation of the ONH, even by expert observers, can produce marked disagreement in the diagnosis of glaucomatous optic neuropathy (GON).[118, 154] Objective imaging systems, such as the Heidelberg Retina Tomograph (HRT II), provide reproducible ONH measurements and offer improved accuracy in ONH evaluation.[55, 165] Glaucoma is evaluated on the basis of functional as well as structural test results. The Glaucoma Hemifield Test (GHT) was developed to provide a comparative analysis of clusters of test points throughout the superior and inferior visual hemifields to reveal any asymmetry.[166] As a structural counterpart to the functional GHT Jonas et al. constructed the 'Optic Disc Hemifield Test'.[167] Using optic nerve head measurements morphometrically derived from stereo optic disc photographs, they compared superior and inferior neuroretinal rim parameters, corresponding to the upper and lower visual hemifield responses. Using the neuroretinal rim width and area ratios the optic disc hemifield test had, at best, poor sensitivity (25.2%) at a specificity of 80%. They concluded that their test was not helpful in the morphometric diagnosis of GON. However, whilst stereoscopic optic disc photograph measurements offer improved repeatability of ONH measurements[118, 168] interobserver and intraobserver agreement are much better using HRT than planimetry techniques.[57, 77] HRT may also be capable of detecting glaucoma with greater sensitivity than by clinically assessing stereoscopic ONH photographs,[101] although not all studies repeated this finding.[119] This study therefore aimed to determine whether the Optic Disc Hemifield test might display greater diagnostic accuracy if constructed using HRT parameters.

10.2 PATIENTS AND METHODS

10.2.1 Normal Subjects: The Bridlington Eye Assessment Project

BEAP saw it's first subject on 5/11/2002 and had seen 2065 subjects at the start of this study in October 2004. Of these, 880 were defined as normal based on

the criteria stated in Chapter 3. The methodology of subject recruitment, examination and selection is described in full in Chapter 3.

10.2.2 Glaucoma Patients

95 patients with open angle glaucoma were recruited retrospectively over 2 years from the practice of a glaucoma consultant (SAV) at Queen's Medical Centre, Nottingham (see Section 8.2.2).

10.2.3 Confocal Scanning Laser Ophthalmoscope assessment

Individuals were imaged with HRT II, with the scanner's focus being adjusted according to the individual's refraction, and to obtain the best image. The optic disc contour line was drawn on all images by one investigator (MJH). HRT II then calculated disc area (mm^2), reference height (mm) and further stereometric parameters including rim area (mm^2) and rim/disc area ratio. Each of these parameters were expressed for the global disc, and for 6 individual disc sectors (temporal, temporal superior, temporal inferior, nasal, nasal superior, nasal inferior). Subjects with an image mean pixel height standard deviation greater than 50 microns in either eye were excluded from further analysis.

10.2.4 Optic disc hemifield parameter calculations

The ratios (superior/inferior) for temporal-superior/temporal-inferior (TS/TI) and nasal-superior/nasal-inferior (NS/NI) rim area and rim/disc area ratio were derived. The TS/TI ratio and NS/NI ratio comprised the two elements of the optic disc hemifield parameter. To construct the area under receiver-operating characteristic (ROC) curves a transformation was performed such that ratio values were all greater than 1 (the inverse function of any values less than 1). Statistical analyses were undertaken using SPSS 12.0.2 (Statistical Package for Social Sciences, SPSS, Inc, Chicago, Illinois).

10.3 RESULTS

10.3.1 Study group characteristics

After exclusion of subjects with unacceptable image quality, the final study sample consisted of 721 normal subjects, and 58 patients with glaucoma. Characteristics of the datasets are given in Table 30. Mean age was significantly

lower in the glaucoma group compared with the normal individuals (62.6 vs 72.8 years respectively; $p<0.001$). In the glaucoma dataset mean (SD) MD of the visual field test closest to the date of HRT imaging was –5.7 (5.1) dB (range –0.2 to –23.0 dB). Corresponding mean (SD) PSD was 6.6 (3.3) dB (range 1.8 to 13.8 dB).

10.3.2 Rim parameter measurements

Rim area and rim/disc area ratio measures were consistently significantly less in the glaucoma group (Table 31). In normal subjects, rim area was significantly less in males compared with females in the TI sector; rim/disc area ratio was significantly less in males compared with females in all disc sectors (TS, TI, NS, NI; $p<0.05$). There was no significant correlation between any rim-related parameter and subject age.

Table 30. Characteristics of the study populations (Mean (SD))

	Normal subjects (n=712)	**Glaucoma patients (n=58)**	***P****
Age	72.8(4.9)	62.6(13.7)	<0.001
Male:Female (%)	42:58	57:43	
Right:Left eyes (%)	49:51	64:36	
MPHSD (microns)	24.0(10.1)	28.9(10.0)	0.002

MPHSD Mean Pixel Height Standard Deviation

* Mann-Whitney U Test

10.3.3 Optic Disc Hemifield Parameters

Mean ratio of superior/inferior rim/disc area ratio did not differ significantly between the sexes in the temporal (TS/TI) or nasal (NS/NI) hemidisc, although the variance of these measures was greater in males than females (TS/TI standard deviation 0.24 and 0.23, NS/NI standard deviation 0.16 and 0.12 in males and females respectively, Levene test of homogeneity of variance $p<0.01$). The spread of superior/inferior ratio values was greater in the glaucoma

group than the normal group (Table 32; Figure 22). Areas under the ROC curves for the direct sectoral rim-related measurements, along with the ratio TS/TI and NS/NI, separately and together, are given in Table 33.

10.3.4 Diagnostic Algorithm for Optic Disc Hemifield test

Using the normal dataset, 95% and 99% limits of normality were constructed for the ratio of TS/TI and NS/NI rim/disc area ratios. These limits were calculated separately for males (n=301) and females (n=420). Specificity and sensitivity was similar for TS/TI RDAR and NS/NI RDAR when these limits were used to detect glaucoma. Sensitivity was found to be much better when limits of normality were considered for the TS/TI and NS/NI RDAR ratios separately compared with combining the values into superior/inferior (TS+NS/TI+NI) RDAR ratio (Table 34). Patient sex had no significant effect on the chance of being classified normal or glaucoma for any of the parameters. Of the 58 glaucoma patients, 42 had a visual field mean deviation of up to -6 decibels (mild), 9 of up to -12 decibels (moderate), and 7 of greater than -12 decibels (severe). Sensitivity of the optic disc hemifield test did not differ significantly between these categories (at the 95% level of normality sensitivity was 57.1% in the mild group, 33.3% in the moderate group, and 42.9% in the severe group; X^2=2.37 with 4 degrees of freedom, *p*=0.47).

Table 31. Mean (SD) of selected HRT II parameters. Results are for 721 normal elderly subjects and 58 patients with glaucoma.

Parameter	**Normal**	**Glaucoma**	***P****
TS disc area (mm^2)	0.25 (0.05)	0.26 (0.06)	0.03
TS rim area (mm^2)	0.18 (0.04)	0.12 (0.05)	<0.001
TS rim/disc area ratio	0.76 (0.17)	0.48 (0.22)	<0.001
TI disc area (mm^2)	0.26 (0.05)	0.28 (0.06)	0.02
TI rim area (mm^2)	0.20 (0.05)	0.12 (0.06)	<0.001
TI rim/disc area ratio	0.76 (0.17)	0.45 (0.22)	<0.001
NS disc area (mm^2)	0.25 (0.05)	0.26 (0.06)	0.17
NS rim area (mm^2)	0.21 (0.04)	0.15 (0.05)	<0.001
NS rim/disc area ratio	0.87 (0.13)	0.61 (0.22)	<0.001
NI disc area (mm^2)	0.24 (0.05)	0.25 (0.06)	0.10
NI rim area (mm^2)	0.21 (0.04)	0.17 (0.05)	<0.001
NI rim/disc area ratio	0.90 (0.12)	0.68 (0.17)	<0.001

* Mann-Whitney U Test
TS temporal-superior
TI temporal-inferior
NS nasal-superior
NI nasal-inferior

Table 32. Mean (SD) of the comparison of superior and inferior rim area and rim/disc area ratio in 721 normal subects and 58 glaucoma patients.

Parameter	Normal	Glaucoma
Ratio TS/TI rim area	0.97 (0.24)	1.24 (0.92)
Ratio NS/NI rim area	1.03 (0.18)	0.95 (0.34)
Ratio TS/TI rim/disc area ratio	1.02 (0.23)	1.31 (0.98)
Ratio NS/NI rim/disc area ratio	0.98 (0.14)	0.91 (0.30)

TS Temporal/Superior
TI Temporal/Inferior
NS Nasal/Superior
NI Nasal/Inferior

Figure 22. Boxplots displaying the ratio of superior and inferior rim/disc area ratio in 721 normal individuals and 58 glaucoma patients. Results shown for the temporal (TS/TI) (1a) and the nasal (NS/NI) hemidisc (1b).

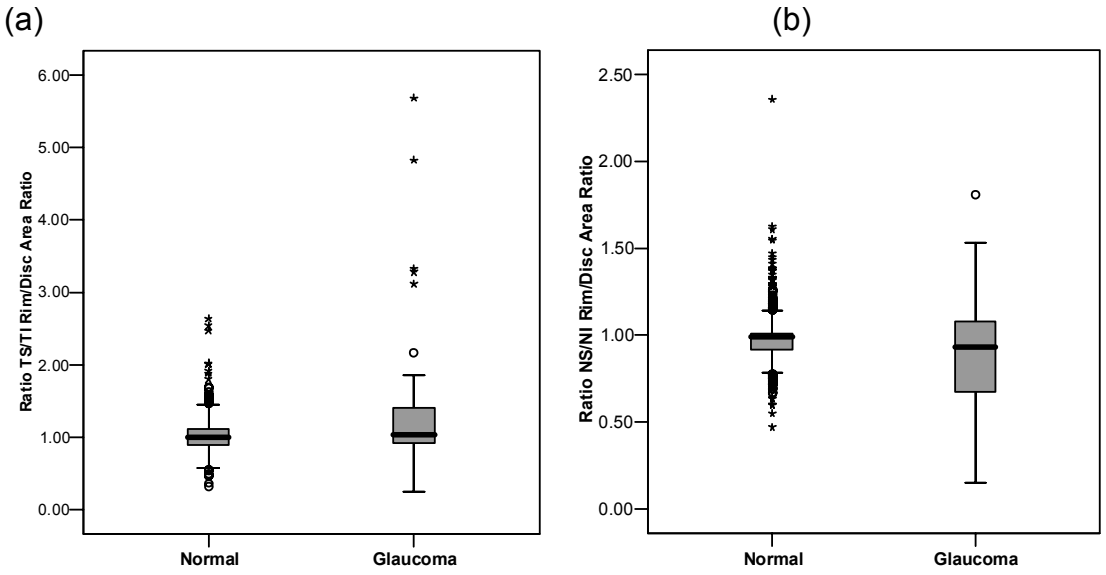

Table 33. Areas under the receiver-operating characteristic (ROC) curves for different HRT II optic disc parameters. Results based on 721 normal subjects and 58 glaucoma patients.

Parameter	**Area under ROC curve (SE)**	**Sn/Sp (Sp>95%)**	**Sn/Sp (Sp>80%)**
TS rim area (mm^2)	0.81 (0.03)	52/95	64/80
TS rim/disc area ratio	0.85 (0.03)	52/95	76/80
TI rim area (mm^2)	0.83 (0.03)	48/95	72/80
TI rim/disc area ratio	0.87 (0.03)	52/95	78/80
NS rim area (mm^2)	0.82 (0.03)	53/95	71/80
NS rim/disc area ratio	0.84 (0.03)	59/95	74/80
NI rim area (mm^2)	0.75 (0.04)	38/95	53/80
NI rim/disc area ratio	0.85 (0.03)	38/95	76/80
Ratio TS/TI rim/disc area ratio	0.66 (0.04)	26/95	45/80
Ratio NS/NI rim/disc area ratio	0.75 (0.04)	40/95	59/80
Ratio superior/inferior rim/disc area ratio*	0.72 (0.04)	36/95	53/80

TS Temporal/Superior
TI Temporal/Inferior
NS Nasal/Superior
NI Nasal/Inferior
* =TS+NS/TI+NI rim/disc area ratio

Table 34. Sensitivity and specificity using the rim/disc area ratio for different disc sectors to discriminate normal (n=712) from glaucoma (n=58) testing at the 95% limit of normality. Numbers in parentheses represent limits at 99% cut offs.

Parameter	**Sensitivity (%)**	**Specificity (%)**
Sup/Inf RDAR	36.2 (22.4)	95.3 (99.2)
TS/TI RDAR	32.8 (19.0)	95.3 (99.2)
NS/NI RDAR	36.2 (15.5)	95.1 (99.2)
Ratio TS/TI and NS/NI combined RDAR	51.7 (27.6)	91.7 (98.3)

Sup Superior (=TS+NS)
Inf Inferior (=TI+NI)
TS Temporal Superior
TI Temporal Inferior
NS Nasal Superior
NI Nasal Inferior
RDAR Rim/disc area ratio

10.4 DISCUSSION

The morphology of the ONH correlates with the presence of glaucomatous visual field defects.[87-91] Unsurprisingly, this correlation is stronger when analysed for ONH sectors compared with the global ONH analysis.[92] As the comparison of the superior and inferior visual fields in the GHT is a useful and highly sensitive and specific test,[166] it would seem logical that a similar comparison of the superior and inferior neuroretinal rims of the optic disc may be helpful, and as ONH changes predate field losses, may allow for earlier detection of GON. Using data obtained by HRT II a new optic disc hemifield test has been constructed with an overall specificity of 91.7% and sensitivity of 51.7% at the 95% limit of normality. Diagnostic performance was significantly better than that derived by Jonas et al. (sensitivity of 25.2% at a specificity of 80%) using planimetric measurements from stereoscopic optic disc photographs.[167] One reason for this may be the greater accuracy and

reproducibility of HRT.[55, 165] Another improvement may lie in the use of rim/disc area ratio which more accurately reflects changes in rim area due to GON as opposed to interindividual differences in disc area. Additionally, HRT allowed construction of a test with greater resolution, since the temporal and nasal hemifields could be separately compared (confirmed in this study, Table 33). Other advantages of HRT over planimetry are objectivity in follow-up examinations, the fast availability of results, ability to gain good quality images without pupillary dilation, and that HRT examination is a reproducible, semiautomated technique which can be used by non medical staff.[63, 169-172] The test cannot be conducted using HRT or planimetry interchangeably, since ONH parameters can differ significantly between these techniques.[115, 116, 173]

Jonas et al. concluded that the test is not markedly helpful in diagnosing GON. Whilst not offering diagnostic accuracy sufficient for use alone as a test for glaucoma, we conclude that with HRT this test is moderately capable of detecting the disease. As such, it is possible that it may significantly contribute to glaucoma detection when used in combination with other morphometric discriminators such as the Moorfields Regression Analysis.[17] Further research is required in this regard. As the test is more likely to be useful in early disease, it is interesting that the sensitivity of the test tended to be greater in early glaucoma compared with later stages, although not to statistically significant levels. This is perhaps the opposite of what may be expected. This finding may be artefactual due to the small numbers of patients with moderate and severe glaucoma in this study. It may also reflect differences in the relationship between structural and functional parameters for each individual compounded by the small sample size. Alternatively, this might suggest that as glaucoma becomes more advanced the ONH is more generally involved and differences between the superior and inferior sectors equalise.[37] A similar phenomenon can be seen in those with advanced glaucoma but normal GHT.[174]

A key advantage of this study lies in the definition of normality. The Bridlington Eye Assessment Project[158] provides a population-based cohort of elderly normal subjects, mean age 72.8 (compared to Jonas' previous study with a mean age of 45.4 for the normal group[167]) Thus, the age profile of subjects defining normal tolerances is more representative of those who develop acquired glaucoma.[132] However, as stated previously, a limitation of this study lies in its selection of cases with glaucoma. These were drawn from a highly selected sample found within the glaucoma clinic setting. Thus, the demographic profile of glaucoma patients was significantly different from the normative subjects. This will inevitably create confounds that affect the estimation of test sensitivity. The true sensitivity of the optic disc hemifield test may be lower than the 52% in this study, although further studies in different demographic settings are required to confirm this.

Image quality was another significant limiting factor in this study, with poor quality images resulting in the exclusion of 19% of normals and 39% of glaucoma patients. This issue has been discussed in previous chapters.

11.0 Combined Use of Three Diagnostic Algorithms to Detect Glaucoma Using the Heidelberg Retina Tomograph

11.1 INTRODUCTION

Heidelberg Retina Tomography (HRT) is an objective means of characterising the optic nerve head (ONH) with superior inter-observer repeatability over planimetry,[77] and less dependence upon operator experience.[57] The major advantage of HRT is its ability to employ objective statistical determinants of normality by which to discriminate normality from glaucoma. One such technique, the Moorfields Regression Analysis (MRA), uses linear regression modelling of rim area to correct for the effects of disc size and age, and can achieve specificities of 94-96%, with lower sensitivities of 74-84%,[17, 100] although a variable diagnostic accuracy across the disc size range. [104, 105] It is reported that this approach may be more sensitive than expert clinical evaluation in detecting glaucoma.[101] A modified linear regression analysis using normative data from an elderly population examined by the Bridlington Eye Assessment Project (BEAP; Nottingham correction of the MoorfieldsRegression Analysis, NRA) is presented in Chapter 8.[175] This addressed the issue of variable diagnostic accuracy across the disc size range as determined by the MRA to produce an algorithm with constant diagnostic accuracy independent of disc size.

In addition, two further statistical evaluations of the ONH using HRT morphometric data have been developed. The rim area/disc area asymmetry ratio (RADAAR, first described by Harasymowycz et al.[152]) compares the rim/disc area ratio in the bigger disc with that in the smaller disc (See Chapter 9). Using this concept normative ranges were calculated based on data from BEAP[163] to produce an optic disc asymmetry diagnostic algorithm with a specificity of 95.1% and sensitivity of 55.6%.[176] A further test, the optic disc hemifield test (ODHT, first described by Jonas et al. using planimetric data[167]) was also developed using HRT normative data from BEAP (See Chapter 10). Whilst only offering moderate sensitivity (51.7%) at an acceptable specificity of 91.7%, this was a considerable improvement on the diagnostic accuracy

produced using planimetric data.[167] It was concluded that the test would not be useful in isolation, but may combine with other ONH diagnostic algorithms in a useful and complementary fashion.

Reducing the wealth of topographic data harnessed by HRT into simply 'rim area' or 'RADAAR' or 'ODHT' risks limiting sensitivity by discarding much topographic information. This study aimed to assess whether these three diagnostic algorithms may be usefully combined to complementarily enhance diagnostic accuracy. For statistical reasons, most studies evaluate diagnostic tests on one eye randomly selected from each study subject. However, glaucoma may be a unilateral condition, and patients, being usually in possession of two eyes, are often referred to glaucoma specialists with asymmetric or unilaterally suspicious ONHs. Therefore, this study also aimed to assess the specificity and sensitivity of the diagnostic algorithms when applied to both eyes of each subject compared with only one randomly selected eye.

11.2 PATIENTS AND METHODS

11.2.1 Normal Subjects: The Bridlington Eye Assessment Project

BEAP saw it's first subject on 5/11/2002 and had seen 2065 subject at the start of this study in October 2004. Of these, 880 were defined as normal based on the criteria stated in Chapter 3. The methodology of subject recruitment, examination and selection is described in full in Chapter 3.

11.2.2 Glaucoma Patients

95 patients with open angle glaucoma were recruited retrospectively over 2 years from the practice of a glaucoma consultant (SAV) at Queen's Medical Centre, Nottingham (see Section 8.2.2).

11.2.3 Confocal Scanning Laser Ophthalmoscope assessment

Individuals were imaged with HRT II, with the scanner's focus being adjusted according to the individual's refraction, and to obtain the best image. The optic disc contour line was drawn on all images by one investigator (MJH). HRT II then calculated disc area (mm2), reference height (mm) and further stereometric

parameters including rim area (mm2) and rim/disc area ratio. Each of these parameters were expressed for the global disc, and for 6 individual disc sectors (temporal, temporal superior, temporal inferior, nasal, nasal superior, nasal inferior). Subjects with an image mean pixel height standard deviation greater than 50 microns in either eye were excluded from further analysis. The diagnostic algorithms described were generated using data from one randomly selected eye from each normal subject (RADAAR was generated using both eyes). The algorithms were applied individually and in combination to study subjects in two analyses: A uniocular analysis where one eye was randomly selected from each subject for analysis and a binocular analysis where both eyes were subjected to analysis simultaneously. The RADAAR algorithm, which comprises one test per patient involving both eyes, was included in both the uniocular and binocular analyses. All statistical analyses were undertaken using SPSS 12.0.2 (Statistical Package for Social Sciences, SPSS, Inc, Chicago, Illinois).

11.2.4 Linear regression analysis

The development of this diagnostic algorithm is described in Section 8.2.4.

11.2.5 RADAAR diagnostic algorithm

The development of this diagnostic algorithm is described in Section 9.2.4.

11.2.6 Optic disc hemifield test

The development of this diagnostic algorithm is described in Section 10.2.4.

11.2.7 Combination of the diagnostic algorithms

The three different algorithms were applied according to the OR logic function for disease, and the AND function for normality. Thus, an eye was considered ‘disease’ if it was diagnosed ‘outside normal limits’ by any of the three algorithms. Eyes that were diagnosed ‘within normal limits’ by all three algorithms were classed as normal. Using this method of combining tests, the sensitivity of the combined test will be at least as great as that of the most sensitive component test, and the specificity of the combined test will be no greater than the component test with the lowest specificity. The tests were not

combined in a probabilistic fashion as it was anticipated that a degree of interdependence (convergence) would exist between the tests.

11.3 RESULTS

11.3.1 Study group characteristics

After exclusion of subjects with unacceptable image quality, the final study sample consisted of 622 normal subjects, and 45 patients with glaucoma with acceptable images in both eyes (MPHSD less than 50 microns). In the Uniocular Analysis a greater number of subjects were included in the normal and glaucoma groups (721 and 58 individuals respectively) since only the study eye of each subject was required to meet the image quality criteria. On average, the normal subjects were older than the glaucoma patients (mean(SD) age 72.5(4.8) and 62.1(14.1) years respectively, $P<0.001$, Mann-Whitney U test). Average visual field mean deviation in the worse eye of each of the glaucoma patients was –6.9dB.

11.3.2 Uniocular Analysis

The specificity and sensitivity of the three separate diagnostic algorithms applied to one randomly selected eye from each subject is examined in Table 35. The values for the RADAAR measure are included here since this comprises one measure per patient. The NRA and RADAAR had similar specificities at the 99% limit, though RADAAR maintained a lower sensitivity than the NRA at this limit (51.7% and 72.4% respectively). The ODHT had the highest specificity but the lowest sensitivity of the three algorithms (98.5% and 27.6% at the 99% limit respectively).

The specificity and sensitivity of different combinations of the three diagnostic algorithms is given in Table 36. Combining the RADAAR and NRA algorithms resulted in a 5.2% decrease in specificity and a 13.8% increase in sensitivity at the 99% limit compared with NRA alone. Further combining the ODHT with the other two algorithms gave no further increase in sensitivity with a small drop in specificity. These results are displayed graphically in Figure 23.

11.3.3 Binocular Analysis

The specificity and sensitivity of the three separate diagnostic algorithms applied simultaneously to both eyes of each subject is given in Table 37. Applying the NRA to both eyes resulted in a 6.2% reduction in specificity with a 9.8% rise in sensitivity at the 99% limit compared with uniocular application. Applying the ODHT to both eyes resulted in a 2% drop in specificity with a 12.3% rise in sensitivity at the 99% limit compared with uniocular application.

The specificity and sensitivity of different combinations of the three diagnostic algorithms is given in Table 38. Applying all three algorithms on a binocular basis at the 99% limit achieved a specificity of 82.8% with a sensitivity of 88.9%. The inclusion of the ODHT made almost no difference to the overall diagnostic accuracy. Application of the combination of NRA and RADAAR on a binocular basis resulted in a 2.6% drop in specificity with a 2.7% rise in sensitivity at the 99% level compared with uniocular application. Combining RADAAR with the NRA when applied binocularly (at the 99% level) resulted in a 1.6% drop in specificity with a 6.7% rise in sensitivity compared with NRA alone applied binocularly. These results are displayed graphically in Figure 24. Positive and negative predictive values of the three separate diagnostic algorithms at the 99% limit are compared in uniocular and binocular application in Table 39.

Table 35. Uniocular specificity and sensitivity of three different diagnostic algorithms at the 95% and 99% limits of normality. Results based on one eye randomly selected from 721 normal elderly subjects and 58 patients with glaucoma.

Algorithm	**Specificity (%)**		**Sensitivity (%)**	
	95%	**99%**	**95%**	**99%**
NRA	82.9	90.8	81.0	72.4
RADAAR	74.6	93.0	75.8	51.7
ODHT	91.7	98.5	51.7	27.6

Table 36. Uniocular specificity and sensitivity of different combinations of the three diagnostic algorithms at the 95% and 99% limits of normality. Results based on one eye randomly selected from 721 normal elderly subjects and 58 patients with glaucoma.

Algorithm	Specificity (%)		Sensitivity (%)	
	95%	99%	95%	99%
NRA/RADAAR/ODHT	65.9	85.4	93.1	86.2
NRA/RADAAR	67.4	85.6	91.4	86.2
NRA/ODHT	80.6	90.7	84.5	72.4
RADAAR/ODHT	70.7	91.4	84.5	62.1

Table 37. Binocular specificity and sensitivity of three different diagnostic algorithms at the 95% and 99% limits of normality. Results based on 622 normal elderly subjects and 45 subjects with glaucoma.

Algorithm	Specificity (%)		Sensitivity (%)	
	95%	99%	95%	99%
NRA	73.8	84.6	86.6	82.2
RADAAR	74.6	93.0	75.8	51.7
ODHT	85.7	96.5	75.6	40.0

Table 38. Binocular specificity and sensitivity of different combinations of the three diagnostic algorithms at the 95% and 99% limits of normality. Results based on 622 normal elderly subjects and 45 patients with glaucoma.

Algorithm	Specificity (%)		Sensitivity (%)	
	95%	99%	95%	99%
NRA/RADAAR/ODHT	65.1	82.8	93.3	88.9
NRA/RADAAR	67.4	83.0	91.1	88.9
NRA/ODHT	70.1	84.1	91.1	82.2
RADAAR/ODHT	72.0	92.1	88.9	66.7

Figure 23. Venn diagrams showing the uniocular (A) Specificity (number of normal subjects categorised as normal) and (B) Sensitivity (number of glaucoma patients categorised as glaucoma) of the three different diagnostic algorithms at the 99% limit. Results based on one eye randomly selected from 721 normal elderly subjects and 58 patients with glaucoma.

(A) Specificity

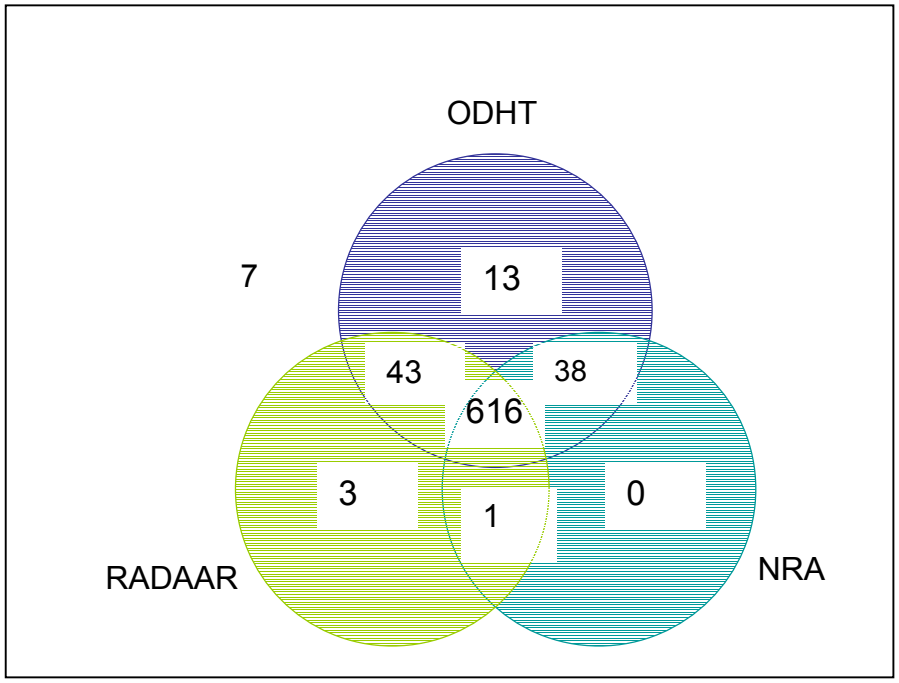

B) Sensitivity

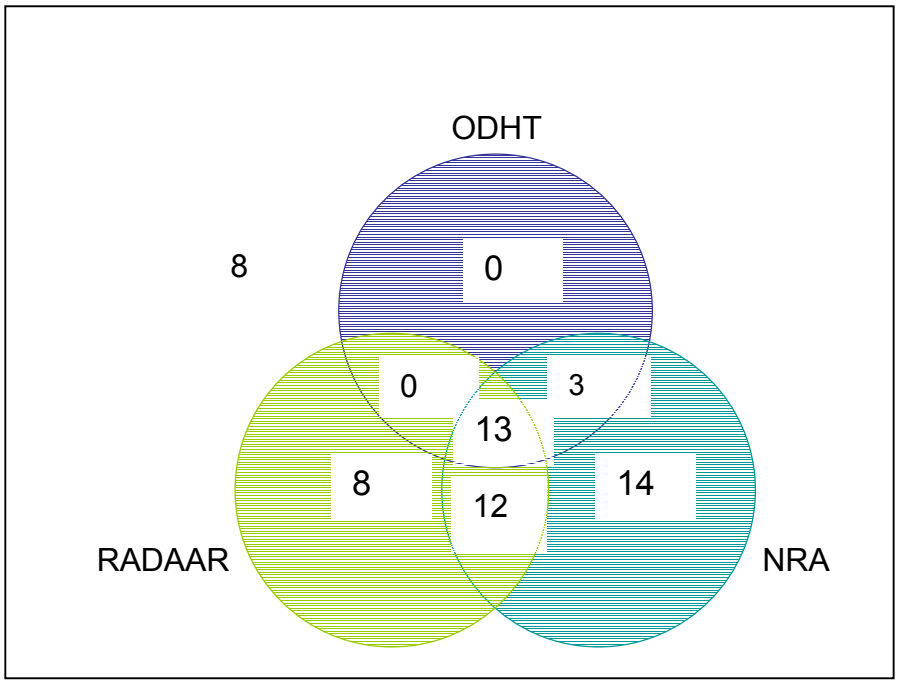

Figure 24. Venn diagrams showing the binocular (A) Specificity (number of normal subjects categorised as normal) and (B) Sensitivity (number of glaucoma patients categorised as glaucoma) of the three different diagnostic algorithms at the 99% limit. Results based on 622 normal elderly subjects and 45 patients with glaucoma.

(A) Specificity

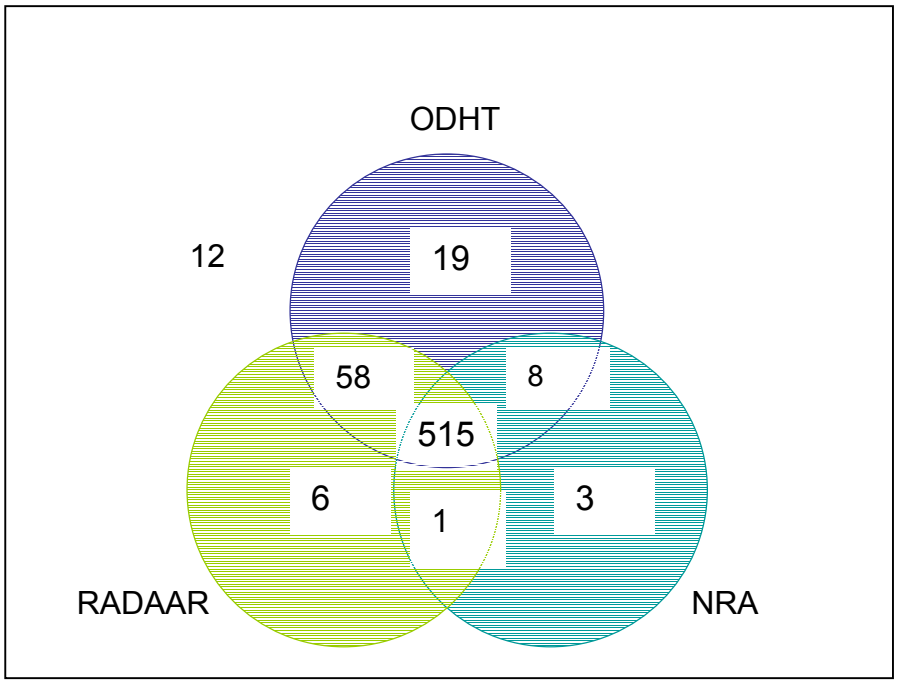

(B) Sensitivity

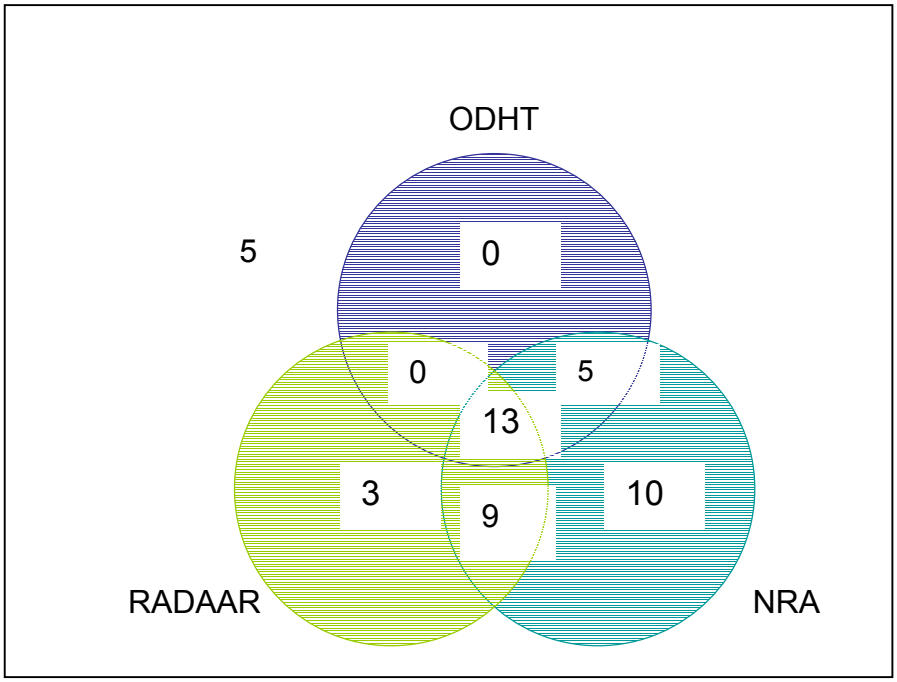

Table 39. Uniocular and Binocular positive and negative predictive values for the Nottingham Regression Analysis (NRA), Optic Disc Hemifield Test (ODHT), and Rim Area/Disc Area Asymmetry Ratio (RADAAR) at the 99% limit for normality.

Algorithm		Uniocular	Binocular
NRA	**PPV**	0.98	0.99
NPV		0.61	0.72
ODHT	**PPV**	0.96	0.97
NPV		0.30	0.62
RADAAR	**PPV**	0.96	-
	NPV	0.64	-

PPV Positive predictive value
NPV Negative predictive value

11.4 DISCUSSION

For statistical reasons, most studies of diagnostic imaging in glaucoma select only one eye per subject for inclusion. Thus, the unit of analysis is the 'eye', as opposed to the 'subject' who comprises two eyes. Random sampling of individual eyes minimises pairing effects within the study data which might compromise the assumptions of independence of data points made by statistical tests. However, the difficulty then arises in applying the results of studies where the unit of analysis is an 'eye' to the clinical situation where the unit of analysis becomes the 'patient'. A previous study found a specificity of 91.4% and sensitivity of 72.4% of the Nottingham correction of the Moorfields Regression Analysis (NRA) when applied to one eye per subject at the 99% limit of normality (see Chapter 8).[175] When the NRA was applied binocularly in this study the sensitivity rose to 82.2%, though with a corresponding drop in specificity to 84.6%. When a diagnostic test is applied in multiple there is a greater probability of an abnormal result occurring by chance alone. However, the differential benefit of greater sensitivity over reduced specificity suggests that the greater sensitivity of binocular application is a real effect. The drop in specificity may be too great to allow use of the regression analysis in screening of populations with

low prevalence of glaucoma. However, the 99% limit of normality employed was based on optimal balancing between specificity and sensitivity in single eyes. Further studies are required to evaluate the optimal cut-off for normality when the test is applied binocularly. To the author's knowledge, this is the first study to report diagnostic accuracy data of the HRT with the unit of data being the 'patient'. A previous study looking at the performance of the Moorfields Regression Analysis on the HRT machine in screening a local population reported results separately for left and right eyes to comply with the theoretical statistical assumptions described.[177] However, if HRT is to be used to screen 'patients' for glaucoma then data on the diagnostic accuracy of the machine when applied binocularly are required to optimise diagnostic performance.

Patients with POAG frequently present with bilateral field loss at diagnosis. However, particularly in the early stages, the disease may be asymmetric[132] or unilateral,[178] with fellow eyes at greater risk of glaucoma compared with ocular hypertensive eyes.[179, 180] Therefore, the use of linear regression of rim area alone in detecting glaucoma with the HRT may lack sensitivity in detecting early disease which is asymmetric. This study found that utilising asymmetry analysis (rim area/disc area asymmetry ratio, RADAAR) in addition to binocular linear regression analysis using the NRA resulted in a further rise in sensitivity of 6.7% to 88.9% with a small fall in specificity of 1.6% to 83.0%. 21 tests are therefore applied to each subject in this analysis (each test comprises 7 analyses of the individual disc sectors), with a 21-fold increase in an abnormal result by chance alone. However, the differentially greater rise in sensitivity compared with fall in specificity suggests that the benefit of the combination is real. Chapter 10 described accuracy of the Optic Disc Hemifield Test (ODHT) developed for the HRT machine using normative data from BEAP with a specificity of 91.7% and a sensitivity of 51.6%. Whilst the sensitivity was not great enough to be a useful standalone test, it was postulated that the ODHT might be usefully combined with other tests in a complementary fashion. Thus, further characteristics of optic nerve head (ONH) topography are analysed to maximise use of the topographic

data available. However, this study found that there was no further rise in sensitivity when the ODHT was added to the combination of NRA and RADAAR at the 99% limit of normality. Thus, glaucoma patients with differential rim loss of the superior and inferior hemidiscs additionally manifest glaucomatous optic neuropathy detectable by the NRA, although not by RADAAR (Figure 23 and Figure 24).

With all three diagnostic algorithms combined, the greatest sensitivity at the 99% limit of normality was 86.2%. Thus, even with statistical evaluation of the many different sectoral ONH characteristics in combination, a minority of clinically-diagnosed glaucomatous optic discs are not detected by the HRT tools. Further research is required to identify the morphological characteristics of these optic discs to aid further development of diagnostic algorithms. A further statistical tool to classify ONHs using statistical shape analysis techniques has recently been incorporated into the software of HRT (HRT III).[157] This has the advantages of utilising much more of the topographic information available (in a single statistical test) compared with linear regression of 'rim area', whilst being independent of optic disc contour and reference plane requirements. A recent study has shown that the shape analysis tool has similar diagnostic performance to the Moorfields Regression Analysis.[181]

This study has some important limitations. Image quality was surprisingly poor, both in the normal and glaucoma groups. This issue has been discussed in previous chapters. Any HRT diagnostic algorithm will be of limited usefulness if significant numbers of patients produce unusable images. Another limitation lies in the definition of glaucoma, which did not require longitudinal confirmation of the diagnosis. Thus, although diagnosis was made by an experience glaucoma specialist based on ONH and visual field evaluation, no attempt was made to confirm ONH status with another expert opinion, or to confirm visual field status with a follow-up examination.

12.0 Concluding remarks

12.1 Concluding Remarks

The primary initial aims of this work were to describe normal optic nerve head morphometry and asymmetry in the elderly population, and the specificity of existing HRT II diagnostic algorithms when applied to the normal elderly population of Bridlington.

This study has found that in the elderly, perimetric normal males have larger cup-related parameters than normal females. Given that elderly males have twice the prevalence of open angle glaucoma compared to females[132], this novel finding may reflect the progression of a greater proportion of males towards glaucoma. Having found significant sex-related differences, for the purposes of using these data to distinguish normal and glaucoma, sex-specific normal ranges for HRT II optic nerve head parameters should be used in the elderly. Although rim and nerve fibre-related measurements tended to decrease with age, no significant effect of age on optic nerve head parameters was found. However, with a minimum age of 65 years, it is likely that the sample lacks power in detecting a significant effect without younger subjects for comparison. Whilst age should still be considered for inclusion in a diagnostic algorithm using this data, the magnitude of variability in normal tolerances is minimal.

In agreement with previous work, this study has found that rim and cup-related measures increase in magnitude with disc area. However, the increase in cup parameters is much greater than rim parameters. To generate consistent asymmetry parameters therefore the bigger disc should be compared with the smaller, rather than the right with the left. Asymmetry of rim parameters calculated in this way were not affected by sex or age. Although rim area asymmetry was positively correlated with disc area asymmetry, this effect for asymmetry in rim/disc area ratio was minimal. The major advantage of rim/disc area ratio asymmetry is therefore that it is a descriptor of normality that is not affected by demographic or disc size variables. It is possible that it may

discriminate glaucoma from normality with greater accuracy as a result, and with less interobserver variability.

The Moorfields Regression Analysis and two linear discriminant functions showed a specificity in the study population of between 88.2% and 94.3%. The percentage of optic discs classified 'outside normal limits' by the Moorfields Regression Analysis in the smallest and largest quartiles for disc size was 0.9% and 14.9%. This association was statistically significant only in males. The two linear discriminant functions also tended to reduced specificity in larger optic nerve heads. This may reflect the finding of significantly larger cups in males compared with females in the normal elderly population. This divergence was not predicted by these diagnostic functions which were developed on samples of younger subjects.

Disagreement between two investigators independently placing ONH contours on perimetrically normal optic discs was found to be substantial for some parameters. One investigator traced significantly larger contours on average than the other. 95% coefficients of agreement ranged from 26.7% for disc area, to 76.5% for rim volume. Rim/disc area ratio showed consistent high agreement, both on an inter- and intra-observer analysis (12.7% for inter-observer agreement). Linear regression analysis revealed that disagreement in rim-related parameters was highly correlated with disagreement in disc area, whilst disagreement in cup-related parameters was highly correlated with disagreement in reference height. By dividing rim area by disc area, rim disc area ratio substantially corrected for disagreement in disc area, thus producing high levels of agreement.

Following these initial findings, subsequent aims were to reproduce the methodology of the Moorfields Regression Analysis using BEAP data to try and improve diagnostic accuracy. In the BEAP data, the relationship between log rim area and disc area was not linear and showed significant heteroscedasticity.

These factors violate the assumptions of linear regression and explain the variable diagnostic accuracy of the technique with optic disc size. By conducting the linear regression separately for each disc area quartile, the assumptions of linear regression were met. The Nottingham correction of the Moorfields Regression Analysis (NRA) did not result in higher diagnostic accuracy overall, but did achieve a uniform diagnostic accuracy across the disc size range. By including sex in the NRA, specificity was equalised between the sexes.

The potential advantages of asymmetry analysis were explored using the Rim Area/Disc Area Asymmetry Ratio (RADAAR). Whilst RADAAR variance was significantly greater in glaucoma compared with normal subjects, there was significant symmetry resulting in only a moderate sensitivity in detection of disease (55.6% at the 99^{th} percentile limit with a specificity of 95.1%). Males with glaucoma showed greater RADAAR variance than females, with males also tending to be detected with greater sensitivity compared with females (63.0% and 44.4% respectively, p=0.43).

The Optic Disc Hemifield Test (ODHT) was created as morphometrically analogous to the functional Glaucoma Hemifield Test calculated by the Humphrey Visual Field Analyser. The ratios for temporal-superior/temporal-inferior (TS/TI) and nasal-superior/nasal-inferior (NS/NI) rim area and rim/disc area ratio were derived. Using the 95% limit of normality sensitivity was 32.8% and 36.2% for the ratio of TS/TI and NS/NI rim/disc area ratio respectively. Combining these two ratios into a single diagnostic test (positive if outside normal limits in either) resulted in a specificity of 91.7% and sensitivity of 51.7%. Whilst the sensitivity of neither the RADAAR nor ODHT diagnostic algorithms was considered great enough to be used as a stand-alone test, it was postulated that these tests may be usefully combined with the NRA in a complementary fashion to further enhance diagnostic accuracy.

The three diagnostic algorithms developed in this study were further investigated in combination. In applying the algorithms to one eye selected from each subject, it was found that combining RADAAR with the NRA achieved a 13.8% increase in sensitivity at the cost of a 5.2% decrease in specificity. Further combination with the ODHT provided no greater sensitivity, with a small decrease in specificity. Interestingly, when all three algorithms were applied to both eyes of each subject at the 99% limit of normality, sensitivity was only 88.9%. Thus, significant numbers of patients with glaucoma were not detected by the multiple application of these tests.

12.2 Future Work

As a result of this thesis, several areas for future enquiry have been identified:

1) Image quality in the elderly

Significant numbers of study subjects were excluded on the basis of a mean pixel height standard deviation (MPHSD) greater than 50 microns. Further work is required on ways to enhance the quality of the raw image in the elderly age group. As this age group is most at risk of glaucoma, the usefulness of the HRT machine in screening for the disease will be significantly limited if it cannot be applied to a substantial minority. Further work is also required to assess the usefulness of the MPHSD measure to the overall assessment of image quality. Since pixel height standard deviation is significantly positively skewed the median value may be more informative. It may be that maps displaying colour-coded pixel height standard deviation values may aid in assessing the relative contribution of structures such as blood vessels to overall MPHSD. It may therefore become apparent if structures of no interest are resulting in an image being rejected.

2) Linear Regression of Rim Area

This study overcame the issue of non-linearity and heteroscedasticity by conducting linear regression separately for each disc area quartile. Whilst this achieved the aim it is not the ‘cleanest’ of statistical methods. Further work is

required to adequately model the relationship between these variables simultaneously across the entire disc size range.

3) Statistical Shape Analysis

The reduction of the wealth of topographic data harnessed by HRT to 'rim area' and other such variables wastes potentially useful information. Statistical shape analysis has the potential to harness this information in an automated way. A technique developed by Swindale et al. has been incorporated into the most recent version of HRT.[157] Future work is required to optimise statistical shape analysis techniques on population-based elderly subjects such as those screened by BEAP.

4) Limitations of HRT in Detecting Glaucoma

A diagnostic test with a sensitivity of around 75% at high specificity can not usefully be applied to a population with a prevalence of disease around 2%. Thus, low sensitivity at suitable specificity remains a significant limiting factor for this technology. Further work is required to look specifically at the topographic features of those glaucomatous ONHs that are not detected as diseased by HRT. Identification of morphological features such as tilted disc which might contribute to reduced sensitivity may lead to the development of improved diagnostic techniques.

13.1 REFERENCES

1. Leske MC. The epidemiology of open-angle glaucoma: a review. Am J Epidemiol 1983;118(2):166-91.

2. Quigley HA. Number of people with glaucoma worldwide. Br J Ophthalmol 1996;80(5):389-93.

3. Ogden TE. Nerve fiber layer of the primate retina: morphometric analysis. Invest Ophthalmol Vis Sci 1984;25(1):19-29.

4. Dacey DM, Petersen MR. Dendritic field size and morphology of midget and parasol ganglion cells of the human retina. Proc Natl Acad Sci U S A 1992;89(20):9666-70.

5. Quigley HA, Nickells RW, Kerrigan LA, Pease ME, Thibault DJ, Zack DJ. Retinal ganglion cell death in experimental glaucoma and after axotomy occurs by apoptosis. Invest Ophthalmol Vis Sci 1995;36(5):774-86.

6. Quigley HA, Dunkelberger GR, Green WR. Chronic human glaucoma causing selectively greater loss of large optic nerve fibers. Ophthalmology 1988;95(3):357-63.

7. Dandona L, Hendrickson A, Quigley HA. Selective effects of experimental glaucoma on axonal transport by retinal ganglion cells to the dorsal lateral geniculate nucleus. Invest Ophthalmol Vis Sci 1991;32(5):1593-9.

8. Chaturvedi N, Hedley-Whyte ET, Dreyer EB. Lateral geniculate nucleus in glaucoma. Am J Ophthalmol 1993;116(2):182-8.

9. Yucel YH, Zhang Q, Gupta N, Kaufman PL, Weinreb RN. Loss of neurons in magnocellular and parvocellular layers of the lateral geniculate nucleus in glaucoma. Arch Ophthalmol 2000;118(3):378-84.

10. Vickers JC, Hof PR, Schumer RA, Wang RF, Podos SM, Morrison JH. Magnocellular and parvocellular visual pathways are both affected in a macaque monkey model of glaucoma. Aust N Z J Ophthalmol 1997;25(3):239-43.

11. Osborne NN, Wood JP, Chidlow G, Bae JH, Melena J, Nash MS. Ganglion cell death in glaucoma: what do we really know? Br J Ophthalmol 1999;83(8):980-6.

12. Kupfer C, Chumbley L, Downer JC. Quantitative histology of optic nerve, optic tract and lateral geniculate nucleus of man. J Anat 1967;101(Pt 3):393-401.

13. Mikelberg FS, Drance SM, Schulzer M, Yidegiligne HM, Weis MM. The normal human optic nerve. Axon count and axon diameter distribution. Ophthalmology 1989;96(9):1325-8.

14. Jonas JB, Muller-Bergh JA, Schlotzer-Schrehardt UM, Naumann GO. Histomorphometry of the human optic nerve. Invest Ophthalmol Vis Sci 1990;31(4):736-44.

15. Kerrigan-Baumrind LA, Quigley HA, Pease ME, Kerrigan DF, Mitchell RS. Number of ganglion cells in glaucoma eyes compared with threshold visual field tests in the same persons. Invest Ophthalmol Vis Sci 2000;41(3):741-8.

16. Repka MX, Quigley HA. The effect of age on normal human optic nerve fiber number and diameter. Ophthalmology 1989;96(1):26-32.

17. Wollstein G, Garway-Heath DF, Hitchings RA. Identification of early glaucoma cases with the scanning laser ophthalmoscope. Ophthalmology 1998;105(8):1557-63.

18. Britton RJ, Drance SM, Schulzer M, Douglas GR, Mawson DK. The area of the neuroretinal rim of the optic nerve in normal eyes. Am J Ophthalmol 1987;103(4):497-504.

19. Jonas JB, Budde WM. Diagnosis and pathogenesis of glaucomatous optic neuropathy: morphological aspects. Prog Retin Eye Res 2000;19(1):1-40.

20. Jonas JB, Gusek GC, Naumann GO. Optic disc, cup and neuroretinal rim size, configuration and correlations in normal eyes. Invest Ophthalmol Vis Sci 1988;29(7):1151-8.

21. Jonas JB, Gusek GC, Naumann GO. Optic disk morphometry in high myopia. Graefes Arch Clin Exp Ophthalmol 1988;226(6):587-90.

22. Varma R, Tielsch JM, Quigley HA, Hilton SC, Katz J, Spaeth GL, et al. Race-, age-, gender-, and refractive error-related differences in the normal optic disc. Arch Ophthalmol 1994;112(8):1068-76.

23. Chi T, Ritch R, Stickler D, Pitman B, Tsai C, Hsieh FY. Racial differences in optic nerve head parameters. Arch Ophthalmol 1989;107(6):836-9.

24. Jonas JB, Gusek GC, Guggenmoos-Holzmann I, Naumann GO. Correlations of the neuroretinal rim area with ocular and general parameters in normal eyes. Ophthalmic Res 1988;20(5):298-303.

25. Jonas JB, Kling F, Grundler AE. Optic disc shape, corneal astigmatism, and amblyopia. Ophthalmology 1997;104(11):1934-7.

26. Caprioli J, Miller JM. Optic disc rim area is related to disc size in normal subjects. Arch Ophthalmol 1987;105(12):1683-5.

27. Quigley HA, Coleman AL, Dorman-Pease ME. Larger optic nerve heads have more nerve fibers in normal monkey eyes. Arch Ophthalmol 1991;109(10):1441-3.

28. Balazsi AG, Drance SM, Schulzer M, Douglas GR. Neuroretinal rim area in suspected glaucoma and early chronic open-angle glaucoma. Correlation with parameters of visual function. Arch Ophthalmol 1984;102(7):1011-4.

29. Jonas JB, Schmidt AM, Muller-Bergh JA, Schlotzer-Schrehardt UM, Naumann GO. Human optic nerve fiber count and optic disc size. Invest Ophthalmol Vis Sci 1992;33(6):2012-8.

30. Dandona L, Quigley HA, Brown AE, Enger C. Quantitative regional structure of the normal human lamina cribrosa. A racial comparison. Arch Ophthalmol 1990;108(3):393-8.

31. Jonas JB, Mardin CY, Schlotzer-Schrehardt U, Naumann GO. Morphometry of the human lamina cribrosa surface. Invest Ophthalmol Vis Sci 1991;32(2):401-5.

32. Minckler DS, McLean IW, Tso MO. Distribution of axonal and glial elements in the rhesus optic nerve head studied by electron microscopy. Am J Ophthalmol 1976;82(2):179-87.

33. Budde WM, Jonas JB, Martus P, Grundler AE. Influence of optic disc size on neuroretinal rim shape in healthy eyes. J Glaucoma 2000;9(5):357-62.

34. Jonas JB, Budde WM, Panda-Jonas S. Ophthalmoscopic evaluation of the optic nerve head. Surv Ophthalmol 1999;43(4):293-320.

35. Tuulonen A, Airaksinen PJ. Initial glaucomatous optic disk and retinal nerve fiber layer abnormalities and their progression. Am J Ophthalmol 1991;111(4):485-90.

36. Pederson JE, Anderson DR. The mode of progressive disc cupping in ocular hypertension and glaucoma. Arch Ophthalmol 1980;98(3):490-5.

37. Jonas JB, Fernandez MC, Sturmer J. Pattern of glaucomatous neuroretinal rim loss. Ophthalmology 1993;100(1):63-8.

38. Quigley HA, Sanchez RM, Dunkelberger GR, L'Hernault NL, Baginski TA. Chronic glaucoma selectively damages large optic nerve fibers. Invest Ophthalmol Vis Sci 1987;28(6):913-20.

39. Jonas JB, Gusek GC, Naumann GO. Optic disc morphometry in chronic primary open-angle glaucoma. I. Morphometric intrapapillary characteristics. Graefes Arch Clin Exp Ophthalmol 1988;226(6):522-30.

40. Caprioli J. Discrimination between normal and glaucomatous eyes. Invest Ophthalmol Vis Sci 1992;33(1):153-9.

41. Jonas JB, Fernandez MC. Shape of the neuroretinal rim and position of the central retinal vessels in glaucoma. Br J Ophthalmol 1994;78(2):99-102.

42. Jonas JB, Mardin CY, Grundler AE. Comparison of measurements of neuroretinal rim area between confocal laser scanning tomography and planimetry of photographs. Br J Ophthalmol 1998;82(4):362-6.

43. Jonas JB, Fernandez MC, Naumann GO. Glaucomatous parapapillary atrophy. Occurrence and correlations. Arch Ophthalmol 1992;110(2):214-22.

44. Quigley HA, Katz J, Derick RJ, Gilbert D, Sommer A. An evaluation of optic disc and nerve fiber layer examinations in monitoring progression of early glaucoma damage. Ophthalmology 1992;99(1):19-28.

45. Airaksinen PJ. Retinal nerve fiber layer and neuroretinal rim changes in ocular hypertension and early glaucoma. Surv Ophthalmol 1989;33 Suppl:413-4; discussion 21-2.

46. Quigley HA, Addicks EM, Green WR, Maumenee AE. Optic nerve damage in human glaucoma. II. The site of injury and susceptibility to damage. Arch Ophthalmol 1981;99(4):635-49.

47. Quigley HA, Addicks EM, Green WR. Optic nerve damage in human glaucoma. III. Quantitative correlation of nerve fiber loss and visual field defect in glaucoma, ischemic neuropathy, papilledema, and toxic neuropathy. Arch Ophthalmol 1982;100(1):135-46.

48. Quigley HA, Dunkelberger GR, Green WR. Retinal ganglion cell atrophy correlated with automated perimetry in human eyes with glaucoma. Am J Ophthalmol 1989;107(5):453-64.

49. Sommer A, Katz J, Quigley HA, Miller NR, Robin AL, Richter RC, et al. Clinically detectable nerve fiber atrophy precedes the onset of glaucomatous field loss. Arch Ophthalmol 1991;109(1):77-83.

50. Zeyen TG, Caprioli J. Progression of disc and field damage in early glaucoma. Arch Ophthalmol 1993;111(1):62-5.

51. Katz J, Quigley HA, Sommer A. Repeatability of the Glaucoma Hemifield Test in automated perimetry. Invest Ophthalmol Vis Sci 1995;36(8):1658-64.

52. Landers JA, Goldberg I, Graham SL. Detection of early visual field loss in glaucoma using frequency-doubling perimetry and short-wavelength automated perimetry. Arch Ophthalmol 2003;121(12):1705-10.

53. Girkin CA, Emdadi A, Sample PA, Blumenthal EZ, Lee AC, Zangwill LM, et al. Short-wavelength automated perimetry and standard perimetry in the detection of progressive optic disc cupping. Arch Ophthalmol 2000;118(9):1231-6.

54. Wild JM, Moss ID, Whitaker D, O'Neill EC. The statistical interpretation of blue-on-yellow visual field loss. Invest Ophthalmol Vis Sci 1995;36(7):1398-410.

55. Rohrschneider K, Burk RO, Kruse FE, Volcker HE. Reproducibility of the optic nerve head topography with a new laser tomographic scanning device. Ophthalmology 1994;101(6):1044-9.

56. Burk RO, Vihanninjoki K, Bartke T, Tuulonen A, Airaksinen PJ, Volcker HE, et al. Development of the standard reference plane for the Heidelberg retina tomograph. Graefes Arch Clin Exp Ophthalmol 2000;238(5):375-84.

57. Garway-Heath DF, Poinoosawmy D, Wollstein G, Viswanathan A, Kamal D, Fontana L, et al. Inter- and intraobserver variation in the analysis of optic disc images: comparison of the Heidelberg retina tomograph and computer assisted planimetry. Br J Ophthalmol 1999;83(6):664-9.

58. Vihanninjoki K, Burk RO, Teesalu P, Tuulonen A, Airaksinen PJ. Optic disc biomorphometry with the Heidelberg Retina Tomograph at different reference levels. Acta Ophthalmol Scand 2002;80(1):47-53.

59. Tan JC, White E, Poinoosawmy D, Hitchings RA. Validity of rim area measurements by different reference planes. J Glaucoma 2004;13(3):245-50.

60. Park KH, Caprioli J. Development of a novel reference plane for the Heidelberg retina tomograph with optical coherence tomography measurements. J Glaucoma 2002;11(5):385-91.

61. Bathija R, Zangwill L, Berry CC, Sample PA, Weinreb RN. Detection of early glaucomatous structural damage with confocal scanning laser tomography. J Glaucoma 1998;7(2):121-7.

62. Caprioli J, Park HJ, Ugurlu S, Hoffman D. Slope of the peripapillary nerve fiber layer surface in glaucoma. Invest Ophthalmol Vis Sci 1998;39(12):2321-8.

63. Chauhan B, Le Blanc R, McCormick TA, Rogers JB. Test-retest variability of topographic measurements with confocal scanning laser tomography in patients with glaucoma and control subjects. Am J Ophthalmol 1994;118(1):9-15.

64. Tomita G, Honbe K, Kitazawa Y. Reproducibility of measurements by laser scanning tomography in eyes before and after pilocarpine treatment. Graefes Arch Clin Exp Ophthalmol 1994;232(7):406-8.

65. Weinreb RN, Lusky M, Bartsch DU, Morsman D. Effect of repetitive imaging on topographic measurements of the optic nerve head. Arch Ophthalmol 1993;111(5):636-8.

66. Brigatti L, Weitzman M, Caprioli J. Regional test-retest variability of confocal scanning laser tomography. Am J Ophthalmol 1995;120(4):433-40.

67. Zangwill L, Irak I, Berry CC, Garden V, de Souza Lima M, Weinreb RN. Effect of cataract and pupil size on image quality with confocal scanning laser ophthalmoscopy. Arch Ophthalmol 1997;115(8):983-90.

68. Chauhan BC, McCormick TA. Effect of the cardiac cycle on topographic measurements using confocal scanning laser tomography. Graefes Arch Clin Exp Ophthalmol 1995;233(9):568-72.

69. Rohrschneider K, Burk RO, Volcker HE. [Comparison of two laser scanning tomography systems for three-dimensional analysis of the optic papilla]. Ophthalmologe 1993;90(6):613-9.

70. Strouthidis NG, White ET, Owen VM, Ho TA, Hammond CJ, Garway-Heath DF. Factors affecting the test-retest variability of Heidelberg retina tomograph and Heidelberg retina tomograph II measurements. Br J Ophthalmol 2005;89(11):1427-32.

71. Sihota R, Gulati V, Agarwal HC, Saxena R, Sharma A, Pandey RM. Variables affecting test-retest variability of Heidelberg Retina Tomograph II stereometric parameters. J Glaucoma 2002;11(4):321-8.

72. Miglior S, Albe E, Guareschi M, Rossetti L, Orzalesi N. Intraobserver and interobserver reproducibility in the evaluation of optic disc stereometric parameters by Heidelberg Retina Tomograph. Ophthalmology 2002;109(6):1072-7.

73. Hatch WV, Flanagan JG, Williams-Lyn DE, Buys YM, Farra T, Trope GE. Interobserver agreement of Heidelberg retina tomograph parameters. J Glaucoma 1999;8(4):232-7.

74. Roff EJ, Hosking SL, Barnes DA. The influence of contour line size and location on the reproducibility of topographic measurement with the Heidelberg Retina Tomograph. Ophthalmic Physiol Opt 2001;21(3):173-81.

75. Iester M, Mikelberg FS, Courtright P, Burk RO, Caprioli J, Jonas JB, et al. Interobserver variability of optic disk variables measured by confocal scanning laser tomography. Am J Ophthalmol 2001;132(1):57-62.

76. Hatch WV, Trope GE, Buys YM, Macken P, Etchells EE, Flanagan JG. Agreement in assessing glaucomatous discs in a clinical teaching setting with stereoscopic disc photographs, planimetry, and laser scanning tomography. J Glaucoma 1999;8(2):99-104.

77. Boros AS, Jonescu-Cuypers CP, Bartz-Schmidt KU. Variability of the normalised rim/disc area quotient estimated by laser scanning tomography. A comparison with conventional planimetry. Int Ophthalmol 2001;24(5):263-7.

78. Sung VC, Bhan A, Vernon SA. Agreement in assessing optic discs with a digital stereoscopic optic disc camera (Discam) and Heidelberg retina tomograph. Br J Ophthalmol 2002;86(2):196-202.

79. Meyer T, Howland HC. How large is the optic disc? Systematic errors in fundus cameras and topographers. Ophthalmic Physiol Opt 2001;21(2):139-50.

80. Rudnicka AR, Burk RO, Edgar DF, Fitzke FW. Magnification characteristics of fundus imaging systems. Ophthalmology 1998;105(12):2186-92.

81. Holden AL, Fitzke FW. Image size in the fundus: structural evidence for wide-field retinal magnification factor. Br J Ophthalmol 1988;72(3):228-30.

82. Lotmar W. Dependence of magnification upon the camera-to-eye distance in the Zeiss fundus camera. Acta Ophthalmol (Copenh) 1984;62(1):131-4.

83. Hosking SL, Flanagan JG. Prospective study design for the Heidelberg Retina Tomograph: the effect of change in focus setting. Graefes Arch Clin Exp Ophthalmol 1996;234(5):306-10.

84. Tan JC, Poinoosawmy D, Fitzke FW, Hitchings RA. Magnification changes in scanning laser tomography. J Glaucoma 2004;13(2):137-41.

85. Orgul S, Cioffi GA, Bacon DR, Van Buskirk EM. Sources of variability of topometric data with a scanning laser ophthalmoscope. Arch Ophthalmol 1996;114(2):161-4.

86. Sheen NJ, Aldridge C, Drasdo N, North RV, Morgan JE. The effects of astigmatism and working distance on optic nerve head images using a Heidelberg Retina Tomograph scanning laser ophthalmoscope. Am J Ophthalmol 2001;131(6):716-21.

87. Brigatti L, Caprioli J. Correlation of visual field with scanning confocal laser optic disc measurements in glaucoma. Arch Ophthalmol 1995;113(9):1191-4.

88. Eid TM, Spaeth GL, Katz LJ, Azuara-Blanco A, Agusburger J, Nicholl J. Quantitative estimation of retinal nerve fiber layer height in glaucoma and the relationship with optic nerve head topography and visual field. J Glaucoma 1997;6(4):221-30.

89. Iester M, Mikelberg FS, Courtright P, Drance SM. Correlation between the visual field indices and Heidelberg retina tomograph parameters. J Glaucoma 1997;6(2):78-82.

90. Tole DM, Edwards MP, Davey KG, Menage MJ. The correlation of the visual field with scanning laser ophthalmoscope measurements in glaucoma. Eye 1998;12 (Pt 4):686-90.

91. Teesalu P, Vihanninjoki K, Airaksinen PJ, Tuulonen A. Hemifield association between blue-on-yellow visual field and optic nerve head topographic measurements. Graefes Arch Clin Exp Ophthalmol 1998;236(5):339-45.

92. Iester M, Swindale NV, Mikelberg FS. Sector-based analysis of optic nerve head shape parameters and visual field indices in healthy and glaucomatous eyes. J Glaucoma 1997;6(6):370-6.

93. Chauhan BC, McCormick TA, Nicolela MT, LeBlanc RP. Optic disc and visual field changes in a prospective longitudinal study of patients with glaucoma: comparison of scanning laser tomography with conventional perimetry and optic disc photography. Arch Ophthalmol 2001;119(10):1492-9.

94. Cioffi GA, Liebmann JM, Johnson CA, Weinreb RN. Structural-functional relationships of the optic nerve in glaucoma. J Glaucoma 2000;9(1):3-4.

95. Schlottmann PG, De Cilla S, Greenfield DS, Caprioli J, Garway-Heath DF. Relationship between visual field sensitivity and retinal nerve fiber layer thickness as measured by scanning laser polarimetry. Invest Ophthalmol Vis Sci 2004;45(6):1823-9.

96. Garway-Heath DF, Holder GE, Fitzke FW, Hitchings RA. Relationship between electrophysiological, psychophysical, and anatomical measurements in glaucoma. Invest Ophthalmol Vis Sci 2002;43(7):2213-20.

97. Teesalu P, Vihanninjoki K, Airaksinen PJ, Tuulonen A, Laara E. Correlation of blue-on-yellow visual fields with scanning confocal laser optic disc measurements. Invest Ophthalmol Vis Sci 1997;38(12):2452-9.

98. Greenstein VC, Thienprasiddhi P, Ritch R, Liebmann JM, Hood DC. A method for comparing electrophysiological, psychophysical, and structural measures of glaucomatous damage. Arch Ophthalmol 2004;122(9):1276-84.

99. Salgarello T, Colotto A, Falsini B, Buzzonetti L, Cesari L, Iarossi G, et al. Correlation of pattern electroretinogram with optic disc cup shape in ocular hypertension. Invest Ophthalmol Vis Sci 1999;40(9):1989-97.

100. Miglior S, Guareschi M, Albe E, Gomarasca S, Vavassori M, Orzalesi N. Detection of glaucomatous visual field changes using the Moorfields regression analysis of the Heidelberg retina tomograph. Am J Ophthalmol 2003;136(1):26-33.

101. Wollstein G, Garway-Heath DF, Fontana L, Hitchings RA. Identifying early glaucomatous changes. Comparison between expert clinical assessment of optic disc photographs and confocal scanning ophthalmoscopy. Ophthalmology 2000;107(12):2272-7.

102. Bowd C, Zangwill LM, Medeiros FA, Hao J, Chan K, Lee TW, et al. Confocal scanning laser ophthalmoscopy classifiers and stereophotograph evaluation for prediction of visual field abnormalities in glaucoma-suspect eyes. Invest Ophthalmol Vis Sci 2004;45(7):2255-62.

103. Logan JF, Rankin SJ, Jackson AJ. Retinal blood flow measurements and neuroretinal rim damage in glaucoma. Br J Ophthalmol 2004;88(8):1049-54.

104. Agarwal HC, Gulati V, Sihota R. The normal optic nerve head on Heidelberg Retina Tomograph II. Indian J Ophthalmol 2003;51(1):25-33.

105. Ford BA, Artes PH, McCormick TA, Nicolela MT, LeBlanc RP, Chauhan BC. Comparison of data analysis tools for detection of glaucoma with the Heidelberg Retina Tomograph. Ophthalmology 2003;110(6):1145-50.

106. Mikelberg F, Parfitt C, Swindale N, others. Ability of the Heidelberg Retina Tomograph to detect early glaucomatous visual field loss. J Glaucoma 1995;4:242-7.

107. Bowd C, Chan K, Zangwill LM, Goldbaum MH, Lee TW, Sejnowski TJ, et al. Comparing neural networks and linear discriminant functions for glaucoma detection using confocal scanning laser ophthalmoscopy of the optic disc. Invest Ophthalmol Vis Sci 2002;43(11):3444-54.

108. Iester M, Mikelberg FS, Drance SM. The effect of optic disc size on diagnostic precision with the Heidelberg retina tomograph. Ophthalmology 1997;104(3):545-8.

109. Zangwill LM, Chan K, Bowd C, Hao J, Lee TW, Weinreb RN, et al. Heidelberg retina tomograph measurements of the optic disc and parapapillary retina for detecting glaucoma analyzed by machine learning classifiers. Invest Ophthalmol Vis Sci 2004;45(9):3144-51.

110. Orgul S, Croffi GA, Van Buskirk EM. Variability of contour line alignment on sequential images with the Heidelberg Retina Tomograph. Graefes Arch Clin Exp Ophthalmol 1997;235(2):82-6.

111. Derado G, Mardia KV, Patrangenaru V, Thompson HW. A shape-based glaucoma index for topographic images. Journal of Applied Statistics 2004;31(10):1241-8.

112. Medeiros FA, Zangwill LM, Bowd C, Weinreb RN. Comparison of the GDx VCC scanning laser polarimeter, HRT II confocal scanning laser ophthalmoscope, and stratus OCT optical coherence tomograph for the detection of glaucoma. Arch Ophthalmol 2004;122(6):827-37.

113. Zangwill LM, Bowd C, Berry CC, Williams J, Blumenthal EZ, Sanchez-Galeana CA, et al. Discriminating between normal and glaucomatous eyes using the Heidelberg Retina Tomograph, GDx Nerve Fiber Analyzer, and Optical Coherence Tomograph. Arch Ophthalmol 2001;119(7):985-93.

114. Ikram MK, Borger PH, Assink JJ, Jonas JB, Hofman A, de Jong PT. Comparing ophthalmoscopy, slide viewing, and semiautomated systems in optic disc morphometry. Ophthalmology 2002;109(3):486-93.

115. Azuara-Blanco A, Spaeth GL, Nicholl J, Lanzl IM, Augsburger JJ. Comparison between laser scanning tomography and computerised image analysis of the optic disc. Br J Ophthalmol 1999;83(3):295-8.

116. Dichtl A, Jonas JB, Mardin CY. Comparison between tomographic scanning evaluation and photographic measurement of the neuroretinal rim. Am J Ophthalmol 1996;121(5):494-501.

117. Spencer AF, Sadiq SA, Pawson P, Vernon SA. Vertical optic disk diameter: discrepancy between planimetric and SLO measurements. Invest Ophthalmol Vis Sci 1995;36(5):796-803.

118. Varma R, Steinmann WC, Scott IU. Expert agreement in evaluating the optic disc for glaucoma. Ophthalmology 1992;99(2):215-21.

119. Greaney MJ, Hoffman DC, Garway-Heath DF, Nakla M, Coleman AL, Caprioli J. Comparison of optic nerve imaging methods to distinguish normal eyes from those with glaucoma. Invest Ophthalmol Vis Sci 2002;43(1):140-5.

120. Medeiros FA, Zangwill LM, Bowd C, Sample PA, Weinreb RN. Use of progressive glaucomatous optic disk change as the reference standard for evaluation of diagnostic tests in glaucoma. Am J Ophthalmol 2005;139(6):1010-8.

121. Budde WM, Jonas JB, Hayler JK, Mardin CY. Determination of optic cup depth by confocal scanning laser tomography. Eur J Ophthalmol 2003;13(1):42-8.

122. Lim CS, O'Brien C, Bolton NM. A simple clinical method to measure the optic disc size in glaucoma. J Glaucoma 1996;5(4):241-5.

123. Schuman JS, Wollstein G, Farra T, Hertzmark E, Aydin A, Fujimoto JG, et al. Comparison of optic nerve head measurements obtained by optical coherence tomography and confocal scanning laser ophthalmoscopy. Am J Ophthalmol 2003;135(4):504-12.

124. Bowd C, Zangwill LM, Berry CC, Blumenthal EZ, Vasile C, Sanchez-Galeana C, et al. Detecting early glaucoma by assessment of retinal nerve fiber layer thickness and visual function. Invest Ophthalmol Vis Sci 2001;42(9):1993-2003.

125. Guedes V, Schuman JS, Hertzmark E, Wollstein G, Correnti A, Mancini R, et al. Optical coherence tomography measurement of macular and nerve fiber layer thickness in normal and glaucomatous human eyes. Ophthalmology 2003;110(1):177-89.

126. Sanchez-Galeana C, Bowd C, Blumenthal EZ, Gokhale PA, Zangwill LM, Weinreb RN. Using optical imaging summary data to detect glaucoma. Ophthalmology 2001;108(10):1812-8.

127. Weinreb RN, Shakiba S, Zangwill L. Scanning laser polarimetry to measure the nerve fiber layer of normal and glaucomatous eyes. Am J Ophthalmol 1995;119(5):627-36.

128. Weinreb RN. Evaluating the retinal nerve fiber layer in glaucoma with scanning laser polarimetry. Arch Ophthalmol 1999;117(10):1403-6.

129. Weinreb RN, Zangwill L, Berry CC, Bathija R, Sample PA. Detection of glaucoma with scanning laser polarimetry. Arch Ophthalmol 1998;116(12):1583-9.

130. Tjon-Fo-Sang MJ, Lemij HG. The sensitivity and specificity of nerve fiber layer measurements in glaucoma as determined with scanning laser polarimetry. Am J Ophthalmol 1997;123(1):62-9.

131. Weinreb RN, Bowd C, Zangwill LM. Glaucoma detection using scanning laser polarimetry with variable corneal polarization compensation. Arch Ophthalmol 2003;121(2):218-24.

132. Wolfs RC, Borger PH, Ramrattan RS, Klaver CC, Hulsman CA, Hofman A, et al. Changing views on open-angle glaucoma: definitions and prevalences--The Rotterdam Study. Invest Ophthalmol Vis Sci 2000;41(11):3309-21.

133. Hermann MM, Theofylaktopoulos I, Bangard N, Jonescu-Cuypers C, Coburger S, Diestelhorst M. Optic nerve head morphometry in healthy adults using confocal laser scanning tomography. Br J Ophthalmol 2004;88(6):761-5.

134. Durukan AH, Yucel I, Akar Y, Bayraktar MZ. Assessment of optic nerve head topographic parameters with a confocal scanning laser ophthalmoscope. Clin Experiment Ophthalmol 2004;32(3):259-64.

135. Nakamura H, Maeda T, Suzuki Y, Inoue Y. Scanning laser tomography to evaluate optic discs of normal eyes. Jpn J Ophthalmol 1999;43(5):410-4.

136. Gherghel D, Orgul S, Prunte C, Gugleta K, Lubeck P, Gekkieva M, et al. Interocular differences in optic disc topographic parameters in normal subjects. Curr Eye Res 2000;20(4):276-82.

137. Bartz-Schmidt KU, Sengersdorf A, Esser P, Walter P, Hilgers RD, Krieglstein GK. The cumulative normalised rim/disc area ratio curve. Graefes Arch Clin Exp Ophthalmol 1996;234(4):227-31.

138. Chylack LT, Jr., Wolfe JK, Singer DM, Leske MC, Bullimore MA, Bailey IL, et al. The Lens Opacities Classification System III. The Longitudinal Study of Cataract Study Group. Arch Ophthalmol 1993;111(6):831-6.

139. Mardin CY, Horn FK, Jonas JB, Budde WM. Preperimetric glaucoma diagnosis by confocal scanning laser tomography of the optic disc. Br J Ophthalmol 1999;83(3):299-304.

140. Iester M, Broadway DC, Mikelberg FS, Drance SM. A comparison of healthy, ocular hypertensive, and glaucomatous optic disc topographic parameters. J Glaucoma 1997;6(6):363-70.

141. Perneger TV. What's wrong with Bonferroni adjustments. Bmj 1998;316(7139):1236-8.

142. Saruhan A, Orgul S, Kocak I, Prunte C, Flammer J. Descriptive information of topographic parameters computed at the optic nerve head with the Heidelberg retina tomograph. J Glaucoma 1998;7(6):420-9.

143. Bowd C, Zangwill LM, Blumenthal EZ, Vasile C, Boehm AG, Gokhale PA, et al. Imaging of the optic disc and retinal nerve fiber layer: the effects of age, optic disc area, refractive error, and gender. J Opt Soc Am A Opt Image Sci Vis 2002;19(1):197-207.

144. Rudnicka AR, Frost C, Owen CG, Edgar DF. Nonlinear behavior of certain optic nerve head parameters and their determinants in normal subjects. Ophthalmology 2001;108(12):2358-68.

145. Ramrattan RS, Wolfs RC, Jonas JB, Hofman A, de Jong PT. Determinants of optic disc characteristics in a general population: The Rotterdam Study. Ophthalmology 1999;106(8):1588-96.

146. Garway-Heath DF, Wollstein G, Hitchings RA. Aging changes of the optic nerve head in relation to open angle glaucoma. Br J Ophthalmol 1997;81(10):840-5.

147. Healey PR, Mitchell P, Smith W, Wang JJ. The influence of age and intraocular pressure on the optic cup in a normal population. J Glaucoma 1997;6(5):274-8.

148. Burk RO, Rendon R. Clinical detection of optic nerve damage: measuring changes in cup steepness with use of a new image alignment algorithm. Surv Ophthalmol 2001;45 Suppl 3:S297-303; discussion S32-4.

149. Iester M, Mikelberg FS, Swindale NV, Drance SM. ROC analysis of Heidelberg Retina Tomograph optic disc shape measures in glaucoma. Can J Ophthalmol 1997;32(6):382-8.

150. Vernon S, Hawker M, Ainsworth G, Hillman J, HK M, HS. D. Laser scanning tomography of the optic nerve head in a normal elderly population: The Bridlington Eye Assessment Project. Invest Ophthalmol 2005;In Press.

151. Yablonski ME, Zimmerman TJ, Kass MA, Becker B. Prognostic significance of optic disk cupping in ocular hypertensive patients. Am J Ophthalmol 1980;89(4):585-92.

152. Harasymowycz P, Davis B, Xu G, Myers J, Bayer A, Spaeth GL. The use of RADAAR (ratio of rim area to disc area asymmetry) in detecting glaucoma and its severity. Can J Ophthalmol 2004;39(3):240-4.

153. Ong LS, Mitchell P, Healey PR, Cumming RG. Asymmetry in optic disc parameters: the Blue Mountains Eye Study. Invest Ophthalmol Vis Sci 1999;40(5):849-57.

154. Azuara-Blanco A, Katz LJ, Spaeth GL, Vernon SA, Spencer F, Lanzl IM. Clinical agreement among glaucoma experts in the detection of glaucomatous changes of the optic disk using simultaneous stereoscopic photographs. Am J Ophthalmol 2003;136(5):949-50.

155. Iester M, Jonas JB, Mardin CY, Budde WM. Discriminant analysis models for early detection of glaucomatous optic disc changes. Br J Ophthalmol 2000;84(5):464-8.

156. Miglior S, Casula M, Guareschi M, Marchetti I, Iester M, Orzalesi N. Clinical ability of Heidelberg retinal tomograph examination to detect glaucomatous visual field changes. Ophthalmology 2001;108(9):1621-7.

157. Swindale NV, Stjepanovic G, Chin A, Mikelberg FS. Automated analysis of normal and glaucomatous optic nerve head topography images. Invest Ophthalmol Vis Sci 2000;41(7):1730-42.

158. Vernon SA, Hawker MJ, Ainsworth G, Hillman JG, Macnab HK, Dua HS. Laser Scanning Tomography of the Optic Nerve Head in a Normal Elderly Population: The Bridlington Eye Assessment Project. Invest Ophthalmol Vis Sci 2005;46(8):2823-8.

159. Cleveland W, Devlin S. Locally Weighted Regression: An Approach to Regression Analysis by Local Fitting. Journal of the American Statistical Association 1988;83:596-610.

160. Jonas JB, Budde WM. Is the nasal optic disc sector important for morphometric glaucoma diagnosis? Br J Ophthalmol 2002;86(11):1232-5.

161. Quigley HA, Enger C, Katz J, Sommer A, Scott R, Gilbert D. Risk factors for the development of glaucomatous visual field loss in ocular hypertension. Arch Ophthalmol 1994;112(5):644-9.

162. Graham SL, Klistorner AI, Grigg JR, Billson FA. Objective VEP perimetry in glaucoma: asymmetry analysis to identify early deficits. J Glaucoma 2000;9(1):10-9.

163. Hawker MJ, Vernon SA, Ainsworth G, Hillman JG, MacNab HK, Dua HS. Asymmetry in optic disc morphometry as measured by heidelberg retina tomography in a normal elderly population: the Bridlington Eye Assessment Project. Invest Ophthalmol Vis Sci 2005;46(11):4153-8.

164. Guzowski M, Fraser-Bell S, Rochtchina E, Wang JJ, Mitchell P. Asymmetric refraction in an older population: the Blue Mountains Eye Study. Am J Ophthalmol 2003;136(3):551-3.

165. Janknecht P, Funk J. Optic nerve head analyser and Heidelberg retina tomograph: accuracy and reproducibility of topographic measurements in a model eye and in volunteers. Br J Ophthalmol 1994;78(10):760-8.

166. Asman P, Heijl A. Glaucoma Hemifield Test. Automated visual field evaluation. Arch Ophthalmol 1992;110(6):812-9.

167. Jonas JB, Budde WM, Martus P. The optic disc hemifield test. J Glaucoma 2004;13(2):108-13.

168. Tielsch JM, Katz J, Quigley HA, Miller NR, Sommer A. Intraobserver and interobserver agreement in measurement of optic disc characteristics. Ophthalmology 1988;95(3):350-6.

169. Dreher AW, Tso PC, Weinreb RN. Reproducibility of topographic measurements of the normal and glaucomatous optic nerve head with the laser tomographic scanner. Am J Ophthalmol 1991;111(2):221-9.

170. Burk RO, Rohrschneider K, Takamoto T, Volcker HE, Schwartz B. Laser scanning tomography and stereophotogrammetry in three-dimensional optic disc analysis. Graefes Arch Clin Exp Ophthalmol 1993;231(4):193-8.

171. Zangwill L, Shakiba S, Caprioli J, Weinreb RN. Agreement between clinicians and a confocal scanning laser ophthalmoscope in estimating cup/disk ratios. Am J Ophthalmol 1995;119(4):415-21.

172. Uchida H, Brigatti L, Caprioli J. Detection of structural damage from glaucoma with confocal laser image analysis. Invest Ophthalmol Vis Sci 1996;37(12):2393-401.

173. Jayasundera T, Danesh-Meyer HV, Donaldson M, Gamble G. Agreement between stereoscopic photographs, clinical assessment, Heidelberg retina tomograph and digital stereoscopic optic disc camera in estimating vertical cup:disc ratio. Clin Experiment Ophthalmol 2005;33(3):259-63.

174. Blumenthal EZ, Sapir-Pichhadze R. Misleading statistical calculations in far-advanced glaucomatous visual field loss. Ophthalmology 2003;110(1):196-200.

175. Hawker MJ, Vernon SA, Tattersall CL, Dua HS. Linear Regression Modeling Of Rim Area To Discriminate Between Normal And Glaucomatous Optic Nerve Heads:
The Bridlington Eye Assessment Project. J Glaucoma 2006;In Press.

176. Hawker MJ, Vernon SA, Tattersall CL, Dua HS. Detecting glaucoma with RADAAR: the Bridlington Eye Assessment Project. Br J Ophthalmol 2006;90(6):744-8.

177. Harasymowycz PJ, Papamatheakis DG, Fansi AK, Gresset J, Lesk MR. Validity of screening for glaucomatous optic nerve damage using confocal scanning laser ophthalmoscopy (Heidelberg Retina Tomograph II) in high-risk populations: a pilot study. Ophthalmology 2005;112(12):2164-71.

178. Drance SM, Wheeler CA, Pattullo M. Uniocular open-angle glaucoma. Am J Ophthalmol 1968;65:891-902.

179. Harbin TS, Jr., Podos SM, Kolker AE, Becker B. Visual field progression in open-angle glaucoma patients presenting with monocular field loss. Trans Sect Ophthalmol Am Acad Ophthalmol Otolaryngol 1976;81(2):253-7.

180. Susanna R, Drance SM, Douglas GR. The visual prognosis of the fellow eye in uniocular chronic open-angle glaucoma. Br J Ophthalmol 1978;62:327-9.

181. Harizman N, Zelefsky JR, Ilitchev EV, Tello CA, Ritch R, Liebmann JM. Detection of Glaucoma Using Operator-Dependent versus Operator-Independent Classification in the HRT-III. Br J Ophthalmol 2006.

Appendix 1 The Heidelberg Retina Tomograph I

Appendix 2: The Heidelberg Retina Tomograph II